

**GEOCHEMICAL AND ISOTOPIC STUDIES IN
SEDIMENTS AND WATERS OF THE
NORTHERN INDIAN OCEAN**

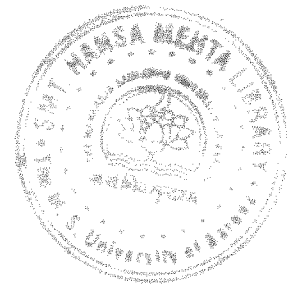


A thesis submitted to
The Maharaja Sayajirao University of Baroda
for the award of
the degree of
Doctor of Philosophy
in
Geology

By
RAVI BHUSHAN

Department of Geology
Faculty of Science
The Maharaja Sayajirao University of Baroda
Vadodara - 390002, Gujarat, India

June, 2008



Dedicated

To

My Father & Mother

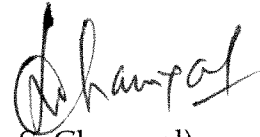
DECLARATION

This is to certify that the contents of this thesis comprise original research work of the candidate and have at no time been submitted for any other degree.

A handwritten signature in black ink, appearing to read 'Rbushan', with a long diagonal stroke extending from the bottom right of the signature.

(Ravi Bhushan)

Candidate

A handwritten signature in black ink, appearing to read 'L. S. Chamyat', with a circular flourish at the beginning.

(L. S. Chamyat)

Guide



ACKNOWLEDGEMENTS

I am very thankful and indebted to my guide Prof. L.S. Chamyal, whose guidance, encouragement and generous support made this thesis possible. His scientific suggestions and critical arguments were very helpful in enhancing the quality of this work.

I am extremely thankful to Head, Department of Geology, The M.S. University of Baroda, Vadodara for providing departmental facilities and support. I am thankful to the Director, Physical Research Laboratory (PRL) for granting me permission to register for Ph.D. as an external candidate. I would like to thank Ministry of Earth Sciences (MOES, earlier Department of Ocean Development) for their kind support with ship time for sample collection. I am grateful to Director, Centre for Marine Living Resources and Ecology (CMLRE), Cochin and their staff for their support with ship time onboard oceanographic research vessel FORV Sagar Sampada. I am thankful to Dr. A.J.T. Jull and G.S. Burr of NSF AMS facility at University of Arizona for providing me AMS radiocarbon dates. I am thankful to the Stable Isotope Laboratory for help and support.

I have the pleasure of working with two great oceanographers of the country, Prof. B.L.K. Somayajulu and Prof. S. Krishnaswami. I will always remain grateful to Prof. B.L.K. Somayajulu who introduced me to this fantastic world of oceanography. Prof. Krishnaswami with his critical suggestion was insatiable. His meticulous ways of approach to any problem though was painful to pursue but yielded some of the best outcome noticed ever. I am grateful to him for his scientific thoughts, critical remarks and teaching me nuances of research. I am highly grateful to Prof. M.M. Sarin for his scientific suggestions and meticulous ways of laboratory techniques. His encouragement and help with various experiments has benefited me immensely.

Dr. R. Rengarajan, Dr. Sunil K. Singh, and Mr. A.K. Sudheer were very supportive to me for any laboratory help and scientific suggestions. I am thankful to my colleagues of PRL in liquid nitrogen, glass blowing, workshop, library, maintenance, and administration for their constant support. I am thankful to Rajesh Agnihotri for stable isotope analysis and vigorous discussions. There are some colleagues who deserve special thanks for their constant support I had from them at various occasions. The first person who immediately comes to my mind is Mr. J.P. Bhavsar. I have a great appreciation for his selfless attitude and meticulous work ethics. I am very thankful to Navin, a friend, philosopher and a guide in various aspects of my personal and professional life. He deserves special thanks for his encouragement and help in shaping of my thesis. My good old friend, Kailash Dilli was very generous and spontaneous for help in thesis reorganisation. Jyoti, Ratan, Anjan, Dipu, Anil, Rama, Pauline, Ramani, Som, Deshpande, and Yadava are very special to me, whose

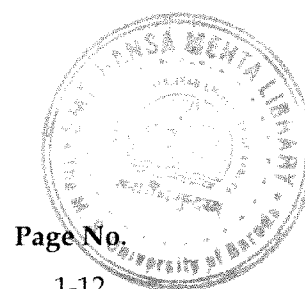
soothing company over long lasting period had a great impact. The present and past chemistry lab students Baskaran, Supriyo, Yadav, Rajesh, Koushik, Anirban, Santosh, Neeraj, Gyana, Kirpa, Rahaman, Ashwini and Vineet need special acknowledgement for their support, intense discussion and keeping a sound laboratory environment. The encouragement and fruitful scientific suggestions from Dr. R.K. Pant, Prof. A.K. Singhvi, Dr. P.N. Shukla, Prof. R. Ramesh and Prof. Kanchan Pande benefited me immensely. My sincere gratitude to my friend and late colleague Viswanathan for his support. I am very thankful to Sneha for her secretarial help with the thesis and Subhash for editorial help. Last but not the least, the Chemistry Gang needs special appreciation for the laboratory atmosphere it provided to me for over two decades.

Being active in various extra-co-curricular activities, I had opportunity to interact with large spectrum of people associated with various divisions. It is impossible to name all of them but they find a special place. Special mention needs to be there for the weekend football club and PRL tea club. I have nostalgic memories of my good old group of yesteryears "BAG", which made my earlier days exciting at PRL..

I dedicate this thesis to my belated father, who always wished to see it one day. I am grateful to my mother for her love and support. Shrabani (my wife) was a very encouraging factor in my life whose constant support and love not only at home but also in my scientific work kept me going. My cheerful daughter Maitreyi made my home a place of joy and her love and affection was my strength. I shall always remain grateful to my two younger brothers Shyam and Vijay, who were always there with me to support for any cause of the family.

(Ravi Bhushan)

CONTENTS



	Page No.
Chapter-I INTRODUCTION	1-12
Scope of the present study	10
Chapter-II EXPERIMENTAL DETAILS	13-21
Sampling Procedures	13
Onboard Processing and Measurements	14
Measurements Procedures	17
Sediment Measurements	18
Chapter-III Estimates of Upwelling Rates in the Arabian Sea	22-33
Determination of bomb ^{14}C inventory and air-sea CO_2 exchange rates	24
Determination of Upwelling Rates	29
Bomb ^{14}C inventory and air-sea CO_2 exchange rates	29
Upwelling Rates	31
Chapter-IV Bay of Bengal: Sediment Provenance	34-54
Sediment Distribution	37
Detrital Components	41
Biogenic Components	46
Strontium (Sr) and Neodymium (Nd) isotopic distribution	49
Chapter-V Bay of Bengal: Palaeoclimatic Implications	55-107
Chronology and the Sedimentation Rates	57
Variation in Lithogenic Proxies	60
Variation in Productivity Proxies	69
Variation in Trace Element Proxies	80
Strontium and Neodymium Isotopic Variations	85
Discussion	88
Regional and Global Correlations	99
Climatic Periodicities from Proxies	103
Chapter-VI Summary and Conclusions	108-113
References	114-137



LIST OF FIGURES

Fig. 1.1:	Surface circulation pattern in the Bay of Bengal during summer and winter monsoon. Note, the reversal of EICC during the two seasons (after Schott and McCreary, 2001).	4
Fig. 2.1:	Water Sampling locations in the Arabian Sea and the Equatorial Indian Ocean. GEOSECS station numbers are given after '#'. The boxed filled circles are the reoccupied GEOSECS stations.	13
Fig. 2.2:	Locations of the sediment core samples collected in the Bay of Bengal. Boxed filled circles are the cores studied in detail.	14
Fig. 3.1:	Location of sampling stations in the Arabian Sea. The boxed filled circles are the GEOSECS stations occupied during this study almost after two decades.	23
Fig. 3.2:	Radiocarbon distribution in the upper 1000 m water column at the equatorial Indian Ocean station 3846. Also, shown the ^{14}C profile of GEOSECS for the station occupied during 1978. Dashed line is the pre-bomb ^{14}C simulated curve.	27
Fig. 3.3:	Model $\Delta^{14}\text{C}$ of tropospheric CO_2 for the atmosphere over the Northern Indian Ocean used in the upwelling calculation (thick gray line). Tropospheric $\Delta^{14}\text{C}$ of Northern Hemisphere Zone 3 (Hua and Barbetti, 2004) is shown as thin line. Tropospheric $\Delta^{14}\text{C}$ values measured over the Arabian Sea during 1993-'95 and over the Bay of Bengal during 1997 (Dutta et al., 2006) are shown as filled circles.	28
Fig. 3.4:	Distribution of $\Delta^{14}\text{C}^*$ (excess bomb ^{14}C) versus depth for different stations. The solid line represents the simulated curve based on 1-D model of Oeschger et al., (1975) for the exchange rate (E), eddy diffusivity (K) and upwelling velocity (w).	32
Fig. 4.1:	Core locations in the Bay of Bengal. Boxed filled circles are the two cores studied in detail. Rivers supplying sediment to the Bay are also identified.	37
Fig. 4.2:	Correlation of Organic Carbon (C_{org}) in the surface sediments with CaCO_3 , C/N ratio and V concentration. No apparent correlation of C_{org} with	41

C/N can be noticed indicating marine source of C_{org} .

- Fig. 4.3:** Distribution of Al (%) in the Bay of Bengal surface sediments. Note, Al decrease from the coast to the open ocean. Western Bay of Bengal show Fe rich sediments, contribution from peninsular river. 42
- Fig. 4.4:** Distribution of Ti (ppm) in the surface sediments of the Bay of Bengal. 43
- Fig. 4.5:** Distribution of Fe (%) in the surface sediments of the Bay of Bengal. Western Bay of Bengal show Fe rich sediments, contribution from peninsular river. 44
- Fig. 4.6:** Distribution of V and Cr in the surface sediments. Erosion of Basaltic rocks from the peninsular India is responsible for higher V and Cr in western region. 45
- Fig. 4.7:** Distribution of Mn (%) in the surface sediments of the Bay of Bengal. Higher Mn concentrations in the northern Bay of Bengal is due to enrichment of surface sediments in high sedimentation regions. 46
- Fig. 4.8:** Distribution of $CaCO_3$ and organic carbon (C_{org}) in the surface sediments of the Bay of Bengal. Increasing $CaCO_3$ from the coast to the open ocean indicates decreasing detrital contribution. Whereas, high C_{org} near the coast reflects its enhanced preservation with increasing detrital flux 47
- Fig. 4.9:** Distribution of Ba/Al, productivity proxy in the surface sediments of the Bay of Bengal. Dilution of Ba due to increasing continental flux from coast to the open ocean can be observed. 48
- Fig. 4.10:** $^{87}Sr/^{86}Sr$ and ϵ_{Nd} of the river mouth samples measured. Irrawaddy river data from Colin et al., 1999 49
- Fig. 4.11:** $^{87}Sr/^{86}Sr$ versus ϵ_{Nd} plot of surface sediments. Also, shown are the boxes representing the end members. G-K (Godavari-Krishna) sediments values are the river mouth value.(Singh et al., 2008; Colin et al., 1999) 51
- Fig. 4.12:** $^{87}Sr/^{86}Sr$ and ϵ_{Nd} of surface sediment samples. Also, shown are the boxes representing the end members. G-K (Godavari-Krishna) sediments values are the river mouth value.(Singh et al., 2008; Colin et al., 1999; Ahmad et al., 2005). 51

Fig. 4.13:	$^{87}\text{Sr}/^{86}\text{Sr}$ vs $1/\text{Sr}$ and ϵ_{Nd} versus $1/\text{Nd}$ plot of the surface sediment.	52
Fig. 4.14:	Contour plot of $^{87}\text{Sr}/^{86}\text{Sr}$ distribution of sediments in the Bay of Bengal.	52
Fig. 4.15:	Contour plot of ϵ_{Nd} distribution of sediments in the Bay of Bengal. Note, third end member with high ϵ_{Nd} from the eastern Bay of Bengal along the coast of Arakan through Irrawaddy River	53
Fig. 5.1:	Sediment core locations in the Bay of Bengal	56
Fig. 5.2:	Age-Depth plot model of the core 4032 and 4040 from the Bay of Bengal.	57
Fig. 5.3:	Mass Accumulation Rate for the core 4032.	59
Fig. 5.4:	Downcore variation of Al (%), Fe(%), Mg(%) and Ti(ppm) in the core 4032. In general, a slow decreasing pattern from 50 kyr to 14 kyr and a gradual decreasing pattern from 14 kyr to 7 kyr can be noticed.	60
Fig. 5.5:	Downcore variation of Al (%), Fe (%), Mg (%) and Ti (ppm) in the core 4040. Note, relatively high variability in their concentrations.	64
Fig. 5.6:	Mass accumulation rate of lithogenic proxies for the core 4032.	67
Fig. 5.7:	Downcore variation of Al, Fe/Al, Mg/Al and Ti/Al in the Core 4032.	68
Fig. 5.8:	Downcore variation of Al, Fe/Al, Mg/Al and Ti/Al in the Core 4040.	69
Fig. 5.9:	Downcore variation of CaCO_3 , C_{org} and C/N in the core 4032.	70
Fig. 5.10:	Downcore variation of CaCO_3 , C_{org} and C/N in the core 4040.	73
Fig. 5.11:	Downcore variation of C_{org} and $\delta^{13}\text{C}$ and $\delta^{15}\text{N}$ of the organic matter in the core 4032.	74
Fig. 5.12:	Downcore variation of Ca/Al, Ba/Al and Sr/Al in the core 4032.	79
Fig. 5.13:	Downcore variation of Ca/Al, Ba/Al and Sr/Al in the	80

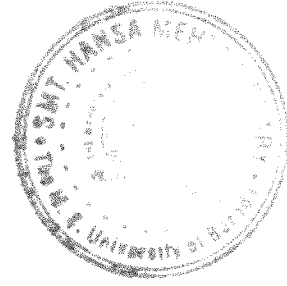
core 4040.

Fig. 5.14:	Downcore variation of fluxes of redox sensitive proxies viz. Mn, Cr and V in the core 4032	81
Fig. 5.15:	Downcore variation of fluxes of trace elemental proxies of Ni, Co, Zn and Cu in the core 4032	82
Fig. 5.16:	Downcore variation of the redox sensitive elements normalized to Al for the core 4032.	83
Fig. 5.17:	Downcore variation of redox proxies normalised to Al in the core 4040	83
Fig. 5.18:	Downcore variation of trace element proxies normalised to Al in the core 4032.	84
Fig. 5.19:	Downcore variation of trace element proxies normalised to Al in the core 4040.	85
Fig. 5.20:	Downcore variation of $^{87}\text{Sr}/^{86}\text{Sr}$ in the core 4032. Three prominent low $^{87}\text{Sr}/^{86}\text{Sr}$ ratios at 14, 20 and 43 kyr are observed.	87
Fig. 5.21:	Downcore variation of ϵ_{Nd} in the silicate fraction of the sediments from the core 4032. Note, the lowest ϵ_{Nd} of -8.8 at 20 kyr.	97
Fig. 5.22:	Downcore variation of ϵ_{Nd} in the silicate fraction of the sediments from the core 4040. Note, the lowest ϵ_{Nd} of -8.0 at 20 kyr.	98
Fig. 5.23:	Comparison of $^{87}\text{Sr}/^{86}\text{Sr}$ with solar insolation and mean effective moisture (Herszchuh et al., 2006). Note, synchronous variation of $^{87}\text{Sr}/^{86}\text{Sr}$ with solar insolation and moisture indicative of global correlation of the Bay of Bengal climate.	101
Fig. 5.24:	Periodicities observed in the core 4032 in its various proxies. Note 3.7 kyr periodicity prominent in all the proxies.	104
Fig. 5.25:	Periodicities observed in the core 4040 in its productivity proxies. Note 2.7 kyr periodicity prominent in all the proxies.	105
Fig. 5.26:	Periodicities observed in the core 4032 for Mn and V/Al. Note 2.4 kyr periodicity prominent in all the proxies.	106

LIST OF TABLES

Table 3.1:	Upwelling rates based on bomb ^{14}C inventory for the Arabian Sea and the Equatorial Indian Ocean stations	30
Table 4.1:	Locations of the cores in the Bay of Bengal.	38
Table 4.2:	Concentration of trace elements, organic carbon (C_{org}), CaCO_3 and C/N ratio in the surface sediments of the Bay of Bengal cores.	39
Table 4.3:	Concentration of major and trace elements in the surface sediments of the Bay of Bengal cores.	40
Table 4.4:	$^{87}\text{Sr}/^{86}\text{Sr}$ and ϵ_{Nd} in the silicate fraction of the surface sediments from the cores in the Bay of Bengal.	50
Table 5.1:	AMS ^{14}C dates of <i>foraminifer</i> shells from the Cores 4032 and 4040	58
Table 5.2:	Concentrations of Major and Trace elements in the bulk sediments of the core 4032.	62
Table 5.3:	Concentrations of Major and Trace elements in the bulk sediments of the core 4040.	65
Table 5.4:	Concentration of total carbon, organic carbon (C_{org}) and CaCO_3 along with C/N ratios in the core 4032.	71
Table 5.5:	Concentration of total carbon, organic carbon (C_{org}) and CaCO_3 along with C/N ratios in the core 4040.	75
Table 5.6:	$\delta^{13}\text{C}$ and $\delta^{15}\text{N}$ of the organic matter in the core 4032 from the Bay of Bengal.	77
Table 5.7:	$^{87}\text{Sr}/^{86}\text{Sr}$ and Sr concentration in the core 4032.	86
Table 5.8:	ϵ_{Nd} and Nd concentration in the core 4032 and 4040.	88

Chapter I



INTRODUCTION

The northern Indian Ocean comprises two major regions, the Arabian Sea and the Bay of Bengal. These two areas which adjoin the two sides of the Indian subcontinent play a dominant role in the climatic pattern of the region. The Southwest Summer Monsoon (SWSM) is one of the most intense systems that influence world climate. In the Indian subcontinent, SWSM is followed by a relatively weak, but nevertheless significant, North East Winter Monsoon (NEWM). These monsoon systems, so unique to this region, occur due to the combined air-sea interaction resulting in not only precipitation over the Indian subcontinent but also lead to significant changes in the sea surface temperature, salinity and biogeochemical cycles of the northern Indian Ocean.

The present investigation addresses two important issues of the northern Indian Ocean: (i) Upwelling rate in the Arabian Sea and (ii) Sediment provenance and climatic history of the Bay of Bengal since the last 50 kyr. The rationale for these objectives is based on the premise that the physical, biological and chemical environment of the Bay of Bengal is closely linked to the variation in the summer and winter monsoon. In the Arabian Sea, the summer monsoon winds induce strong upwelling resulting in enhanced productivity – a surrogate that can be used for reconstructing monsoon induced wind strength.

The Arabian Sea and the Bay of Bengal both experience seasonally reversing monsoon that induce a reversal of wind driven circulation of the surface waters. This results in upwelling along the western margin of both the regions viz. the Arabian Sea and the Bay of Bengal (Currie et al., 1973).

Although these basins experience similar circulation patterns, the upwelling in the Arabian Sea is more intense making it the most productive region of the world (Prasanna Kumar et al., 2002). As compared to this, the Bay of Bengal region experiences enhanced fresh water flux during the monsoon periods from the rivers draining into it leading to a stratification, with a lens of fresh water at the surface, that reduces the vertical mixing in the water column (Wyrski, 1971).

The studies of ocean water circulation has been investigated with the help of radiocarbon (^{14}C) as a tracer to follow pathways of carbon across various exchangeable carbon reservoirs (Broecker et al., 1985, 1995). During the late 1950s and early 1960s, considerable amount of ^{14}C was injected into the atmosphere by nuclear weapon tests thereby leading to increase in the atmospheric ^{14}C levels (Nydal and Lövseth, 1983; Broecker and Peng, 1994). This transient of bomb ^{14}C in the environment during early 1960s has been used as a tracer and provides an opportunity for studying ocean circulation in the upper part of the water column and exchange of CO_2 at the air-sea interface processes that normally take place on decadal time scales.

The Arabian Sea and the equatorial Indian Ocean regions are typically associated with high wind speeds due to the seasonally reversing monsoon and the associated wind induced upwelling. The upwelling areas associated with high productivity are expected to experience a higher than average exchange rate. To ascertain the temporal variation in the bomb ^{14}C distribution in the upper layers of the Arabian Sea and the equatorial Indian Ocean, a number of oceanographic expeditions onboard *FORV Sagar Sampada* were made between 1994 and 1999 for the collection of samples from the water column (Somayajulu et al., 1999; Bhushan et al., 2000, 2003; Dutta, 2001). It is also expected that an understanding of upwelling rates could provide better insight into the wind driven circulation in the ocean's upper layers. In view of this, the present study aimed at determining the upwelling rates at various locations in the Arabian Sea and the equatorial Indian Ocean,

based on temporal variation in the bomb ^{14}C distribution over the past two decades (Broecker et al., 1985, 1995; Bhushan et al., 2000). Towards this, vertical profiles of seawater samples from the various locations in the Arabian Sea were collected for analyses of radiocarbon, total dissolved CO_2 (ΣCO_2), nutrients and dissolved oxygen, along with other hydrographic parameters.

In the Arabian Sea and the Bay of Bengal, the denitrification layer in the subsurface waters varies between water depths of 200–1000 m. The sediment traps deployed in western, central and eastern parts of the deep northern Arabian Sea recorded strong seasonality in particle fluxes during the southwest and northeast monsoons (Ramaswamy et al., 1991; Ramaswamy and Nair, 1994). High primary productivity during the monsoons resulting from wind-induced mixed-layer deepening and the associated nutrient injection to the euphotic zone appeared to be the main factor controlling the observed particle flux pattern (Nair et al, 1989). This process had implications on the CO_2 uptake during glaciation when the wind speeds were higher. Further, the areas of high surface productivity and low bottom-water oxygen concentrations are caused by contribution of nutrients from the continental runoff. $\delta^{15}\text{N}$ analyses of sediment cores from areas with high accumulation rates off the Oman continental margin have shown millennial-scale variability in the Arabian Sea denitrification and productivity during the last glacial period. This would imply that $\delta^{15}\text{N}$ can be used as a proxy for reconstructing the monsoon driven wind strength in the past. Further, studies have shown that global marine productivity has been influenced by changes in denitrification and this could be related to climatic and atmospheric CO_2 oscillations as has been observed in the Antarctica ice cores during the past 20–60 kyr (Altabet et al., 2002).

In the Bay of Bengal, the boundary current shows a strong seasonal variability leading to a reversal of the local monsoon wind field by several months. This is attributed to the topography of the northern Bay and the

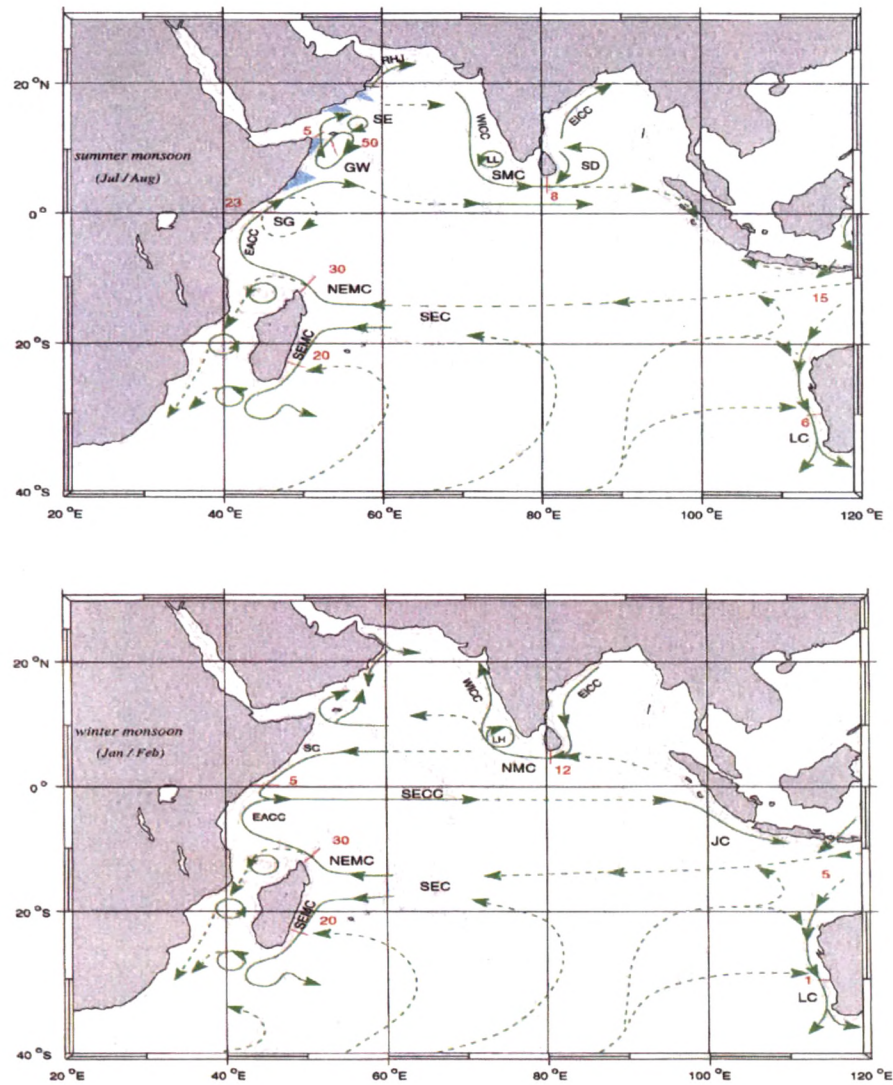


Fig. 1.1: Surface circulation pattern in the Bay of Bengal during summer and winter monsoon. Note, the reversal of East India Coastal Current (EICC) during the two seasons (after Schott and McCreary, 2001).

proximity of the Himalaya and the Tibetan Plateau (Kennett and Toumi, 2005). The total vorticity generation over the Himalayan region as a whole is at least half as that over the Bay of Bengal thus implying that the Himalayan

rainfall plays a central role in amplifying the circulation of the monsoon (Kennett and Toumi, 2005).

The Bay of Bengal is characterized by the East India Coastal Current (EICC) that reverses direction twice a year, flowing northeastward from February to September, with a strong peak in March–April, and southeastward from October to January with the peak flow in November (Shetye et al., 1996). During the Southwest monsoon, currents in the entire bay are weak. The EICC is a major system in the Bay of Bengal that not only influences the coastal productivity but also seems to have a strong bearing on the sediment dispersion pattern as is evident from the present study (Fig. 1.1, Schott and McCreary, 2001).

The Bay of Bengal is a natural repository of sediments brought in by the various river systems draining the Indian subcontinent. During the last few decades as a part of the ocean circulation studies, large number of sediment cores were collected from a wide geographical area in the Bay of Bengal. The sediment distribution in the Bay of Bengal is dominated by three sediment sources viz. the Ganga–Brahmaputra River system (henceforth G–B River system) in the north, the peninsular river system in the west and the Irrawaddy–Salween River system in the Andaman Sea to the east. About 30% of the sediment load of the G–B River system gets deposited in the shelf region, another 40% in the sub-aqueous delta, while the remainder 30% reaches the “*Swatch of No Ground*” (Goodbred and Kuel, 1999). In the case of the Irrawaddy, nearly 15% of the sediment load is deposited beyond the delta shelf (Rodolfo, 1969). The sedimentation rates in the central and southern Bay of Bengal ranges from 2–4 cm/kyr (Prell et al., 1980). The average accumulation rate in the Andaman Basin (15 cm/kyr) is higher than that in the Bay of Bengal (10 cm/kyr) (Frerichs, 1968; Sarin et al., 1979; Venkatchala et al., 1992).

The enormous fluvial input to the Bay during the South West Summer Monsoon (SWSM) is reflected in the high average content of lithogenic matter with a relative increase in the flux of biogenic opal. In addition, the high carbonate-dominated flux observed during SWSM and Northeast Winter Monsoon (NEWM) is mainly due to wind-induced nutrient supply, while the high opal-rich fluxes during SW-NE inter-monsoon is due to both upwelling as well as supply of riverine and shelf derived matter (Unger et al., 2003). In the northeastern part, the sediment flux is dominated by inputs from the G-B River system, while in the western part it is the peninsular rivers that drain regions of India that contribute largely to the sediment budget. The narrow margins along the coastal regions in the Bay of Bengal are dominated by sand, silt and clay with a large area covered only by clay (Rao, 1991; Rao and Kessarkar, 2001). In the G-B delta region, silt deposits occupy a wide area while west of the Andaman coast, silty-clay is the dominant material that occupies a very large area extending westwards almost to the central region of the Bay of Bengal (Kolla and Coumes, 1984). The transport of clastic material from the land to the deep sea results in turbidite sedimentation. Sediments brought by the G-B River system are deposited partly near the shelf and in the "*Swatch of No Ground*", a submarine canyon deeply incised into the shelf off Bangladesh. The "*Swatch of No Ground*" connects the present shelf depocenter to a channel-levee system. There is a general increase in foraminifera as well as unidentifiable calcareous fragments towards the central and southeastern parts of the Bay with a decrease in terrigenous material and insoluble matter (Siddiquie, 1967). The Bengal Fan, one of the world's largest submarine fan systems is formed by long-term input of riverine sediments moderated by glacio-eustatic sea-level fluctuations, climate change and tectonic activity (Flood et al., 1995).

The average annual particle flux to the Bay of Bengal is highest in the central Bay area ($\sim 50 \text{ g.m}^{-2}.\text{yr}^{-1}$) and lowest in the southern part of the Bay ($\sim 37 \text{ g.m}^{-2}.\text{yr}^{-1}$) and this coincides with the freshwater discharge pattern of the G-B River system (Ramaswamy and Nair, 1994). Based on the sediment

trap studies, it has been noticed that the southern Bay of Bengal (~1500 km away from major rivers) has the highest lithogenic flux as compared to western or eastern Arabian Sea areas located ~400 km away from landmasses and in areas known for high aeolian and fluvial input (Kolla et al., 1981; Nair et al., 1989; Ittekkot et al., 1991; Sirocko et al., 1991). Sarin et al. (1979) reported sedimentation rates of 2 to 40 mm/kyr during the Holocene in the Bay of Bengal which is comparable to the trap fluxes in the northern Bay of Bengal.

In terms of biogenic contribution to the surface sediments of the Bay of Bengal, carbonate constitutes a major component which acts as a dilutant for the terrigenous fluxes (Kolla et al., 1976). The sediment brought into the Bay of Bengal comprising varied mineralogical assemblages, due to complex provenances sources (lithology) and is dispersed as per the changing circulation patterns. For example, high quartz and low calcium carbonate percentages in the surface sediments of the Bay of Bengal adjacent to the Indian subcontinent result from the massive influx of terrigenous clastics. Mineralogy and heavy minerals assemblages in the surface sediments of the western margins of the Bengal Fan suggest that they have been derived from the peninsular Indian regions, whereas, the rest of the fan sediment have signatures of a Himalayan origin. The sediments on the Ninety East Ridge and in the deep southern areas beyond the reach of fan deposition result from the *in situ* alteration of volcanics (Kolla and Rao, 1990). The Ninety East Ridge acts as a barrier preventing the coalescence of two Bengal Fan lobes (Kolla and Biscaye, 1973).

The influence of continental inputs on the Bay of Bengal sediments is further illustrated by the Ti/Al and Fe/Al ratios. The higher ratios in samples from the east coast areas of India compared to the Bengal Fan sediments indicate the influence of material derived from the Deccan basalts and mafic rocks of the Indian Peninsula. The clay mineral assemblages of the upper Bengal Fan sediments show dominance of illite and chlorite suggesting a Himalayan source (Roonwal et al., 1997). It has been observed that the

distribution of Al and Fe give a representative picture of the nature of distribution of sediment in the Bay of Bengal. The Al content varies considerably (up to 9%) with the highest values (>6.5%) are found in the terrigenous sediments off the east coast of India, west of Burma, the Java Trench, in the pelagic sediments of the Wharton Basin, and in a few isolated patches in the Central Indian Basin. The above variation is attributed to the varying continental sources. Fe also shows considerable variation with the high values (>5.5%), found proximal to the Indian subcontinent and in some pelagic sediments of the Wharton and the Central Indian Basins. The concentration however decreases off the east coast of India towards the central Bay of Bengal (Wijayananda and Cronan, 1994).

One of the major components of the tropical climate system is the Indian summer monsoon, which results in a differential land-sea sensible heating, producing seasonal reversals in wind direction and intense rainfall. Clemens et al. (1991) suggested that variations of the summer monsoon intensity are mainly forced by the contrast in insolation between the northern and the southern hemispheres. In addition, recent investigations of deep-sea sediment cores of the Arabian Sea (Sirocko et al., 1993, 1996; Heusser and Sirocko, 1997; Schulz, et al., 1998) indicate that the intensity of the Indian monsoon has also experienced changes that are independent from insolation variations. It has been suggested that these rapid changes should be related to the high-amplitude climatic changes, observed in the $\delta^{18}\text{O}$ records of the Greenland ice core GRIP (GRIP member, 1993; Dansgaard et al., 1993) and GISP2 (Grootes et al., 1993; Stuiver et al., 1995) and in the North Atlantic sediment cores (Heinrich, 1988; Bond et al., 1992; Bender et al., 1994; Bond and Lotti, 1995), via an atmospheric and/or oceanic tele-connection (Zonneveld et al., 1997). On a regional scale, the Indian summer monsoon represents an important factor driving weathering and erosion of the Himalayan and Burmese mountain ranges. On geological time scales, changes in the strength of the summer monsoon rainfall are likely to affect the chemical and physical weathering intensity of the Ganges-Brahmaputra and the Irrawaddy

catchment and drainage areas. Sediments of the Bay of Bengal and the Andaman Sea thus provide a record of the variability of the intensity of erosion of the Himalayan and Burmese mountain ranges that in turn relate to palaeoclimatic and palaeoenvironmental variations that have affected the dynamics of the monsoon (Colin et al., 1998).

For example, using the magnetic grain size in the Bay of Bengal sediment core samples, Colin et al. (1998) have reconstructed a detailed record of monsoon variability during the last glacial period which they attributed to the rapid temperature variations in the northern latitude (Dansgaard-Oeschger cycles and Heinrich events). According to them, rapid cold events of the North Atlantic (Heinrich events) during the last glacial stages are characterized by a weaker summer monsoon rainfall over the Himalaya via an atmospheric tele-connection. During the Last Glacial Maximum (LGM), the high value and low gradient of $\delta^{18}\text{O}$ (Duplessy, 1982) has been interpreted as a decrease in the fresh water inflow from the Himalayas (Cullen, 1981). Based on SST and $\delta^{18}\text{O}$ record obtained from foraminifera, Chauhan (2003) suggested that between 20 and 15 kyr the Himalayas were extensively glaciated with a minimum fluvial discharge (until 15 kyr) reaching the Bay of Bengal. Rashid et al. (2007) have used the Mg/Ca and $\delta^{18}\text{O}$ data of the planktonic foraminifera from the Andaman Sea to reconstruct the SST and $\delta^{18}\text{O}$ of sea water during the last 25 kyr. According to them, SST was $\sim 3^\circ\text{C}$ lower during the LGM than the late Holocene. The study suggests decreased evaporation-precipitation in the Andaman Sea with increased outflow of the Irrawaddy River during LGM. The above studies indicate that in strategically selected core samples, geochemical and isotopic proxies can be used to reconstruct the climate (monsoon intensity) and provenance variability over long as well as short time scales.

In the present study, the surface sections of sediment cores from the Bay of Bengal were analysed to understand the sediment distribution and provenance. Two cores, that were radiocarbon dated using Accelerated Mass

Spectrometry (AMS) were analysed to reconstruct the Late Quaternary climatic history spanning the last 50 kyr using geochemical and isotopic parameters. A highlight of the present study is the successful use of $^{87}\text{Sr}/^{86}\text{Sr}$ ratio and ϵ_{Nd} in the sediment core that enabled the recognition of the summer and winter monsoon variability and also helped ascertain the spatial and temporal changes in sediment provenance.

Scope of the Present Study

The unique biogeochemistry of the Arabian Sea and the Bay of Bengal areas of the northern Indian Ocean and their typical hydrological and geographic characteristics require special attention as it provides a unique opportunity to understand upwelling processes and rates, sediment provenance and climate changes. Recognizing the importance of the region in its role in influencing climate, particularly the well known monsoon systems of the Indian subcontinent, this investigation was initiated for detailed studies on the water column in the Arabian Sea, the sediments of the Bay of Bengal and representative samples from the estuaries of major rivers draining into the Bay of Bengal.

The Arabian Sea is known for its high productivity due to the wind associated seasonally reversing monsoon system and upwelling of nutrient rich deep waters to the surface. To understand these processes, the air-sea CO_2 exchange rate and the upwelling rate in the Arabian Sea have been estimated from measurements in the water column and atmospheric samples using radiocarbon as a tracer for the following:

- Bomb ^{14}C inventory of the water column in the Arabian Sea,
- Atmospheric inventory of the ^{14}C ,
- Hydrological parameters in the water column at select depths,
- Nutrients, ΣCO_2 and Salinity in seawater,
- Pre-bomb concentrations of radiocarbon from archived shells.

To ascertain the provenance of sediments and to understand the climatic changes during the last 50 kyr in the region, various chemical and isotopic proxies were measured. Analyses of sediment cores distributed spatially in the Bay of Bengal included the following:

- Radiocarbon dating of cores based on select planktonic foraminifer species,
- Major and Trace element analysis on bulk sediments,
- CaCO_3 , Carbon and Nitrogen measurements on bulk sediments
- Carbon ($\delta^{13}\text{C}$) and Nitrogen ($\delta^{15}\text{N}$) isotopic composition of the organic matter in the sediments from the central Bay of Bengal core.
- $^{87}\text{Sr}/^{86}\text{Sr}$ and ϵ_{Nd} in the silicate fraction of the sediments from the central Bay of Bengal core.
- ϵ_{Nd} in the silicate fraction of the sediments from the southern Bay of Bengal core.

These analyses were done to understand:

- 1) Provenance of sediments in the Bay of Bengal,
- 2) Variations in detrital flux and surface productivity during the past 50 kyr,
- 3) Source variation of the sediment deposited in the central and southern Bay of Bengal during the last 50 kyr.
- 4) Climatic implications of the detrital and productivity variations.

The present investigation has been carried out as part of this doctoral dissertation and has been presented in six chapters as:

Chapter-I presents the general introduction to the above two mentioned themes and the rationale for undertaking this study. Also highlighted here are salient observations made by previous workers that are relevant to the objectives of this study.

Chapter-II describes the sample details, sampling procedures and measurement techniques employed for various analyses.

Chapter-III addresses the procedures followed for obtaining the upwelling rates in the Arabian Sea.

Chapter-IV pertains to the sediment distribution pattern and provenance in the Bay of Bengal.

Chapter-V discusses the history of the climatic variation during the past 50 kyr.

Chapter-VI summarizes the results and discusses the understanding developed in respect of the objectives outlined.

Chapter II

EXPERIMENTAL DETAILS

The northern Indian Ocean is an ideal repository of signatures that help us understand various biogeochemical processes operating in the region. The present study aims to address some of these issues that would help in determining upwelling rates in the Arabian Sea, the provenance of sediments being deposited in the Bay of Bengal and to trace the climatic and provenance changes during the past 40-50 kyr. Towards these objectives several vertical profiles of water samples and numerous sediment cores were collected during cruises in the Arabian Sea and the Bay of Bengal.

Sampling Procedures

Seawater sampling

Several depth profiles were occupied in the Arabian Sea during three ocean expeditions in 1994, 1995 and 1997 onboard *FORV Sagar Sampada*,

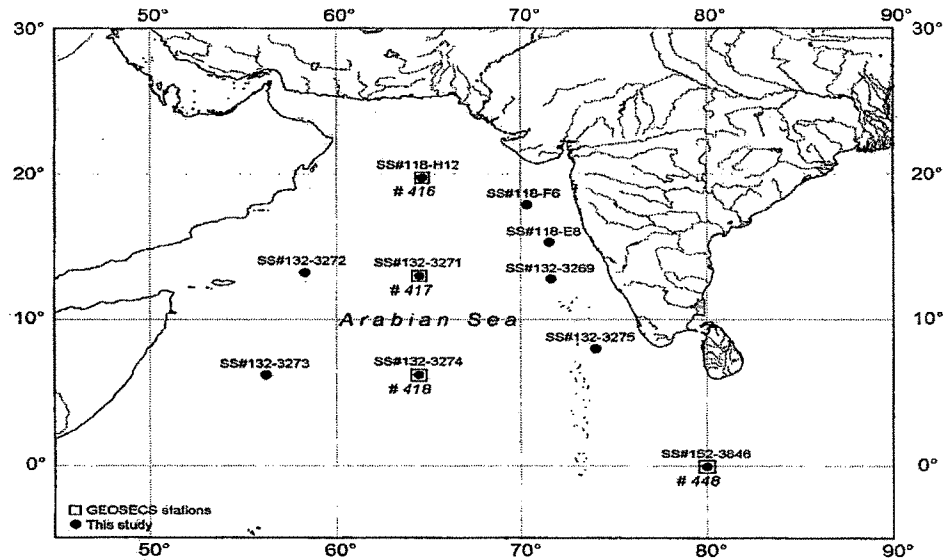


Fig. 2.1: Water Sampling locations in the Arabian Sea and the Equatorial Indian Ocean. GEOSECS station numbers are given after '#'. The boxed filled circles are the reoccupied GEOSECS stations.

oceanographic research vessel belonging to Ministry of Earth Sciences (MOES, earlier Department of Ocean Development (DOD), Government of India) for the collection of seawater at various depths. For the present study, a total of ten sampling stations in the Arabian Sea and one in the equatorial Indian Ocean were identified (Fig. 2.1). For ^{14}C analysis, about ten samples were collected per profile from pre-selected depths, except in the equatorial Indian Ocean station where samples from twenty depths were collected. Nearly 120 lit. of seawater samples were collected from each depth for onboard measurements (laboratory analysis) and processing for various parameters (Narvekar et al., 1997).

Sediment Sampling

Seventeen sediment core samples from the Bay of Bengal were used in the present study (Fig. 2.2). Only the top sections of the cores were analyzed for their chemical and isotopic composition to ascertain their source (provenance). In addition, numerous grab samples from the deltaic regions of rivers draining into the Bay of Bengal were analyzed to understand the source of the sediments.

Onboard Processing and Measurements

Seawater Measurements

For seawater sampling, 100 lit. Go-Flo bottles with the hydrographic wire were used at various depths at each station. The

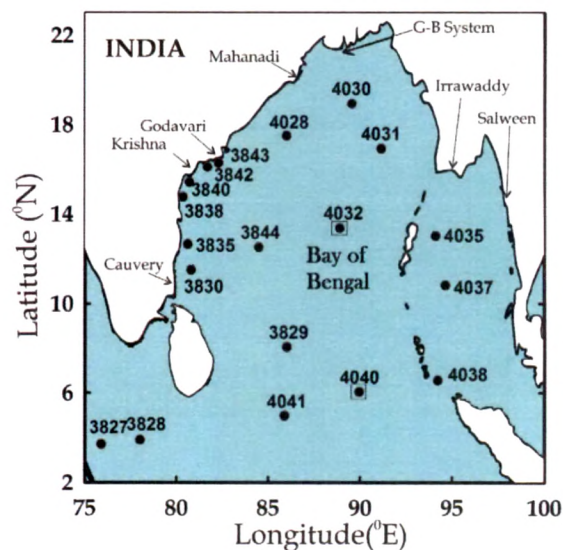


Fig. 2.2: Locations of sediment core samples collected in the Bay of Bengal. Boxed filled circles are the cores studied in detail

seawater collected was immediately sub-sampled for dissolved oxygen measurements, dissolved inorganic carbon (ΣCO_2), nutrients (silicate, phosphate and nitrate), salinity and radiocarbon. About 125 ml of the seawater sample was used for dissolved oxygen (measurements done on duplicate samples), 60 ml of the seawater sample was used for ΣCO_2 , 500 ml for nutrients, 200 ml for salinity and ~100 l for radiocarbon measurements.

Dissolved Oxygen Measurement

Immediately upon collection of the seawater samples in the BOD bottles, Winkler A and Winkler B were added to the sample to estimate the dissolved oxygen content using the modified Winkler titration method (Carpenter, 1965). The bottles were tightly capped and agitated vigorously. They were agitated again after 30 min and then stored in a dark place for ~8-16 hrs. After this, 0.5 ml of conc. H_2SO_4 was added to liberate iodine. This iodine was titrated with 0.2 N sodium thiosulfate solution by a *Metrohm 655 Dosimat* auto-titrator to the end point using starch as an indicator. Based on repeat analysis of samples, the precision for dissolved oxygen by Winkler titration was $\pm 2 \mu\text{mol kg}^{-1}$ (1σ).

Estimation of Dissolved Inorganic Carbon (ΣCO_2)

Seawater samples were collected in a 60 ml ground joint bottle and immediately upon collection, two drops of saturated solution of mercuric chloride was added to inhibit organic growth. The sample bottle was capped tight using non-carbon silicone grease and then stored in a refrigerator till analysis. The total dissolved inorganic carbon (ΣCO_2) of seawater is defined as the total molar concentrations of all species of inorganic carbon present in dissolved phase, and is given by,

$$\Sigma\text{CO}_2 = [\text{CO}_2^*] + [\text{HCO}_3^-] + [\text{CO}_3^{2-}]$$

where bracket represent total concentrations of these constituents in solution (in mol.kg^{-1}) and $[\text{CO}_2^*]$ represents the total concentration of all un-ionized dissolved carbon dioxide (as H_2CO_3 or CO_2). The ΣCO_2 in the seawater

samples were determined by coulometric method, following the procedures as outlined by Johnson *et al.* (1985) and given in D.O.E. handbook (1994).

ΣCO_2 was measured in a small aliquot of seawater either onboard the ship or in the laboratory. In the latter case, the samples were poisoned with HgCl_2 and refrigerated till the time of measurement. ΣCO_2 measurements were carried out using a Coulometer (model 5012, UIC Inc., Joliet, Illinois). Based on repeat analyses, typical precision of ΣCO_2 measurements was $\pm 3 \mu\text{mol.kg}^{-1}$ (1σ). The accuracy of ΣCO_2 measurements was checked from analyses of certified reference seawater samples (Batch#42, December, 1997), supplied by Prof. Andrew G. Dickson of the Scripps Institute of Oceanography, USA. The mean ΣCO_2 measured during this study for this standard seawater is $1983.2 \pm 2.3 \mu\text{mol.kg}^{-1}$ (1σ , $n=20$), and is in good agreement with its certified value of $1985.1 \pm 0.8 \mu\text{mol.kg}^{-1}$ (Dutta, 2001).

Nutrient Measurements

The nutrients measurements for silicate, nitrate and phosphate were done onboard using a *Technicon Auto-Analyzer* (Gordon et al., 1993). The precision ($\pm 1\sigma$) of measurement for silicate, total nitrate and phosphate based on repeat measurements of seawater samples were $< 2\%$ respectively for all the parameters. Accuracies of silicate and nitrate measurements were about $\pm 5\%$, as checked by analyzing CSK standard solutions (Wako Chemical Industries Ltd., Japan).

Salinity Measurement

The seawater samples were brought to room temperature before the salinity measurement. The salinity of the seawater samples was determined using a *Guildline AutoSal Model 8400A* salinometer. The instrument determines the conductivity ratio (K_{15}) of a sample to that of a potassium chloride (KCl) solution containing 32.4356 g of KCl in 1 kg of solution (Standard Seawater). The software SEACALC was used to calculate salinity from *Autosal* values. The salinometer was calibrated using IAPSO standard seawater. The precision

of salinity measurements by *Autosal* was typically ± 0.0005 PSU, based on repeat measurements of seawater samples. The CTD salinity values were calibrated using the values measured by *Autosal*.

Extraction of DIC from Seawater for Radiocarbon Measurement

Nearly 100 l of seawater sample was collected and transferred immediately to a closed circulation system. For CO₂ extraction from seawater, 2N NaOH solution was kept in series with the circulation line along with a 5% HCl solution used as a gas scrubber. The system was connected and a continuous closed system circulation maintained using a *Cole-Parmer* peristaltic pump. Nearly 1 l of H₂SO₄ acid was added slowly through separating funnels to the seawater to extract DIC from seawater. The system was kept in circulation for nearly 8-10 hours to ensure quantitative extraction of CO₂ from the seawater. The extracted CO₂ was trapped in NaOH solution and brought back to the laboratory for analysis. Details of ¹⁴C analysis methods in seawater samples followed in this study are described in Bhushan et al. (1994), (2000) and Dutta (2001).

Measurement Procedures

¹⁴C measurements in Seawater

Briefly, CO₂ was extracted onboard by acidifying ~100 l of seawater in a closed circulation system trapped in aqueous NaOH solution. In the laboratory, CO₂ was liberated from the alkaline solution upon acidification under vacuum and converted to benzene through formation of Li₂C₂ and C₂H₂, and finally assayed for its ¹⁴C activity using low level Liquid Scintillation Spectrometer. For atmospheric ¹⁴C analysis, CO₂ was trapped from the air of marine boundary layer by pumping air through NaOH during the cruises using a greaseless pump and assayed for ¹⁴C as above. A small aliquot of this CO₂ was used for $\delta^{13}\text{C}$ measurements, and the remaining converted to benzene in a Technical and Applied Scientific Knowledge Inc. (TASK) (Athens, Georgia) synthesizer. The benzene was assayed for its radiocarbon activity using a tricarb packard low background liquid

scintillation counter (model 2250CA, Packard Instruments Co., Meriden, Connecticut). The counter was calibrated using benzene extracted from NBS Oxalic acid standard (Standard Reference Material 4990-C). Marble blanks were run periodically to check the background and blank levels (Bhushan et al., 1994). Based on repeat analysis of modern standards, typical precision for $\Delta^{14}\text{C}$ measurements was $\pm 5\%$.

$\delta^{13}\text{C}$ measurements of CO_2

The $\delta^{13}\text{C}$ measurements were done on about half of the ^{14}C samples using a VG 602D micromass mass spectrometer on a small aliquot of CO_2 liberated in the laboratory during the acidification of NaOH solution containing seawater CO_2 (precision $\pm 0.1\%$). $\delta^{13}\text{C}$ was measured in an aliquot of CO_2 used for benzene synthesis for isotopic fractionation correction of the ^{14}C results and determination of $\Delta^{14}\text{C}$ (Stuiver and Polach, 1977).

Sediment Measurements

AMS Radiocarbon dating

For radiocarbon dating using AMS, nearly 10-15 mg of Planktonic Foraminifera shells of select surface dwelling species (*Globigerina Ruber*, *Globigerina Sacculifer* etc) were extracted from the sediments through wet sieving and physical picking under a microscope. These shells were acidified to liberate CO_2 and this CO_2 was converted to graphite for AMS measurement. The AMS measurements were done at NSF Facility of AMS at University of Arizona, Tucson, USA using a 10 Mev pelletron accelerator connected to a mass spectrometer.

CaCO_3 Estimation

The CaCO_3 measurements in the sediments were carried out using UIC Coulometer Model 5012 (UIC Inc., Illinois, USA) attached to a CO_2 extraction system. Nearly 10-20 mg of the dried sediment sample was taken in the reaction vessel of the extraction system kept at 80°C . Nearly 3-4 ml of 30% H_3PO_4 was added to the sample and the evolved CO_2 was purged from the

extraction system using CO₂ free zero air to the Coulometer. The evolved CO₂ was purged in a monoethanolamine solution in the Coulometer. A three point calibration curve was made using Na₂CO₃ as standard. The measurement precision was 3% based on repeat measurements (Bhushan et al., 2000).

Organic Carbon (C_{org}) Determination

The C_{org} in the samples was estimated based on the difference between the measured total carbon and inorganic carbon. The total carbon along with nitrogen was measured by FISONs NA1500 NC Elemental Analyser (FISONs Inc., Italy) and the inorganic carbon by UIC Coulometer Model 5012 (UIC Inc., Illinois, USA). For the estimation of total carbon and nitrogen using NC elemental analyser, the sediment samples were introduced in small aliquots of 10-30 mg in tin or aluminum cups through an auto-sampler into the combustion tube of the analyzer. The calibration was done using Deer River Black as standard reference material containing 2.53% C and 0.12% N. The average blank concentration measured over a period of about 200 days is 1.31±0.12 µg C. The measurement precision for total carbon is 4% estimated by repeat analysis of Deer River Black Shale over several weeks. The measurement precision in the case of total nitrogen concentrations > 0.1% is 8% (Bhushan et al., 2001).

δ¹³C and δ¹⁵N of Organic Matter

For the measurement of δ¹³C and δ¹⁵N in the organic matter, sediment samples were decarbonated with 0.5M HCl and rinsed with distilled water. The decarbonated samples were sealed in a quartz tube under vacuum along with CuO, silver fillings and O₂ free high purity Cu wire. After evacuation, sealed tubes were heated at 850°C for nearly 8-10 hours. The evolved CO₂ and N₂ were cryogenically separated and further purified by passing it through a U-tube containing Cu wire at 650°C and collected in a sample-bottle containing molecular sieve. The purified CO₂ fraction was purified for moisture using a cold trap (-90°C) and analyzed for ¹³C/¹²C ratio using a GEO-2020 mass spectrometer. N₂ was analysed for isotopic ratio on a VG 903

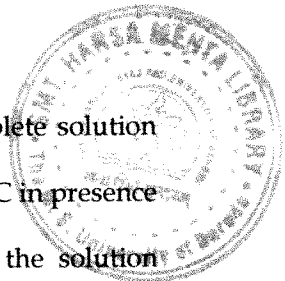
mass spectrometer. Accuracy and precision of the isotopic data were checked using international standard (IAEA-N₂) and replicate analyses of laboratory standard (UBC-ACE; Acetanilide) obtained from the University of British Columbia (Agnihotri, 2001). Carbon and nitrogen isotopic ratios of sedimentary organic matter are expressed as δ values ($\delta^{13}\text{C}_{\text{org}}$ and $\delta^{15}\text{N}$) with reference to V-PDB and atmospheric N₂, respectively. The uncertainties in $\delta^{13}\text{C}_{\text{org}}$ and $\delta^{15}\text{N}$ determinations are $\sim 0.2\text{‰}$ and 0.3‰ , respectively (Agnihotri, 2001).

Major and Trace Elemental Analyses

For major and trace element analyses, the sediment samples were dried and thoroughly homogenized. The samples were digested following conventional HF-HClO₄-HNO₃-HCl procedure and brought to solution in 1M HCl medium. The samples were suitably diluted for the elemental measurements using an ICP-AES (Jobin-Yvon, Model 38S). The USGS rock standards W-2 and MAG-1 were analyzed to check accuracy and precision of the elemental analyses of sediment samples. Among them, MAG-1 (marine mud) was analyzed extensively in this work as it closely matches with the matrix of sediment samples. In addition, an internal laboratory standard NOVA was prepared and standardized during the analyses of sediment samples. NOVA is a deep-sea clay sediment collected from the North Pacific (NOVA III -13; 3° 55.6' N, 178° 47.3' W) at water depth of 5351 m (Amin et al., 1972). Based on repeat measurements of various check standards, the coefficient of variation was about 2% for major elements and ranged from 3-5% for trace elements (Agnihotri, 2001).

Strontium (Sr) and Neodymium (Nd) Isotopic Measurements

To determine the Sr and Nd isotopic values of the silicate fraction of the sediments, ~ 1 g samples were decarbonated by leaching it with 0.6M HCl at 80°C with intermittent ultrasonification to remove the carbonate fractions. Further, the samples were heated at 550°C in a furnace to remove the organic material. About 100 mg of the carbonate and organic matter free



sediments were transferred to teflon vials and brought to complete solution using ultra-pure HF and HNO₃ (Seastar Chemicals) at ~ 130-140°C in presence of ⁸⁴Sr and ¹⁵⁰Nd tracers. Sr and REEs were separated from the solution following standard ion exchange procedure (Pati and Singh, 2007; Singh et al. 2008). From the REE fraction, Nd was separated using HDEHP coated Teflon powder. Sr and Nd concentrations and their ⁸⁷Sr/⁸⁶Sr and ¹⁴³Nd/¹⁴⁴Nd were measured on an Isoprobe-T Thermal Ionization Mass Spectrometer in static multi-collection mode. Mass fractionation corrections for Sr and Nd were made by normalizing ⁸⁶Sr/⁸⁸Sr to 0.1194 and ¹⁴⁶Nd/¹⁴⁴Nd to 0.7219 respectively. During the course of analyses, SRM987 Sr and JNdi Nd standards were repeatedly measured, these yielded values of 0.710233±0.000012 (1σ, n = 48) for ⁸⁶Sr/⁸⁸Sr and 0.512106±0.000006 (1σ, n = 7) for ¹⁴³Nd/¹⁴⁴Nd respectively, well within the recommended values. Several Sr and Nd total procedural blanks were measured along with the samples; typical blank for Sr was ~1.6 ng whereas for Nd it was ~300 pg. These blanks are several orders of magnitude lower than the typical total Sr (~7 mg) and Nd (~2 mg) loads analyzed and hence no corrections for blanks were made. Few duplicate samples were processed to check the reproducibility of results.

Chapter III

ESTIMATES OF UPWELLING RATES IN THE ARABIAN SEA

The Arabian Sea, a part of the northern Indian Ocean regime, is known for its seasonally reversing summer and winter monsoonal wind patterns and associated upwelling and convective mixing (Wyrski, 1971, 1973; Shetye et al., 1994). These processes result in the well-known seasonal oscillation in the biological productivity of these waters (Qasim, 1977, 1982; Lal, 1994; Krishnaswami and Nair, 1996). The upwelling and biological productivity is expected to influence the air-sea exchange of CO₂ and its budget in the atmosphere. A large body of its intermediate water (~200-1000 m) remains suboxic throughout the year, and there is perennial denitrification (Naqvi, 1991). Detailed measurements of various chemical and biological parameters have been made in the Arabian Sea to determine air-sea exchange fluxes of CO₂ during the Indian Joint Global Ocean Flux Study (George et al., 1994; Krishnaswami and Nair, 1996; Sarma et al., 1998).

The phenomenon of upwelling in the Indian Ocean is unique with an absence of equatorial upwelling unlike in the Pacific and the Atlantic Ocean. This is because the Southeast Trades do not cross the equator preventing equatorial divergence responsible for upwelling (Schott and McCreary, 2001). The upwelling in the Indian Ocean is confined to coastal areas north of the equator. This upwelling leads to an upward migration of deep (greater than 50 m), cool, nutrient rich ¹⁴C depleted waters to the surface resulting in enhanced productivity.

Radiocarbon (^{14}C) is a useful tracer, for studies of ocean circulation and pathways of carbon across various exchangeable carbon reservoirs (Broecker et al., 1985). Cosmic ray produced ^{14}C in the atmosphere is now an established geochronometer and is used widely for various archeological and geological date estimation. The atmospheric ^{14}C levels nearly doubled due to injection of considerable amounts of ^{14}C in the environment by nuclear weapon tests conducted during the late 1950s and early 1960s (Nydal and Lovseth, 1983;

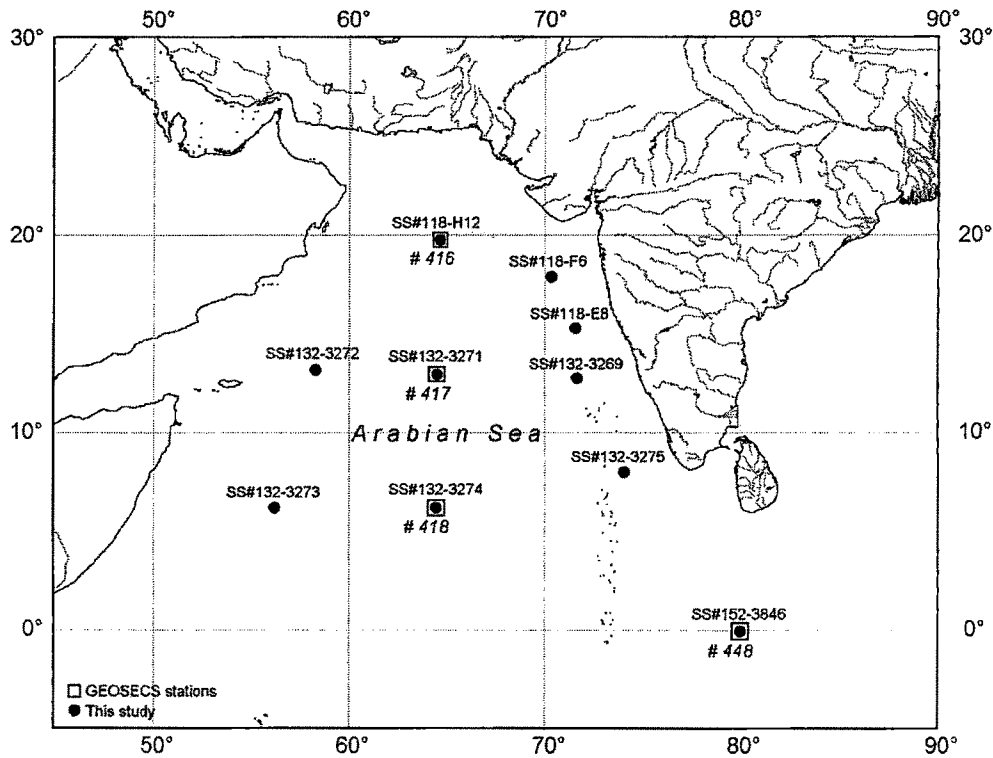


Fig. 3.1: Location of sampling stations in the Arabian Sea. The boxed filled circles are the GEOSECS stations occupied during this study almost after two decades

Broecker and Peng, 1994). This transient of bomb ^{14}C in the environment during early 1960s gave an opportunity to study circulation pattern in the upper water column of oceans and the exchange of CO_2 at the air-sea interface—processes that take place in decadal time scales (Lassey et al., 1990). The earliest ^{14}C measurements in the water column of the Arabian Sea and Indian Ocean were made between 1977-'78, as part of the GEOSECS expedition (Stuiver and Ostlund, 1983).

Several stations in the Arabian Sea and the equatorial Indian ocean were occupied for sampling the water column during the 1994 to 1995 period in various cruises onboard FORV *Sagar Sampada* (Fig. 3.1). Nearly ten samples per profile, from pre-selected depths were collected for ^{14}C analysis. Onboard measurements of nutrients, dissolved inorganic carbon (ΣCO_2) as well as processing for ^{14}C analysis were done on these samples.

Determination of bomb ^{14}C inventory and air-sea CO_2 exchange rates

Knowledge of the inventory of bomb ^{14}C in the sea and its distribution provides useful information on the ventilation in the upper ocean and the air-sea exchange of CO_2 . ^{14}C that has been measured in the water column since the mid-1950s is made of two components, natural (i.e., cosmic ray-produced) and that injected via bomb tests (bomb ^{14}C). Thus, to obtain the inventory of bomb ^{14}C from the measured ^{14}C activity in these waters, accounting for contributions from natural ^{14}C is necessary. Data on pre-bomb ^{14}C profiles in seawater, particularly in the Indian Ocean, are sparse, and hence indirect approaches have been used to derive these profiles in the upper ocean areas using suitable proxies.

To obtain the pre-bomb ^{14}C distribution in the thermocline, various methods have been used. The first method proposed by Broecker et al. (1985) relies on the use of $\Delta^{14}\text{C}$ values of surface waters measured prior to nuclear weapon tests and an estimate made for the penetration depth of bomb ^{14}C based on the vertical distribution of ^3H introduced in the ocean via weapon tests. Available data on ^{14}C in surface waters sampled before 1957 and on corals and shells deposited prior to nuclear weapon tests have been used as pre-bomb $\Delta^{14}\text{C}$ values for surface seawater. There are no measurements of ^{14}C in the Arabian Sea waters prior to the weapon tests. The only available data for pre-bomb ^{14}C in the region are from the measurements of corals in the Gulf of Kutch; 22.6°N, 70°E, a coastal region in the northeastern Arabian Sea (Chakraborty, 1993). The $\Delta^{14}\text{C}$ in a coral sample formed during the 2 year

period between 1949 and 1951, is $-60 \pm 5\%$ (this measurement was made by homogenizing the coral sample deposited during the 2 year period). This, however, compares well with the values of -60 to -65% used by Broecker et al. (1985) in their model for calculating bomb ^{14}C inventory in the Indian Ocean. In this work, a value of -60 to -65% has been used for pre-bomb Arabian Sea surface water $\Delta^{14}\text{C}$. During GEOSECS, ^3H (tritium) measurements were made to determine the penetration depth of bomb ^{14}C (Ostlund et al., 1980; Stuiver, 1980; Broecker et al., 1985). In this study, however, tritium could not be measured as its concentration in water has decreased significantly since the GEOSECS through radioactive decay ($t_{1/2}=12.3$ years) and by mixing during the intervening ~ 2 decades. The bomb ^{14}C inventory in stations H-12, 3271, and 3274 (reoccupation of GEOSECS 416, 417, and 418 respectively) were, however, calculated using the pre-bomb ^{14}C profiles simulated using the GEOSECS tritium data.

In the second method, Broecker et al. (1995) and Peng et al. (1998) have used the correlation between $\Delta^{14}\text{C}$ and dissolved silica in waters deeper than 1000 m (waters devoid of ^3H) to derive pre-bomb ^{14}C profiles in the thermocline. In this study, pre-bomb ^{14}C profiles were simulated using the silica analogy ($\Delta^{14}\text{C} = -70 - \text{SiO}_2$ ($\mu\text{M kg}^{-1}$) (Broecker et al., 1985) using GEOSECS silica data and forcing the surface water $\Delta^{14}\text{C}$ to be in the range of -60 to -65% , as determined from pre-bomb coral samples from the Gulf of Kutch. These profiles form the basis to estimate the bomb ^{14}C component from the measured ^{14}C profiles (regression analysis of SiO_2 versus $\Delta^{14}\text{C}$ data from the Arabian Sea and the Bay of Bengal waters collected during GEOSECS having $\text{SiO}_2 > 50 \mu\text{M kg}^{-1}$) yield a relation of $\Delta^{14}\text{C} = -80 - 0.83\text{SiO}_2$ ($\mu\text{M kg}^{-1}$). The pre-bomb $\Delta^{14}\text{C}$ profiles based on this relation and those derived using Broecker et al. (1995) method are consistent within $\pm 10\%$. Considering this, the Broecker et al. (1995) relation has been used as its intercept is closer to the measured $\Delta^{14}\text{C}$ in pre-bomb corals. In addition, the bomb ^{14}C inventories for these two stations were calculated based on pre-

bomb ^{14}C profiles derived from all the GEOSECS stations in the Arabian Sea (GEOSECS stations 413, 416, 417, 418, and 419). The results show that all the inventories calculated are within $\pm 10\%$. This comparison suggests that the uncertainties introduced in the calculation of bomb ^{14}C inventories, by assuming that pre-bomb ^{14}C profiles in stations from the same latitudinal belt are the same, is unlikely to be more than $\pm 10\%$.

The surface $\Delta^{14}\text{C}$ values, however, show a decrease in 1994–1995 values as compared to 1977–1978. This decrease can be attributed to a cumulative effect of low bomb ^{14}C input from the atmosphere and the vertical mixing in the upper water column. Rhein et al. (1997) observed that the penetration depth of CFC, another transient tracer introduced into the environment predominantly during mid 1900s is ~ 1000 – 1200 m in the Arabian Sea. The mean depth of bomb ^{14}C distribution (Z) (Broecker et al., 1985) in the present study ranged from 218 to 387 m. (In this discussion, Z , the mean depth of the bomb ^{14}C distribution, does not refer to the depth at which bomb ^{14}C can be detected; see Broecker et al. (1985) and the discussion below). The penetration depths of bomb ^{14}C (the depths to which bomb ^{14}C is discernible) as seen from the plots of $\Delta^{14}\text{C}$ versus depth is in the range of 800–1000 m (Fig. 3.2). At the GEOSECS stations 416, 417, and 418, Z increased by ~ 15 – 45% averaging $\sim 25\%$ over ~ 2 decades, from 1977 to 1995.

The bomb ^{14}C inventory is calculated using the relation

$$\Sigma^{14}\text{C} = K [Z \times \Sigma\text{CO}_2 \times (\Delta^{14}\text{C} - \Delta^{14}\text{C}^0)] \quad (1)$$

where, $\Sigma^{14}\text{C}$ = Bomb ^{14}C inventory in atoms cm^{-2} ;

ΣCO_2 = mean ΣCO_2 of the water column containing
bomb ^{14}C ($\mu\text{M kg}^{-1}$);

$$\Delta^{14}\text{C} = \delta^{14}\text{C} - 2(\delta^{13}\text{C} + 25) (1 + \delta^{14}\text{C}/1000)$$

(Stuiver and Polach, 1977);

Z = mean depth of bomb ^{14}C penetration (meters);

$\Delta^{14}\text{C}^0$ = pre-bomb surface water $\Delta^{14}\text{C}$ (-60 to -65‰);

$$= \frac{\text{Area}}{(\Delta^{14}\text{C} - \Delta^{14}\text{C}^o)}$$

Area = area under the curve between measured and pre-bomb ^{14}C profiles;

K is proportionality constant including various conversion factors (such as density, Avogadro's number, and $^{14}\text{C}/\text{C}$ abundance ratio).

Details of exchange rates calculations described by Bhushan et al. (2000) have been revised in this study, following Dutta (2001).

^{14}C concentration in the upper 1000 m of the ocean is a mixture of natural and bomb components. Its measurements in the water column represents sum of the ^{14}C contributions from these two sources but to delineate the bomb ^{14}C component, it is necessary to have precise estimates of pre-bomb ^{14}C activity (i.e. natural ^{14}C)

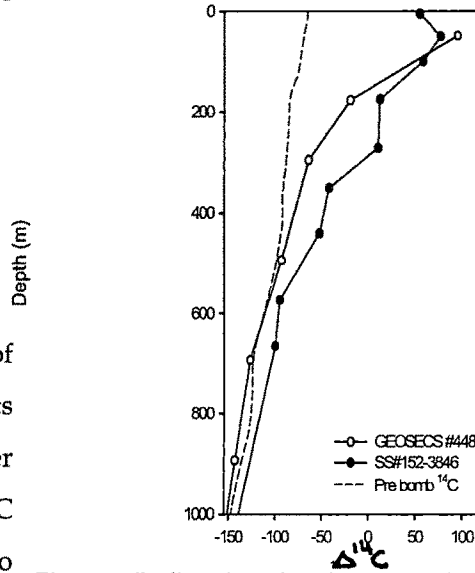


Fig. 3.2: Radiocarbon distribution in the upper 1000 m water column at the equatorial Indian Ocean station 3846. Also, shown the ^{14}C profile of GEOSECS for the station occupied during 1978. Dashed line is the pre-bomb ^{14}C simulated curve.

in these waters. This requirement, however, is not fulfilled in several areas of the ocean including the Arabian Sea and Bay of Bengal as no measurements of ^{14}C were made in these areas during early 1950s. Therefore, indirect approaches based on the distribution of their proxies are used to derive the pre-bomb ^{14}C profile in the upper ocean. Based on bomb ^{14}C inventories, the air-sea CO_2 exchange rates (E) were calculated using the model of Stuiver (1980). The exchange rates are calculated assuming that the observed inventory of bomb ^{14}C is only due to the integrated gradient of ^{14}C between the atmosphere and oceanic mixed layer, with no lateral transport of ^{14}C . The

values of the integrals for $\Delta^{14}\text{C}_{\text{atm}}$ and $\Delta^{14}\text{C}_{\text{mix}}$ are obtained from ^{14}C measurements in the atmosphere and from corals respectively (Chakraborty et al., 1994). The input function of atmospheric ^{14}C used here is based on a model curve, constrained by atmospheric ^{14}C measurements at Israel, Ethiopia and Madagascar between 1963 and 1978 (Nydal and Lovseth, 1983, 1996), tree-ring ^{14}C measurements at Thane, India, near the Arabian Sea coast (Chakraborty et al., 1994), and atmospheric ^{14}C measurements over the Northern Indian Ocean between 1993 and 1997 (Bhushan et al., 1997; Dutta et

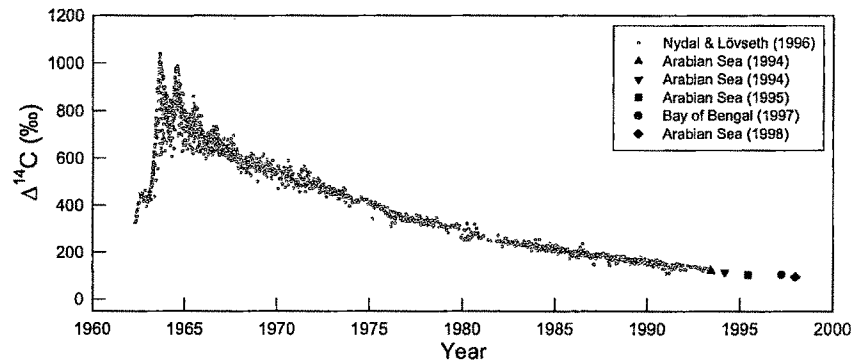


Fig. 3.3 Model $\Delta^{14}\text{C}$ of tropospheric CO_2 for the atmosphere over the Northern Indian Ocean used in the upwelling calculation (thick gray line). Tropospheric $\Delta^{14}\text{C}$ of Northern Hemisphere Zone 3 (Hua and Barbetti, 2004) is shown as thin line. Tropospheric $\Delta^{14}\text{C}$ values measured over the Arabian Sea during 1993-'95 and over the Bay of Bengal during 1997 (Dutta et al., 2006) are shown as filled circles.

al., 2006). The model atmospheric ^{14}C curve rose from 0‰ in 1954, peaking at 730‰ in 1964, and reducing to 570‰ in 1968. From 1968 onwards, an exponentially decreasing atmospheric $\Delta^{14}\text{C}$ trend with an e-folding time (removal time scale of ^{14}C from the atmosphere) of 17 years has been calculated fixing the $\Delta^{14}\text{C}$ for the years 1980 and 1999 at 265‰ and 88‰ respectively. The model atmospheric ^{14}C function is shown in Fig. 3.3, where it is compared with atmospheric ^{14}C compilations as made by Hua and Barbetti (2004) corresponding to the latitudes of the Arabian Sea and the north of equatorial Indian Ocean ("Northern Hemisphere Zone 3"). The integrated

values of atmospheric ^{14}C between 1954 and 1997 of these two curves differ by about 1%, which is not significant as compared to other uncertainties. The overall uncertainty for air-sea CO_2 exchange rates from bomb ^{14}C profiles is about $\pm 15\%$.

Determination of upwelling rates using 1-D model

In this study, upwelling rates are calculated based on the CO_2 exchange rates using a one dimensional (1-D) box diffusion model (Oeschger et al., 1975; Broecker et al., 1978). For this model calculation, the upper 1000 m of the water column is subdivided into 40 boxes, each 25 m thickness with the assumption that ^{14}C concentration within each of these boxes is homogeneous and that the top 100 m is well mixed. The model simulates the bomb ^{14}C depth profile with the defined CO_2 exchange rate (E), upwelling rate (w) and the vertical eddy diffusivity (K) for a given input function of bomb ^{14}C from atmosphere to the ocean surface layer. The same atmospheric ^{14}C input function is used as described in the previous section. The vertical eddy diffusivity (K) and the upwelling rate (w) were varied to generate ^{14}C depth profiles and the values that provided the best fit to the observed bomb ^{14}C profile were chosen as the mixing parameters for the station location. The best fit values of K range from 0.4 to 0.7 $\text{cm}^2 \text{ sec}^{-1}$. In this study, the CO_2 exchange rates (E), as calculated earlier from bomb ^{14}C inventories for each station, have been used (Bhushan et al., 2000; Dutta 2001). However, for some stations, different exchange rates were used to obtain the best fit to observed bomb ^{14}C profiles.

Bomb ^{14}C inventory and air-sea CO_2 exchange rates

The bomb ^{14}C inventory in the Arabian Sea as estimated in this study ranges between $3\text{--}8 \times 10^9$ atoms cm^{-2} (Table 3.1). A relatively large bomb ^{14}C inventory of 8.0×10^9 atoms cm^{-2} was obtained at SS#132-3273 and at the equatorial Indian Ocean station SS#152-3846, the inventory has been 9.5×10^9 atoms cm^{-2} . Lower inventories at other locations in the northern Indian Ocean could have resulted either because of weak diffusive gas exchange leading to

low ^{14}C input or processes favouring vertical penetration (viz. wind speed) which, however, are not vigorous. It is known that on an average the wind speed over the Arabian Sea is $\sim 5 \text{ m s}^{-1}$ (Esbensen and Kushnir, 1981), which is less than the global average value.

Table 3.1: Upwelling rates based on bomb ^{14}C inventory for the Arabian Sea and the Equatorial Indian Ocean stations

Station	Location	Sampling date	Bomb ^{14}C Inventory $\times 10^9$ (atoms cm^{-2})	Air-sea CO_2 Exchange Rate (E) (mol $\text{m}^{-2} \text{yr}^{-1}$)	Eddy diffusivity (K) ($\text{cm}^2 \text{sec}^{-1}$)	Upwelling velocity (w) (m yr^{-1})
<i>Arabian Sea</i>						
SS#118-H-12	19.8°N; 64.6°E	Mar 1994	5.9	12.6	0.7	5
GEOSECS #416	-do-	Dec 1977	6.3	15.4	0.7	7
SS#118-F-6	17.9°N ; 70.3°E	Mar 1994	5.2	11.1	0.7	3
SS#118-E-8	15.3°N ; 71.5°E	Mar 1994	3.5	7.5	0.5	5
SS#132-3272	13.2°N ; 58.3°E	May 1995	6.4	13.7	0.5	4
SS#132-3271	13°N ; 64.5°E	Apr 1995	6.9	14.8	0.4	6
GEOSECS #417	-do-	Jan 1978	5.2	12.7	0.4	9
SS#132-3269	12.8°N ; 71.6°E	Apr 1995	4.8	10.3	0.5	4
SS#132-3275	8°N ; 74°E	May 1995	5.0	10.7	0.5	5
SS#132-3274	6.2°N ; 64.4°E	May 1995	6.4	13.7	0.4	5
GEOSECS #418	-do-	Jan 1978	6.1	15.0	0.4	9
SS#132-3273	5.7°N ; 56.2°E	May 1995	8.0	17.1	0.5	5
<i>Equatorial Indian Ocean</i>						
SS#152-3846	0°N ; 80°E	Mar 1997	9.5	20.4	0.4	5
GEOSECS #448	-do-	Apr 1978	5.0	12.1	0.4	5

The increase in bomb ^{14}C inventories at the Arabian Sea stations during the period between the GEOSECS expeditions and the present study is consistent with the model predictions of Toggweiler et al. (1989b). The increase in inventories are $\leq 30\%$ as compared to GEOSECS, and these are however, expected considering the significantly low $\Delta^{14}\text{C}$ values of the atmosphere since the GEOSECS expedition (Table 3.1).

The station SS#152-3846, reoccupation of the GEOSECS 448, at the equatorial Indian Ocean shows an increase in bomb ^{14}C inventory of ~95%, which could be a result of lateral transport of ^{14}C enriched waters. Bard et al. (1988, 1990) observed ~10-90% increase in the bomb ^{14}C inventory after about a decade of GEOSECS at some of the stations near the equatorial northwestern Indian Ocean. They attributed this increase to the advection of low salinity waters enriched in ^{14}C from the Indonesian through-flow along the equator to the 10°S latitudinal belt.

The CO_2 exchange rates for the Arabian Sea and the equatorial Indian Ocean are in the range of 7.5-20.4 mol $\text{m}^{-2} \text{yr}^{-1}$, and are well within $\pm 30\%$ of the rates derived from the GEOSECS data (Table 3.1). Also, the gas exchange rates, computed using wind speeds, (Wanninkhof, 1992; Wanninkhof et al., 1985) are similar. Toggweiler et al. (1989b) computed CO_2 gas exchange rates for various oceanic regions based on a wind speed dependent model, wherein the exchange rates for the Arabian Sea were computed as 10-15 mol $\text{m}^{-2} \text{yr}^{-1}$, with the highest values near the Somali Basin, a region known for the highest wind speeds and exceptionally strong wind induced upwelling. The exchange rates derived in this study from temporal variation of bomb ^{14}C inventory (Table 3.1) are in good agreement with predicted values (Toggweiler et al., 1989a). In the Arabian Sea, the highest exchange rate of 17.1 mol $\text{m}^{-2} \text{yr}^{-1}$ was obtained for the station SS#132-3273, that is close to the Somali Basin value. The highest exchange rate as obtained for SS#152-3846 could be due to lateral inputs of ^{14}C enriched waters from the Indonesian through-flow along the equator.

Upwelling Rates

The upwelling rates determined for the Arabian Sea and equatorial Indian Ocean stations ranged from 3-9 m yr^{-1} (Table 3.1). In general, it is noticed that the upwelling rates calculated for the stations occupied under this study are lower as compared to the GEOSECS stations. All the GEOSECS stations (416, 417 and 418 except for 448) have higher upwelling rates

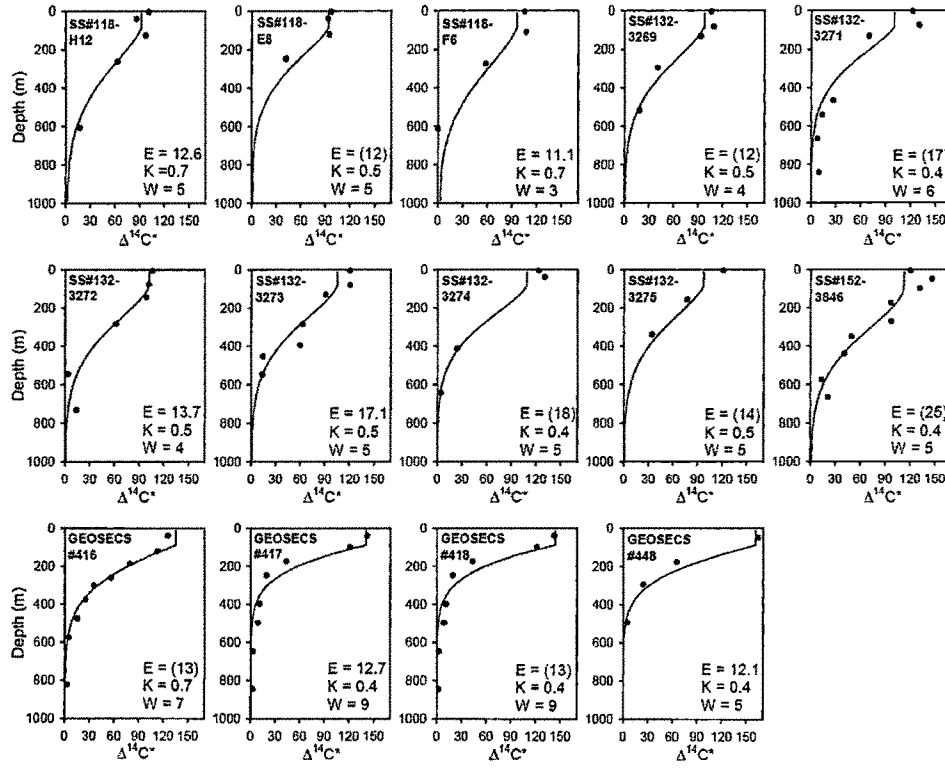


Fig. 3.4: Distribution of $\Delta^{14}\text{C}^*$ (excess bomb ^{14}C) versus depth for different stations. The solid line represents the simulated curve based on 1-D model of Oeschger et al., (1975) for the exchange rate (E), eddy diffusivity (K) and upwelling velocity (w).

compared to that observed for the same stations during this study after a period of nearly two decades (Fig. 3.4). However, GEOSECS station 448 and its reoccupation station SS#152–3846 show similar upwelling rates, with use of higher exchange rate for station SS#152–3846 (Fig. 3.4). As expected, the western region of the Arabian Sea that is known for high wind induced upwelling shows higher upwelling rate (Bhushan et al., 2008).

The difference in bomb ^{14}C inventory from the GEOSECS program (1977–1978) and this study (1994–1995) is in the range of $0.4\text{--}1.3 \times 10^9$ atoms cm^{-2} and are, not wholly inconsistent with the model predictions. Thus, the upwelling rates as derived from this study show values lower than expected. The upwelling rates as deduced from this study may be underestimates as this model does not take into consideration the horizontal advection of ^{14}C along the adjoining isopycnal surfaces. The upwelling rate estimation is

dependent on the gradient of bomb ^{14}C in the water column. This gradient is controlled by the atmospheric ^{14}C concentration, its penetration due to vertical mixing and the air-sea exchange rate and upwelling. The atmospheric ^{14}C concentrations during GEOSECS studies in the Indian Ocean (1977-78) are almost three times higher as compared to the present study (1994-94). As mentioned earlier the Trade winds do not cross the equator thereby inhibiting equatorial divergence that is responsible for the upwelling (Schott and McCreary, 2001). The upwelling in the equatorial region of the Indian Ocean is weak or negligible along the east coast of Kenya (Grumet et al., 2002a). The net result of upwelling is upward advection of relatively depleted $\Delta^{14}\text{C}$ waters enriched in nutrients to the surface thereby causing enhanced productivity. Generally, the surface ocean is depleted in $\Delta^{14}\text{C}$ compared to the atmospheric $\Delta^{14}\text{C}$ due to reservoir mixing time. With atmospheric excess of $\Delta^{14}\text{C}$, there is always an uptake of $\Delta^{14}\text{C}$ enriched CO_2 by the oceans. These processes lead to a vertical gradient of $\Delta^{14}\text{C}$ in the water column as a result of vertical mixing. Since radiocarbon is a transient tracer, the surface water concentrations are expected to have gradients which are time variant (Grumet et al., 2002b). With decreasing atmospheric ^{14}C concentrations, the vertical gradient in the water column ^{14}C distribution is expected to be modulated. This is responsible for the difference in upwelling rate estimates during two different time periods with such vast atmospheric $\Delta^{14}\text{C}$ differences. Although, during GEOSECS period, radiocarbon was more appropriate tracer due to its large air-sea $\Delta^{14}\text{C}$ gradient, however, during the present study it has yielded lower upwelling rates due to reduced water column $\Delta^{14}\text{C}$ gradient caused due to decreasing atmospheric $\Delta^{14}\text{C}$ (Rengarajan et al., 2002). The bomb ^{14}C introduction in the atmosphere proved to be a valuable tracer in understanding many surface processes of the oceans but it is limited by its removal from the atmosphere.

Chapter IV

BAY OF BENGAL: SEDIMENT PROVENANCE

The surface sediment distribution in the Bay of Bengal largely reflects the type of sediments brought by the various rivers draining into it. The coastal sediments comprise of sand, silt and clay. Clay is the major detritus material over most of the region except in areas influenced by the G-B River system. In the G-B delta and Bengal Fan, silt is the major constituent (Mallick, 1976; Meybeck, 1979). To the west of the Andaman coast, silty clay occupies a very large area that extends almost up to the central region of the Bay. Siddiquie (1967) envisaged a general increase in foraminiferal content and unidentifiable calcareous fragments with decrease in terrigenous material and insoluble matter towards the central and southeastern parts of the Bay of Bengal.

The G-B River system not only controls the sediment composition of the Bay of Bengal but is also the largest sediment source to the world oceans (Milliman and Meade, 1983). The other major Indian rivers flowing into the Bay of Bengal derive their sediment load from the Deccan highlands of the Indian peninsula (Archean basement). The fine sand fraction enriched in quartz and heavy minerals settles down in estuarine channels while a predominant part of the fine fraction and suspended matter enriched in clays is transported to the outer shelf of the Bay of Bengal. The suspended matter undergoes compositional changes during its transport, attributed to the grain size distribution, as well as results in the formation of manganese dioxide coatings on the suspended particles (Stummeyer et al., 2002).

The fresh water discharge plays an important role in the circulation of surface waters of the Bay of Bengal (Howden and Murtugudde, 2001). This fresh water inflow coupled with the upwelling winds along the east coast of India during the monsoon period leads to the formation of a cyclonic gyre at the Bay head and occurrence of down welling along the east coast of India. According to Dube et al. (1995), the local effect of the northern fresh water inflow weakens the intensity of wind induced upwelling.

The Andaman Basin in the northeastern Indian Ocean is bound by Myanmar on the north, Thailand and Malaysia on the east and the Andaman and Nicobar Islands on the west and is separated from the rest of the Bay of Bengal. The surface waters of the Andaman Sea receive considerable fresh water inflow from the Irrawaddy River and the G-B River system. The deep water of the Andaman Sea is separated from the main Bay of Bengal area by the Andaman-Nicobar Ridge in the west. The Andaman Sea is connected to the Bay of Bengal by the Preparis and Ten Degree Channels, and by the Great Channel in the south (Sengupta et al., 1981; Kamesh Raju et al., 2004). With Preparis Channel being just ~250 m deep, the exchange of deep water is mainly through the Ten Degrees Channel (where the water depth is ~800 m) and the Great Channel (maximum depth of ~1400 m.) Due to the presence of ridges and surrounding sills, the Andaman Basin is cut off from the deep waters of the Bay of Bengal and the equatorial Indian Ocean. (Okubo et al., 2004; Dutta et al., 2007). The chemical and isotopic composition of the sediments in this basin would provide clues to the intensity and flux component of erosion from the Himalayan and Burman ranges. The sediment to the Andaman basin is mainly supplied by the Irrawaddy and Salween Rivers (Rodolfo, 1969; Kamesh Raju et al. 2004; Rao and Kessarkar, 2001; Vance et al., 2003; Rao et al., 2005).

The sediments carried by the various rivers reflect the lithology of the drainage basin with signatures of mineralogical and isotopic compositions.

This becomes very important in understanding the sediment distribution in the Bay of Bengal and can be used to fingerprint the sediment provenance. The enormous fluvial input to the Bay during the South West Summer Monsoon (SWSM) is reflected in the high average content of lithogenic matter and a relative increase in the flux of biogenic opal. High carbonate dominated fluxes observed during SWSM and North East Winter Monsoon (NEWM) is mainly due to wind-induced nutrient supply, whereas high opal rich fluxes during SW-NE inter-monsoon are controlled by both upwelling as well as supply of riverine and shelf derived matter (Unger et al. 2003). The fluvial sediment input is the major source for detrital flux in the Bay of Bengal. In the northeastern part, the sediment flux is largely due to inputs from the G-B River system, while in the western part it is the peninsular rivers that are responsible for the sediment budget. These fluvial inputs can be differentiated by their contrasting clay mineral assemblages. For example, the sediment of G-B River system are high in illite and chlorite, whereas, the peninsular river sediment are rich in smectite (Goldberg and Griffin 1970; Rao, 1991). Although, the main sediment supplier to the Bay of Bengal has been the G-B River system, the contribution of the peninsular Indian river systems, which has remained a long-lived sedimentary source, cannot be underestimated (Kolla and Rao, 1990; Rao and Kessarkar, 2001). The illite-chlorite rich sediments from G-B River system can be traced right from the eastern Bay of Bengal in the north to the areas well south of the equator. The transport of these sediments has been affected mainly by turbidity currents. The Ninety East Ridge acts as a barrier preventing the coalescence of the two Bengal Fan lobes (Kolla and Biscaye, 1973; Kolla et al., 1976).

Earlier studies on the clay fractions of grab samples from the northwestern part of the Bay of Bengal revealed the presence of major quantities of illite and quartz with minor amounts of smectite, kaolinite and feldspar (Ramamurty and Shrivastava 1979). The surface clay mineral distribution on the southwestern continental margin of India shows high content of illite and chlorite in southern region of the study area pointing to

the evidence of sediment contribution from the Bay of Bengal waters, entering this region after the SW monsoon (Chauhan and Gujar 1996). The Rare Earth Elements (REEs) and metal distribution of the sediments of the G-B River system reflects the excessive crustal erosion in the high Himalayan regions, due to strong physical weathering processes, and the contribution of more material to the Bay of Bengal (Ramesh et al., 2000).

The Bengal Deep Sea Fan *aka* Bengal Fan is the world's largest submarine fan. The sediments are tunnelled to the fan via a delta-front trough, the *Swatch of no Ground*. The sediment distribution patterns of the fan

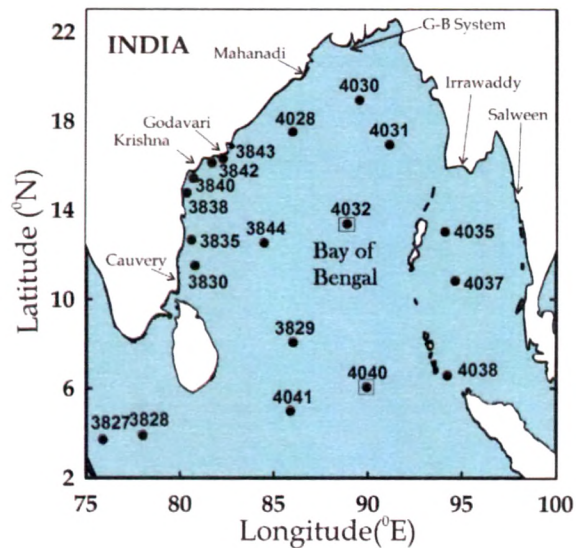


Fig. 4.1: Core locations in the Bay of Bengal. Boxed filled circles are the two cores studied in detail. Rivers supplying sediment to the Bay are also identified.

shows westward inclination, with the thickest accumulation of mud near the submarine canyon, *Swatch of No Ground* incises the western shelf thereby leading to westward transport of sediments (Kuehl et al., 1997). In view of the above understanding of the Bay of Bengal basin in the northern Indian

Ocean and its sediment distribution and characteristics, detailed studies were carried on surface sections of sediments from nearly 17 cores distributed spatially in the Bay of Bengal (including the Andaman Sea) (Fig. 4.1). Details of cores used for the study is given in Table 4.1.

Sediment Distribution

Surface sections of the cores representing the contemporary sediment flux have been analyzed for CaCO_3 , organic carbon (C_{org}), major and trace elements along with Sr and Nd isotopes to identify the source and distribution of modern sediments in the Bay of Bengal. Additionally, few river bed samples near the mouth of the Ganga (near Hooghly Estuary), Mahanadi, Godavari and Krishna Rivers that drain into the Bay of Bengal

Table 4.1: Location and water depth of the cores in the Bay of Bengal.

No.	Core No.	Latitude [°N]	Longitude [°E]	Water depth (m)
1	SS# 152-3827	3°42'	75° 55'	3118
2	SS# 152-3828	3° 54'	78° 4'	3166
3	SS# 152-3829	8° 3'	86° 02'	3669
4	SS# 152-3838	14° 46'	80° 21'	157
5	SS# 152-3840	15° 25'	80° 42'	193
6	SS# 152-3842	16° 7'	81° 41'	173
7	SS# 152-3843	16° 17'	82° 17'	690
8	SS# 152-3844	12° 31'	84° 29'	3327
9	SS# 172-4028	17° 30'	85°60'	2569
10	SS# 172-4030	18° 56'	89° 32'	1848
11	SS# 172-4031	16° 55'	91° 08'	2359
12	SS# 172-4032	13° 21'	88° 54'	3011
13	SS# 172-4035	13° 0.73'	94° 08'	2337
14	SS# 172-4037	10° 49'	94° 39'	3250
15	SS# 172-4038	6° 33'	94° 14'	1314
16	SS# 172-4040	6° 02'	89° 57'	2788
17	SS# 172-4041	4° 59'	85° 54'	4012

* SS- Sagar Sampada

were also analyzed for Sr and Nd isotopes (Fig. 4.1). The isotopic and geochemical composition of surface sediment composition of the Bay of Bengal is governed by three processes viz. detrital, biogenic and diagenetic, with detrital being the most dominant component. Major element geochemistry of the surface sediments show decreasing Al, Mg, Fe, and Ti concentrations from the coast to the open ocean (north to south, Fig. 4.3, Table 4.2), whereas the biogenic proxies CaCO_3 , Sr, Ba show an increasing trend. A strong enrichment of Mn is observed in the surface sediment in near coastal

regions of G-B River system and the Irrawaddy River (Table 4.3). The correlation between organic carbon C_{org} and $CaCO_3$ indicates increasing

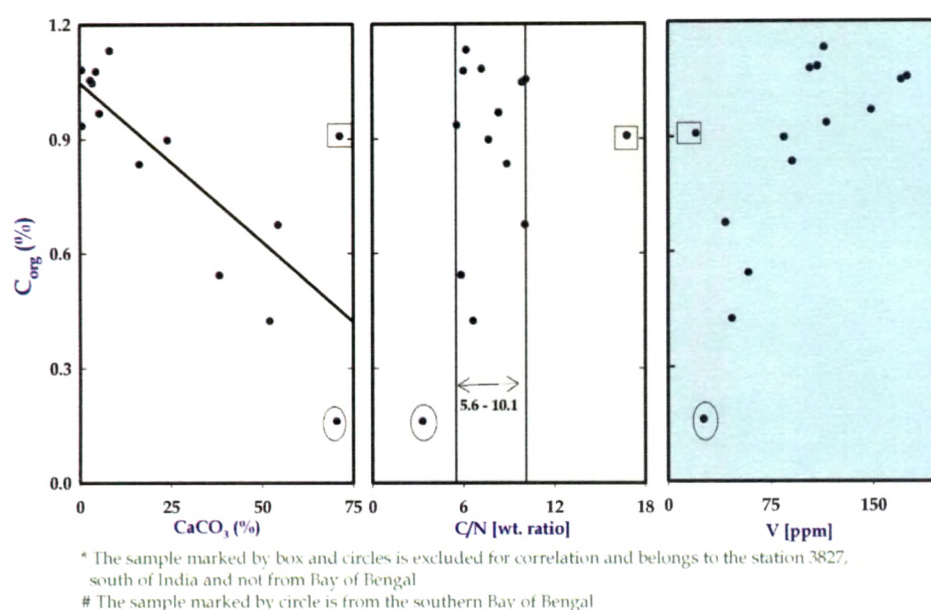


Fig. 4.2: Correlation of Organic Carbon (C_{org}) in the surface sediments with $CaCO_3$, C/N ratio and V concentration. No apparent correlation of C_{org} with C/N can be noticed indicating marine source of C_{org} .

detrital contribution causing enhanced preservation of C_{org} and decrease in $CaCO_3$. There is no apparent correlation of C_{org} with C/N indicates a predominant marine origin of the organic matter. This is corroborated by C/N ratio ranging from 5–10, typical for marine organic carbon. The V shows a positive correlation with C_{org} due to its enrichment with increasing C_{org} (Fig. 4.2).

Detrital Components

The composition, mineralogy and distribution of sediments in the Bay of Bengal reflects the strong physical and chemical weathering prevalent in the drainage basins of all the rivers flowing through the Indian subcontinent. This is strongly dependent on the monsoon intensity especially the SWSM. Besides this, the Bay of Bengal is also influenced by the NEWM. There are evidences

Table 4.2: Concentration of trace elements, organic carbon (C_{org}), $CaCO_3$ and C/N ratio in the surface sediments of the Bay of Bengal cores.

Core No.	Latitude (°N)	Longitude (°E)	Ni (ppm)	Cu (ppm)	Cr (ppm)	Sr (ppm)	Ba (ppm)	$CaCO_3$ (%)	C_{org} (%)	C/N
3827	3.7	75.91	48.8	37.5	21.1	1018	700	71.3	0.90	16.8
3828	3.893	78.03	47.3	39.2	23.5	749	685	69.1	--	--
3829	8.05	86.03	82.1	87.1	55.3	604	1116	38.2	0.54	5.8
3838	14.767	80.35	77.4	86.8	122.3	127	134	5.39	0.96	8.3
3840	15.415	80.70	64.4	115.9	103	147	150	5.55	--	--
3842	16.112	81.68	73.1	87.7	119.9	107	175	3.41	1.04	9.9
3843	16.29	82.28	71.1	102.1	114.4	110	188	2.89	1.05	10.1
3844	12.51	84.49	151.2	113.1	92.9	434	870	24	0.89	7.7
4028	17.5	86.00	89.4	57.1	114.6	101	404	0.61	1.08	7.2
4030	18.933	89.54	109.3	61.1	101.1	182	641	4.41	1.07	6.0
4031	16.917	91.14	136.8	70.8	88.9	343	826	16.3	0.83	8.9
4032	13.362	88.90	40.3	42.5	44.5	726	729	52	0.42	6.6
4035	13.012	94.12	71.9	45.7	94.7	288	535	8.13	1.13	6.2
4037	10.815	94.65	102.5	89.9	101.9	148	665	0.63	0.93	5.6
4038	6.553	94.24	22.2	19.6	26.3	701	2289	54.3	0.67	10.1
4040	6.032	89.94	21.5	26.9	19.6	923	730	70.4	0.16	3.3
4041	4.975	85.89	34.9	73.4	33.5	884	927	58.4	--	--

Table 4.3: Concentration of major and trace elements in the surface sediments of the Bay of Bengal cores.

Core	Latitude (°N)	Longitude (°E)	Al (%)	Fe (%)	Ca (%)	Mg (%)	Ti (ppm)	Mn (%)	V (ppm)	Zn (ppm)	Co (ppm)
3827	3.7	75.91	1.68	1.07	31.2	0.67	697	0.11	21	42	6.2
3828	3.893	78.03	2.13	1.31	29.5	0.64	859	0.11	22	41.3	7.1
3829	8.05	86.03	5.13	3.00	16.4	1.22	2344	0.43	59	90.2	22.6
3838	14.767	80.35	8.42	7.13	3.0	2.25	8088	0.08	149	79	36.1
3840	15.415	80.70	7.57	7.73	4.5	1.96	15340	0.97	230	94	50.7
3842	16.112	81.68	9.14	7.89	2.1	1.98	8358	0.94	171	90	40.7
3843	16.29	82.28	9.27	7.96	2.1	1.92	8545	0.08	175	96	39.4
3844	12.51	84.49	7.41	5.36	11.5	1.75	3530	0.55	85	124	35.3
4028	17.5	86.00	10.44	6.92	0.66	2.09	4074	1.69	109	152	32.3
4030	18.933	89.54	9.05	5.44	2.5	2.01	3889	1.70	104	152	32.2
4031	16.917	91.14	7.97	4.16	7.7	1.74	3155	1.16	91	149	27.4
4032	13.362	88.90	3.82	2.33	23.5	1.10	1567	0.16	47	51	13.4
4035	13.012	94.12	8.25	4.26	4.9	2.11	3007	2.13	114	84	17.5
4037	10.815	94.65	8.92	5.33	0.87	2.21	3214	2.05	116	104	23.4
4038	6.553	94.24	3.45	1.87	23.4	0.85	1360	0.06	42	56	8.1
4040	6.032	89.94	2.06	1.16	28.8	0.68	753	0.06	26	32	6.2
4041	4.975	85.89	3.21	1.89	25.4	0.81	1256	0.19	36	46	10.7

to suggest that both these monsoons have weakened or strengthened during the past several thousand years (Burton and Vance, 2000; Tiwari et al., 2005). At present, the SWSM is the most dominant and contributes abundant sediment flux to the Bay of Bengal.

The Al (%) distribution pattern of the surface sediments from the Bay of Bengal shows a large variation from 2–10% with the highest concentration towards the northern Bay of Bengal. The western Bay of Bengal shows an Al concentration of 9%. The Andaman Sea exhibits almost a uniform distribution of Al (8%) in the surface sediments (Fig. 4.3, Table-1). The open ocean Al concentration in the Bay of Bengal ranges from 4–7%. The decreasing pattern of Al concentration from the coast to the open ocean in the surface sediments of the Bay of Bengal is due to the decreased supply of detrital material to the open ocean and increasing concentration of the biogenic component (Siddique, 1967; Sengupta et al., 1992). The clay mineral assemblage in sediments from the eastern part of the Bay of Bengal is influenced by the G-B River system, in which

the suspended particulates are dominated by illite and chlorite (Ramamurty and Shrivastava, 1979; Kolla and Rao, 1990; Rao, 1991; Kuehl et al., 1997; Weber et al., 1997; Goodbred and Kuehl, 1999; Rao and Kessarkar, 2001). The rivers draining the Himalayas have abundance of illite and chlorite compared to

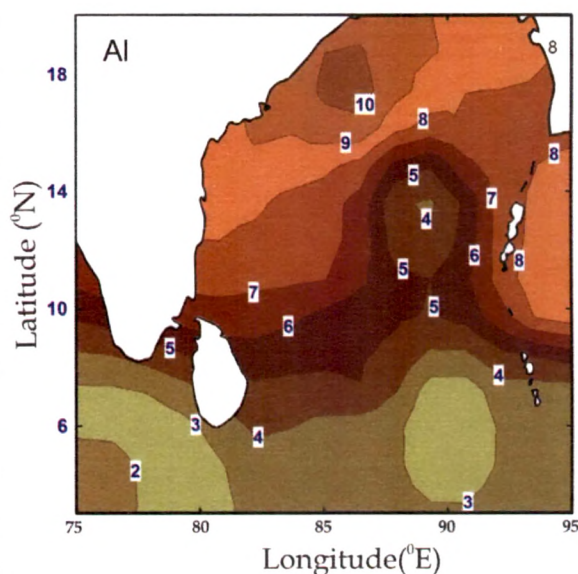


Fig. 4.3: Distribution of Al (%) in the Bay of Bengal surface sediments. Note, Al decrease from the coast to the open ocean.

those draining the Peninsular India. The latter are rich in smectite (Rao and Nath, 1988; Nath, 2001). Clay minerals are the principal carriers of Al_2O_3 with a wide range of concentrations ranging from 28.9% for illite, 25.2% for chlorite, 19.8% for smectite and 38.5% for kaolinite (Degens, 1967). The very high concentration of Al in the northwestern Bay of Bengal (see Fig. 4.3) are due to the sediments enriched with kaolinite brought by the peninsular rivers such as the Mahanadi and Brahmani and rivers draining the Eastern Ghats. Although, the peninsular rivers such as Godavari and Krishna bring sediments enriched with smectite, which has nearly half the Al content compared to kaolinite, the Al concentration in the western Bay of Bengal (off Godavari and Krishna) are comparable to the northern Bay of Bengal (off G-B River) and, a patch of high Al concentrations distinctly occurs in the northwestern Bay of Bengal. This suggests that the influence of sediments derived from G-B River system is insignificant in the northwestern part (off Mahanadi and Brahmani Rivers), may be due to strong northeasterly currents prevailing during the SW monsoon. The Al content in the Andaman Basin is similar to that observed in the Bay of Bengal.

Unlike Al, Ti content increases from granites (~0.3%) to basalts (1.5%) (Lisitsyn, 1996). However, some of the highest concentrations are observed in the western Bay of Bengal unlike that shown by Al due to the sediment contribution from basaltic terrain by the peninsular rivers. The Ti concentration varies from 2000–8000 ppm with

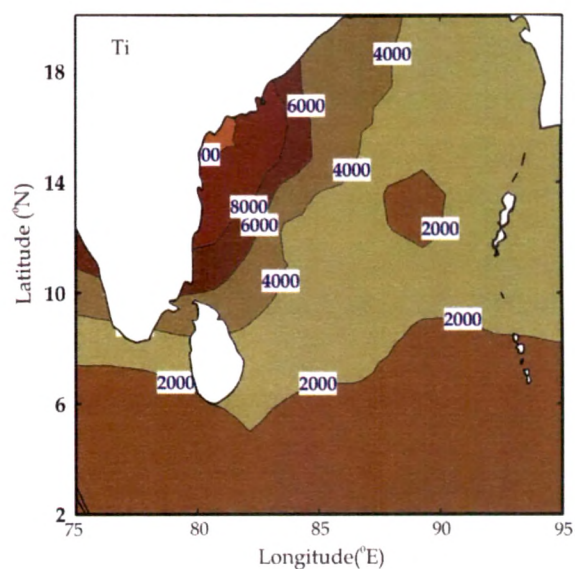


Fig. 4.4: Distribution of Ti (ppm) in the surface sediments of the Bay of Bengal.

decreasing concentration from the coast. Even the Andaman Basin sediment too shows lower values as reflected by the open ocean of 2000 ppm.

In sediment trap, the Al/Ti ratio is found to be much higher when compared to the typical crustal value, thereby implying a non-crustal source of excess Al in the Bay of Bengal. The analyses of sediments from the equatorial Pacific Ocean with low particulate flux of lithogenic material showed that excess Al is associated with the opal rain to the seafloor. In view of this, it has been suggested that Al can be used as a proxy for paleoproductivity, though it should be limited to only productive, open ocean areas which are not strongly influenced by inputs of aluminosilicates (Dymond et al., 1997; Pattan and Shane, 1999).

The distribution of Fe in the Bay of Bengal resembles to the distribution pattern of Ti with its highest concentration on the western shelf areas. The Fe concentration in sediments increases from acidic rocks to basalts and it is one of the most widespread elements in the earth's crust. The

enhanced Fe concentrations observed towards the western Bay of Bengal are due to the

contribution of Fe rich sediments from the peninsular rivers. The Fe content in the western Bay of Bengal ranges from 5–7% while in the eastern Bay of Bengal it is about 3–5% (Fig. 4. 5).

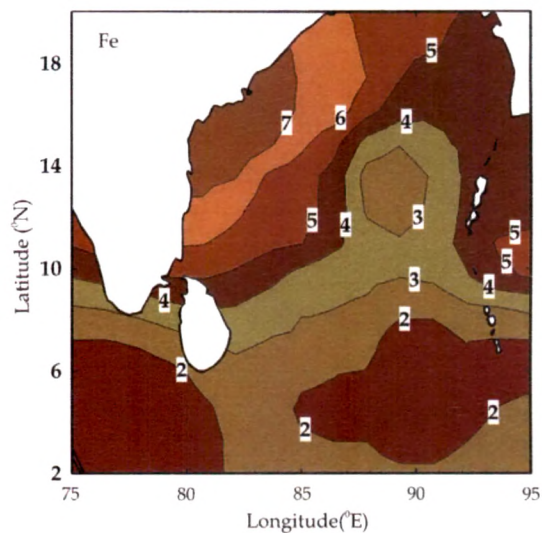


Fig. 4.5: Distribution of Fe (%) in the surface sediments of the Bay of Bengal. Western Bay of Bengal show Fe rich sediments, contribution from peninsular river.

The ionic radius of chromium (Cr, 0.06 nm) is close to that of Fe (0.067 nm) and its concentration increases from granite (~10 ppm) to basalt (~300 ppm) and particularly in ultrabasic rocks (~0.4%). Thus, expectedly, some of the higher concentrations of 90–110 ppm of Cr are observed in the western Bay of Bengal that is influenced by the sediment derived from basaltic rocks of the peninsular India (Fig. 4.6). A general decreasing trend from the coast to the open ocean is observed in the Cr distribution attesting to its terrestrial source. The concentration of vanadium (V) varies like that of Cr but it decreases sharply in ultrabasic rocks (~50 ppm).

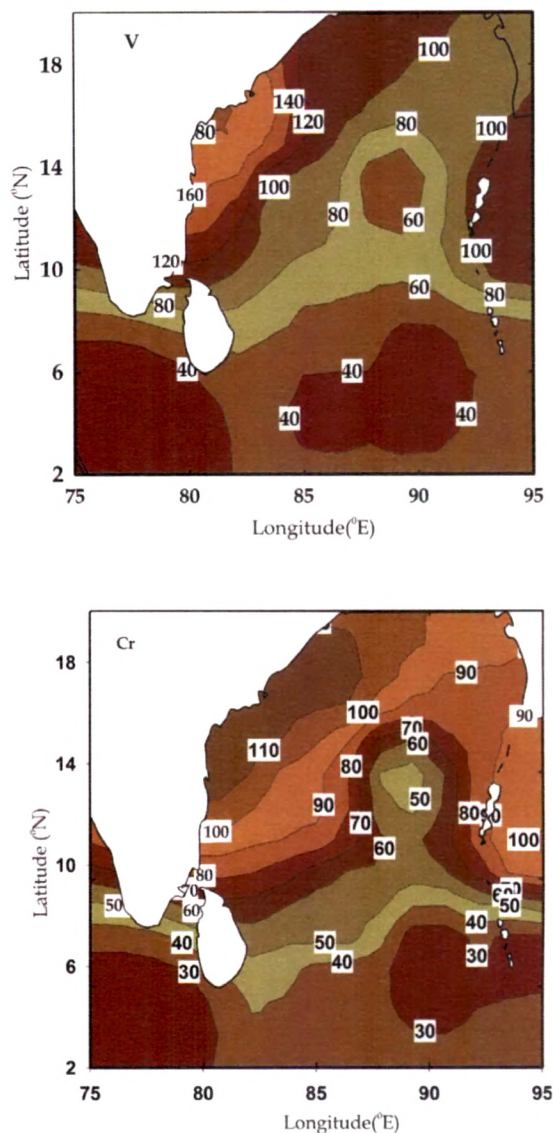


Fig. 4.6: Distribution of V and Cr in the surface sediments. Erosion of Basaltic rocks from the peninsular India is responsible for higher V and Cr in western region.

Some of the highest concentration of Cr in the Bay of Bengal is observed in the western region which is due to the erosion of basaltic rocks in the drainage area of the peninsular rivers (Fig. 4.6). Thus, distribution of V in sediments is an indicator of material from upper basaltic layers, whereas, Cr is an indicator of the lower basaltic layers.

The manganese (Mn) content increases from 0.05% in granites to 0.17% in basalts. Thus, it is to be expected that the high Mn concentrations in the surface sediments have been derived from the basaltic drainage areas, which in the present case lies in western region

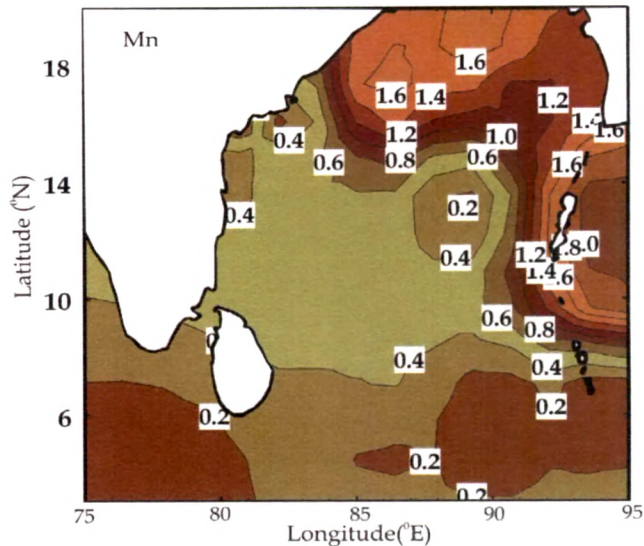


Fig. 4.7: Distribution of Mn (%) in the surface sediments of the Bay of Bengal. Higher Mn concentrations in the northern Bay of Bengal is due to enrichment of surface sediments in high sedimentation regions.

of the Bay of Bengal. However, the surface sediments of the western Bay of Bengal do not show high Mn concentration, whereas unexpectedly the northern Bay of Bengal sediments are highly enriched in Mn (Fig. 4.7). As mentioned earlier, the northern Bay of Bengal receives high sediment flux from the G-B River system. The enhanced sedimentation leads to preservation of organic matter which undergoes slow degradation within the sediments. The diagenetic changes in high sedimentation regions cause Mn from deeper sections to migrate upward to the surface (Chauhan and Rao, 1999; Mangini et al., 2001). Similar trend is observed in the northern Andaman Basin where enhanced sediment flux is contributed by the Irrawaddy and Salween Rivers (Rodolfo, 1969). Over all, detrital proxies show a decreasing trend from coast to the open ocean, due to the fact that majority of the sediment are deposited in the coastal environment.

Biogenic Components

The integrated primary productivity of the Bay of Bengal ranges from ~90–220 mg.C.m⁻².d⁻¹ which is significantly lower compared to ~770–1780

mg.C.m⁻².d⁻¹ observed in the Arabian Sea. The high productivity in the Arabian Sea is attributed to the advection of nutrient-rich waters to the euphotic zone, whereas, in the Bay of Bengal inability of the weaker winds to erode the strongly stratified surface layers leads to reduced vertical mixing and hence the low productivity (Prasanna Kumar et al. 2002). Carbonate, which is contributed by the planktonic foraminifers, constitutes the major fraction of productivity in the Bay of Bengal. As a result, terrestrial contribution gets diluted by the carbonate production (Kolla et al., 1976a). The calcium carbonate content of the sediments ranges from ~2–70%. The highest concentration of CaCO₃ in the surface sediments of the Bay of Bengal is towards the open ocean where the contribution of the detrital component is least and lowest concentration is observed near the coastal regions (Fig. 4.8). The total Ca content of the sediment in the region is mainly due to CaCO₃ with a minor fraction of it coming from the dolomitic detrital sediments (Kolla et al., 1976a; Kolla and Rao, 1990). The Ca distribution of the surface sediments closely resembles to that of CaCO₃ suggesting a biogenic origin and it ranges from 2–28% (Fig. 4.8).

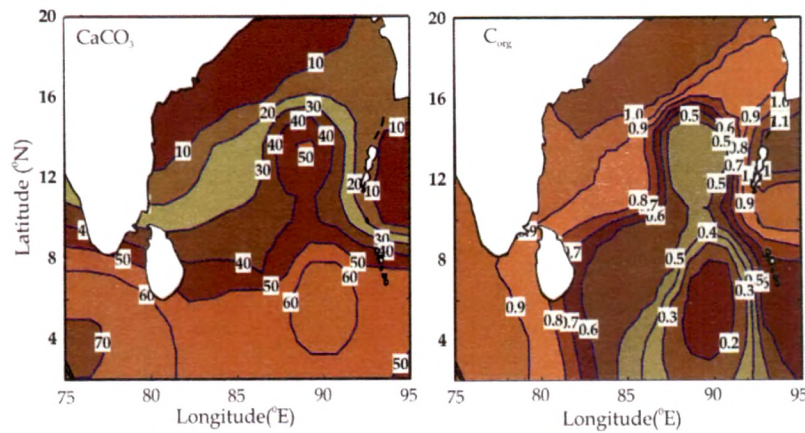


Fig. 4.8: Distribution of CaCO₃ and organic carbon (C_{org}) in the surface sediments of the Bay of Bengal. Increasing CaCO₃ from the coast to the open ocean indicates decreasing detrital contribution. Whereas, high C_{org} near the coast reflects its enhanced preservation with increasing detrital flux.

Barium (Ba) is another productivity indicator and shows an increasing concentration from coast (~200 ppm) to the open ocean (~1000 ppm) thereby

indicating dilution caused due to the continental flux in the Bay of Bengal (Fig. 4.9). Strontium (Sr) concentration too shows a trend similar to that as observed for Ba thus mimicking as a productivity indicator.

While in the coastal sediments, organic carbon (C_{org}) content can be used as a productivity indicator, its reliability in the open ocean is suspect as around 98% of C_{org} gets oxidized in the water column during its traverse to the bottom sediments. In view of this, the decreasing trend of C_{org} in the Bay of Bengal sediments from coast to the open ocean is indicative of the preservation characteristics of the C_{org} rather than productivity (Fig. 4.8). Higher C_{org} near the coast suggests faster sedimentation rates and thereby better

preservation and for the open ocean low sedimentation rate makes it susceptible to oxidation. Naqvi et al. (1996) found lower respiration rates in the Bay of Bengal due to the weak north–south gradients in oxygen and total CO_2 , conflicting with the higher sinking fluxes of organic carbon measured with sediment traps. Large terrigenous input in the Bay of Bengal is attributed for lesser degree of oxidation of particulate organic carbon in the water column as particulate organic matter gets protected from degradation by the inorganic matrix of the sinking particles (Hedges et al. 2001).

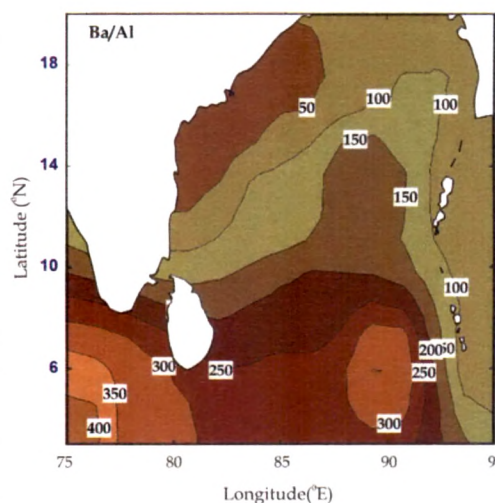


Fig. 4.9: Distribution of Ba/Al (ppm/%), productivity proxy in the surface sediments of the Bay of Bengal. Dilution of Ba due to increasing continental flux from coast to the open ocean can be observed.

Strontium (Sr) and Neodymium (Nd) Isotopic Distribution

The large variation in Sr and Nd isotopic composition in the Bay of Bengal has been attributed to variable contribution from Himalayan and Trans-Himalayan lithologies (Colin et al., 1999; Galy et al., 1996; France-Lanord et al., 1993; Pierson-Wickman et al., 2001; Singh and France-Lanord, 2002).

The higher erosion in

the eastern syntaxes compared to other Himalayan ranges is related to rapid exhumation rates of this region, triggered by higher precipitation and the high incision potential of the Tsang Po River aka Brahmaputra River (Singh and France-Lanord, 2002). The enormous volume of sediments brought to the Bengal Fan is contributed from different Himalayan lithologies having distinct isotopic composition. They are High Himalaya Crystalline (HHC; $^{87}\text{Sr}/^{86}\text{Sr} = 0.75$ and $\epsilon_{\text{Nd}} = -16$), Lesser Himalaya (LH; ≥ 0.8 and -25) and Tethyan Sedimentary Series (TSS; ≤ 0.72 and -12 to -4) (Colin et al., 1999; Galy et al., 1996, 1999; Galy and France-Lanord, 1993; Singh and France-Lanord, 2002; Singh et al., 2008). The $^{87}\text{Sr}/^{86}\text{Sr}$ of the Bengal Fan turbidites ranges from 0.74–0.76 and ϵ_{Nd} values of -16 are similar to the High Himalayan Crystalline (France-Lanord et al., 1993). This indicates that the primary source of sediments to the Bengal Fan has been dominated by the sediments from the HHC (France-Lanord et al., 1993; Galy et al., 1996).

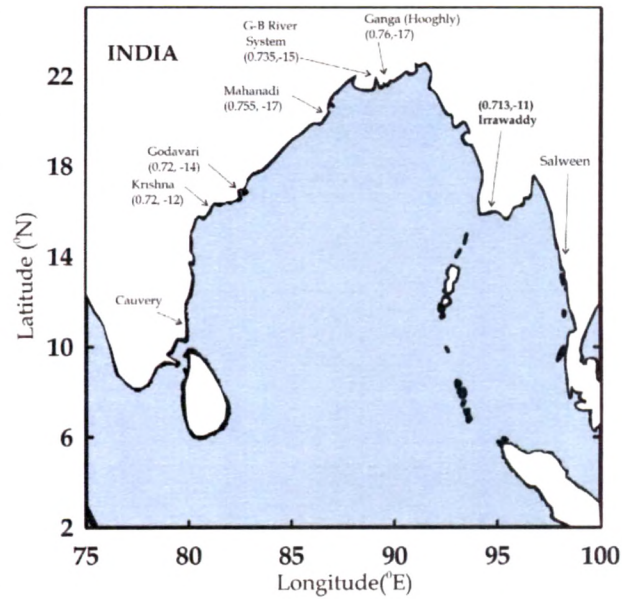


Fig. 4.10: $^{87}\text{Sr}/^{86}\text{Sr}$ and ϵ_{Nd} of the river mouth samples measured. Irrawaddy river data from Colin et al., (1999).

However, relatively lower values of $^{87}\text{Sr}/^{86}\text{Sr}$ observed in the sediments of the Bay of Bengal indicate other sources of sediment and are attributed to the peninsular rivers viz. the Krishna and Godavari (Subramanian 1980; Wijayananda and Cronan 1994). Based on the nature of distribution of elemental and isotopic composition of Sr and Nd in the Bay of Bengal (Colin, et al., 1999), four possible end members have been identified. These are the G-B River system ($^{87}\text{Sr}/^{86}\text{Sr} > 0.735$ and $\epsilon_{\text{Nd}} < -15$), Irrawaddy River (≈ 0.713 , ≈ -11) and the Peninsular Rivers (≈ 0.708 , -18.0) (Ahmad et al., 2005). The fourth member has been inferred as derived from the detrital material from the erosion of the western part of the Indo-Burmese ranges, along the Arakan coast (≈ 0.716 , -7.0).

Table 4.4: $^{87}\text{Sr}/^{86}\text{Sr}$ and ϵ_{Nd} in the silicate fraction of the surface sediments from the cores in the Bay of Bengal.

Core	Latitude (°N)	Longitude (°E)	$^{87}\text{Sr}/^{86}\text{Sr}$	Sr (ppm)	ϵ_{Nd}	Nd (ppm)
3827	3.7	75.908	0.7099	633	-12.97	22.2
3828	3.893	78.033	0.7070	---	-13.86	23.1
3829	8.05	86.033	0.7110	555	---	---
3830	11.495	80.792	0.7208	144	---	---
3835	12.655	80.618	0.7126	499	-17.5	27.1
3838	14.767	80.35	0.7204	82	-12.92	30.9
3840	15.415	80.695	0.7152	174	-17.74	31.5
4028	17.5	85.997	0.7332	94	---	---
4030	18.933	89.538	0.7268	120	-14.6	32.0
4031	16.917	91.14	0.7136	202	-12.72	30.0
4032	13.362	88.9	0.71721	174	---	---
4035	13.012	94.118	0.7125	158	-8.95	28.0
4037	10.815	94.645	0.7164	117	-10.21	33.8
4038	6.553	94.235	0.7138	179	-11.55	24.7
4040	6.032	89.942	0.7125	283	-11.1	29.3
4041	4.975	85.892	0.7134	378	---	---

The Sr and Nd isotopic composition of the silicate fraction of 16 surface sediments of the Bay of Bengal (Table 4.4) and bed sediments of the estuarine regions of the Ganga (Himalaya), Mahanadi, Godavari and Krishna



(peninsular) Rivers near their mouth were analyzed in order to ascertain the sediment provenance (Fig. 4.10).

The high $^{87}\text{Sr}/^{86}\text{Sr}$ (0.725–0.735) and low ϵ_{Nd} (–18 to –12) of the surface sediment samples of the northern Bay of Bengal indicate strong G-B River system influence.

However, samples from

the western Bay of Bengal show mixed signatures of Sr and Nd isotopes

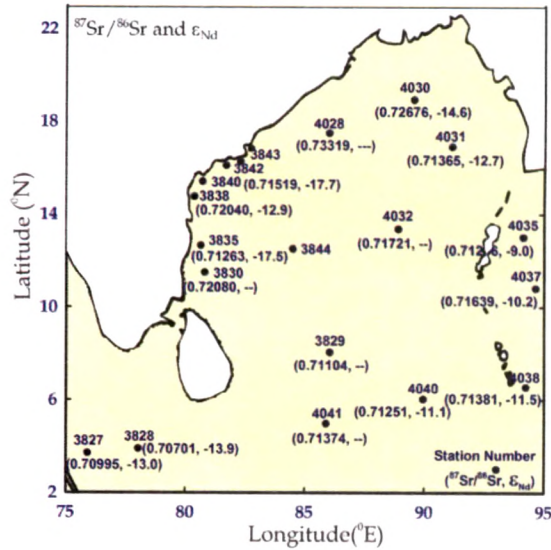


Fig. 4.11: $^{87}\text{Sr}/^{86}\text{Sr}$ and ϵ_{Nd} of surface sediment samples.

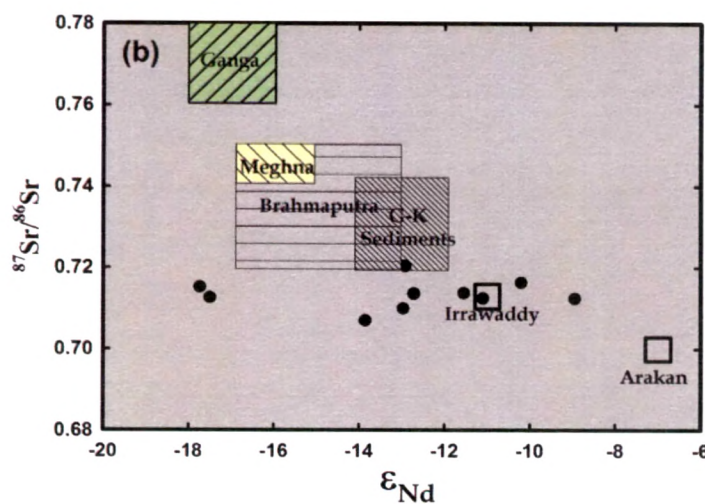


Fig. 4.12: $^{87}\text{Sr}/^{86}\text{Sr}$ versus ϵ_{Nd} plot of surface sediments. Also, shown are the boxes representing the end members. G-K (Godavari-Krishna) sediments values are the river mouth value. (Singh et al., 2008; Colin et al., 1999; Ahmad et al., 2005).

derived mainly from the rivers draining the eastern continental margin of India, viz. Mahanadi, Godavari, Krishna and Cauvery. The low radiogenic Sr with high enriched ϵ_{Nd} in surface sediment samples from the Andaman Sea indicate the Irrawaddy River as the main contributor. The measured value of $^{87}Sr/^{86}Sr$ value of Ganga at Hooghly Estuary in bed sediments was 0.76 and ϵ_{Nd} of -16, for Mahanadi 0.755 and -17, for Godavari 0.72 and -14 and Krishna with 0.72 and -12. The Godavari and Krishna (G-K)

River drain into the Bay of Bengal and contribute sediments from Deccan Traps and Archean basement of peninsular India (Archean). The $^{87}Sr/^{86}Sr$ and ϵ_{Nd} of the sediments analysed as part of this study are shown in Fig. 4.11. The $^{87}Sr/^{86}Sr$ of these sediments is 0.706 and ϵ_{Nd} of -18 (Fig. 4.12; Ahmad et al., 2005). But if we look into the $^{87}Sr/^{86}Sr$ isotopic ratio in the sediments at the junction with the Bay of Bengal, the values are significantly high. This implies the magnitude of the G-B River system influencing the sediment budget and also assisted by the channeling caused due the presence of the 90° East Ridge. This ridge acts as a barrier for the sediment movement towards east (Fig. 4.12). The mixing plot of Sr isotopic ratio versus 1/Sr of the sediments from the Bay of Bengal broadly indicates three sources of sediment to the basin (Fig. 4.13). Three components viz. the G-B River system, Irrawaddy River and the Peninsular Rivers are possibly responsible for the isotopic distribution of

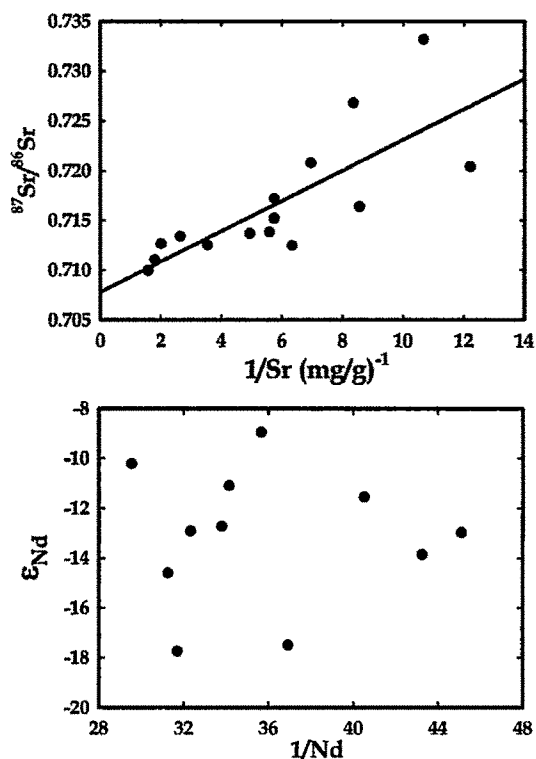


Fig. 4.13: $^{87}Sr/^{86}Sr$ vs $1/Sr$ and ϵ_{Nd} versus $1/Nd$ plot of the surface sediment.

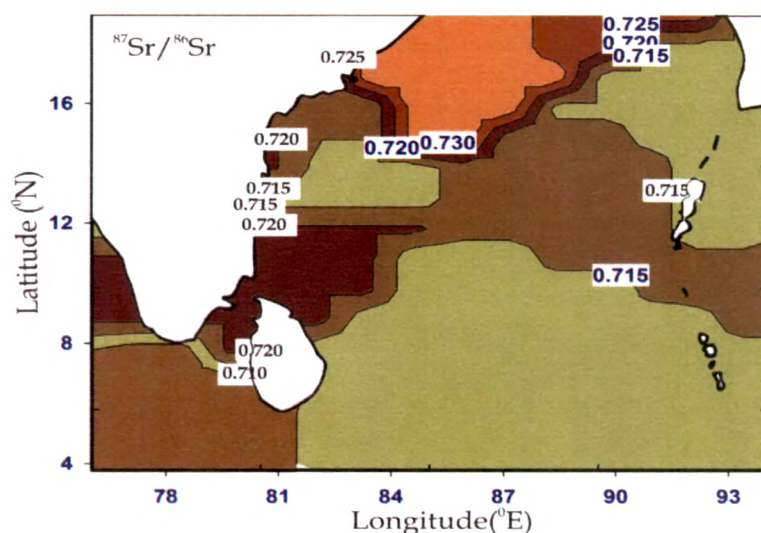


Fig. 4.14: Contour plot of $^{87}\text{Sr}/^{86}\text{Sr}$ distribution of sediments in the Bay of Bengal.

Sr and Nd. Similarly, the isotope plot of $^{87}\text{Sr}/^{86}\text{Sr}$ and ϵ_{Nd} shows that sediment distribution in the region is governed by the three end-members. The main sediment source seems to be G-B River system controlling the isotopic composition in the Bay of Bengal (Fig. 4.13). The Andaman Sea sediments are predominantly controlled by the Irrawaddy River. The sediments in the eastern Bay of Bengal and the northeastern Bay of Bengal display Sr and Nd isotopic characteristics possibly from two end members viz. G-B River system and Irrawaddy River (Fig. 4.14, 4.15). However, Colin et al., 1999 invoke another component of sediments from the Arakan coast responsible for such isotopic characteristics. It is likely that the Irrawaddy River can bring sediment into the Bay of Bengal through Arakan coast, while the Arakan coast by itself, can not account for large supply of the sediments resulting in such isotopic excursions in the sediments from the northeastern Bay of Bengal.

Once the sediment is brought into the Bay of Bengal, its dispersal is controlled by the surface circulation pattern. The surface circulation of the Bay of Bengal experiences seasonal reversal with East India coastal Current (EICC) flowing northeastward during summer monsoon from February until

September with a strong peak in March–April and it flows south–eastward during winter monsoon from October to January with the strongest flow in November (Shetye et al., 1996). During the winter monsoon, it is expected that sediments draining

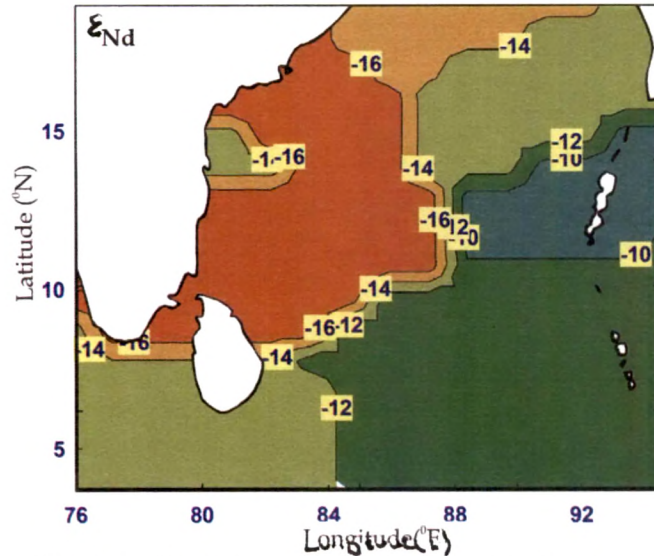


Fig. 4.15: Contour plot of ϵ_{Nd} distribution of sediments in the Bay of Bengal. Note, third end member with high ϵ_{Nd} from the eastern Bay of Bengal along the coast of Arakan through Irrawaddy River

from the Irrawaddy River are brought by the EICC to the Bay of Bengal through the Preparis channel. This seems to be a plausible mechanism for the lower values of $^{87}\text{Sr}/^{86}\text{Sr}$ and ϵ_{Nd} in the eastern Bay of Bengal. The $^{87}\text{Sr}/^{86}\text{Sr}$ and ϵ_{Nd} isotopic composition of the sediment from the station 4032 located strategically between two major sources (G–B and Irrawaddy River) show a mixed isotopic composition to attest for this assumption.

Chapter V

BAY OF BENGAL: PALAEOCLIMATIC IMPLICATIONS

Sedimentation in the Bay of Bengal is governed primarily by detrital input through various rivers draining into it and by overhead primary productivity. The composition of the sediments brought in by the various river systems depends on the terrain through which they flow (Sarin et al., 1989; Somayajulu et al., 1993, 2002). Erosion, composition, transportation and deposition processes of terrigenous sediments into the Bay of Bengal are essentially controlled by crustal deformation (tectonic) and climatic conditions (effect of monsoon). In the open oceans, these sediments serve as an archive of the Earth's geological history where effects of tectonics, climatic changes and eustasy are recorded and preserved. Rivers originating from the Himalayan regions contribute ~20% of the global sediment input to the Bay of Bengal (Milliman and Meade, 1983). The Ganga along with the Brahmaputra (the G-B River system) is one of the major contributors of sediment to the global ocean, transporting about 729×10^6 tons of sediment load annually to the Bay of Bengal (Coleman, 1969; Milliman and Syvitski, 1992; Curray, 1994). Nearly one third of the sediments discharged by the G-B River system is deposited in the shelf areas (Kuehl et al., 1997). As a result, the G-B River system has the largest delta and the largest submarine deep sea fan.

Sediment transfer from the continental areas to the Bay of Bengal is mainly governed by two distinct fluvial regimes, namely the Himalayan and the Peninsular Rivers. The G-B River system is the major contributor, however, in the Andaman Sea on the eastern Bay of Bengal, an additional contribution comes from the Irrawaddy and Salween Rivers (Rodolfo, 1969;

Sarin et al., 1979; Rao and Kessarkar, 2001; Rao et al., 2005; Chauhan et al., 2005). Besides this, the Bay of Bengal experiences a steady rain of biogenic debris which also contributes to the sedimentary budget. Considering that the sediment flux is intimately associated with the tectonic and

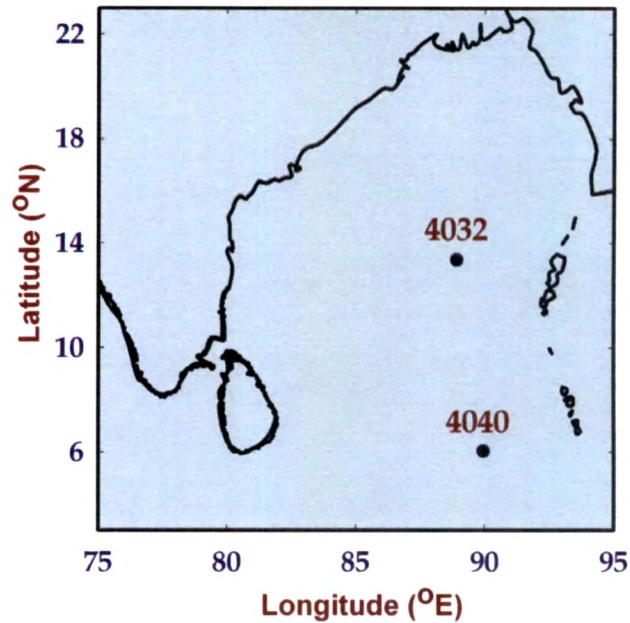


Fig. 5.1: Sediment core locations in the Bay of Bengal

climatic variability (monsoon), the sedimentary archive in the Bay of Bengal provides a rare opportunity to reconstruct the past climatic (Gupta and Thomas, 2003) and tectonic activity (Metivier and Gaudemer, 1999). It has been suggested that the monsoon driven hydrological changes caused significant variability in geochemical and isotopic proxies (Kudrass et al., 2001), so much so that centennial to millennial scale changes can be ascertained by careful investigation of sediment cores (Colin et al., 1998).

In the present study, signatures of geochemical and isotopic composition, total organic carbon (TOC) and carbon/nitrogen (C/N) ratio of the sediments have been used to reconstruct Late Quaternary climatic changes from two gravity cores viz. 4032 and 4040 collected from the central and southern Bay of Bengal respectively (Fig. 5.1). Considering that the detrital contribution is regulated through distinct fluvial systems, this study also attempts to investigate temporal change in contribution from different sources (provenance) during the sedimentation process to study the past erosional patterns. The central Bay of Bengal core 4032 (13.36°N; 88.9°E) was 148 cm in length raised from 3011 m water depth. The sediments in the core are

sandy and light coloured, foraminiferal ooze. However, the southern Bay of Bengal core 4040 (6.03°N; 89.94°E) was raised from relatively shallower water depth (2788 m) and was located at top of the 90° East Ridge (Fig. 5.1). The length of the core 4040 was 140 cm, contained whitish foram rich ooze. The core location 4032 represents a region of high detrital flux and overhead productivity in the central Bay of Bengal, whereas core 4040 (southern Bay of Bengal) has low detrital flux and moderate overhead productivity (Ramaswamy and Nair, 1994). Reconstruction of spatial and temporal changes in Late Quaternary climate and provenance was attempted using the geochemical, lithogenic and isotopic proxies, which were then viewed with respect to regional and global climatic pattern (Naidu and Malmgren, 1996, 1999; Naidu, 2007).

Chronology and Sedimentation Rates

Chronology, which constitutes the major component in any palaeoclimatic study, was obtained using the Accelerated Mass Spectrometry

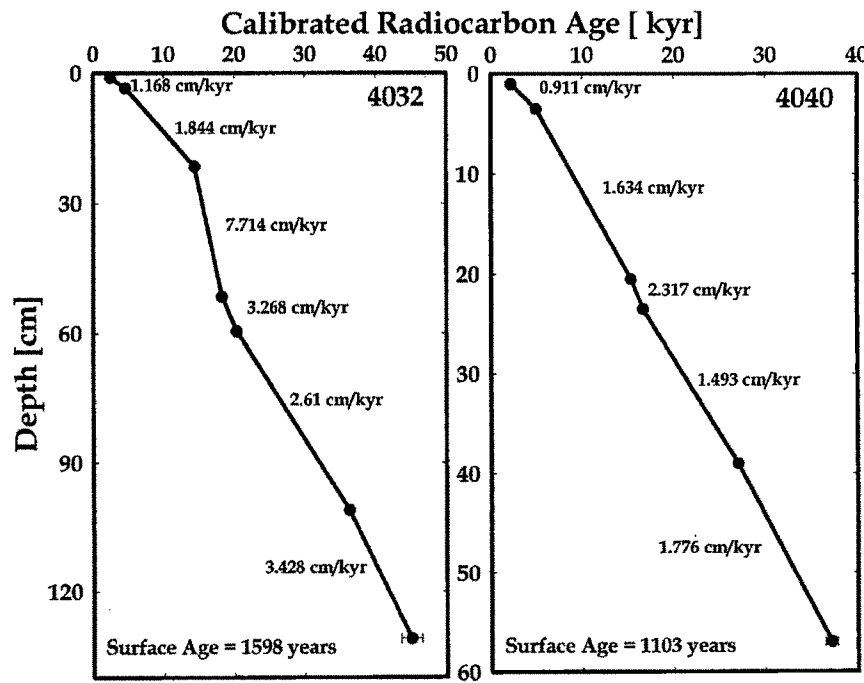


Fig. 5.2: Age-Depth plot model of the core 4032 and 4040 from the Bay of Bengal.

(AMS) radiocarbon dating of surface dwelling planktonic foraminifer (viz. *Globigerina Ruber*, *Globigerina Sacculifer* etc). Samples for AMS radiocarbon dating were collected from selected depths (Fig. 5.2) and a suite of planktonic foraminifer was separated by wet sieving. The AMS radiocarbon dating was carried out at National Science Foundation–Accelerated Mass Spectrometry (AMS) Facility at the University of Arizona, Tucson (USA). In case of core 4040, only the upper 60 cm was considered because it was a double bounce core beyond 80 cm. Ages thus obtained were calibrated

Table 5.1: AMS ^{14}C dates of *foraminifer* shells from the Cores 4032 and 4040
Core: 4040

Depth (cm)	AMS ^{14}C Age (yrs)	Error on ^{14}C Age	Calibrated ^{14}C Age (yrs BP)	Errors on Calibrated Age
0-2	2550	38	2201	67
3-4	4757	49	4946	80
20-21	13437	98	15348	183
23-24	14401	93	16643	223
38-40	23080	180	27028	211
56-58	31990	570	37165	662

Core: 4032

Depth (cm)	AMS ^{14}C Age (yrs)	Error on ^{14}C Age	Calibrated ^{14}C Age (yrs)	Error on Calibrated Age (yrs BP)
0-2	2788	45	2454	96
3-4	4455	46	4595	88
21-22	12958	85	14358	242
51-52	15445	87	18247	135
59-60	17660	110	20337	143
100-102	31140	510	36240	594
130-132	39700	1300	44992	1489

to calendar years using CALIB 4.1 (Stuiver et al., 1998a) with a ΔR value correction of 22 yrs (Dutta et al., 2001). A total of seven samples from core 4032 were dated and the ages range from 44992 ± 1489 (at 130–132 cm) to 2454 ± 96 cal yr (at 0–2 cm). In case of core 4040, six samples were analyzed and the ages range from 37165 ± 662 cal yr to 2201 ± 67 cal yr (Table-5.1). The extrapolated surface age for the core 4032 was 1598 years whereas for core 4040 it was 1103 years (Table 5.1, Fig. 5.2). The ages enabled to develop an age–depth model and the ages of intermediate depths were obtained by interpolation. However, sedimentation rate was calculated between actual adjacent ages (Fig. 5.2).

A significant variability in the sedimentation rate was observed in core 4032 which ranges from 7.714 cm/kyr (between 18247 cal yr to 14358 cal yr) and 1.168 cm/kyr (between 4595 cal yr to 2454 cal yr, Fig. 5.2). Compared to this, core 4040 shows marginal variability in sedimentation rate ranging from 2.317 cm/kyr (between 16643 cal yr to 15348 cal yr) and 0.911 cm/kyr (between 4946 cal yr to 2201 cal yr, Fig. 5.1). In addition, Mass Accumulation Rate (MAR) was calculated ($\text{g}/\text{cm}^2/\text{kyr}$) in the core 4032 to determine the sediment flux of the various elements. It was observed that between 50 kyr to ~21 kyr, the MAR fluctuated around $4 \text{ g}/\text{cm}^2/\text{kyr}$, except around 40 kyr when it marginally increased ($\sim 5 \text{ g}/\text{cm}^2/\text{kyr}$). However, after 20 kyr and 14 kyr, a significant increase of $\sim 13 \text{ g}/\text{cm}^2/\text{kyr}$ was observed.

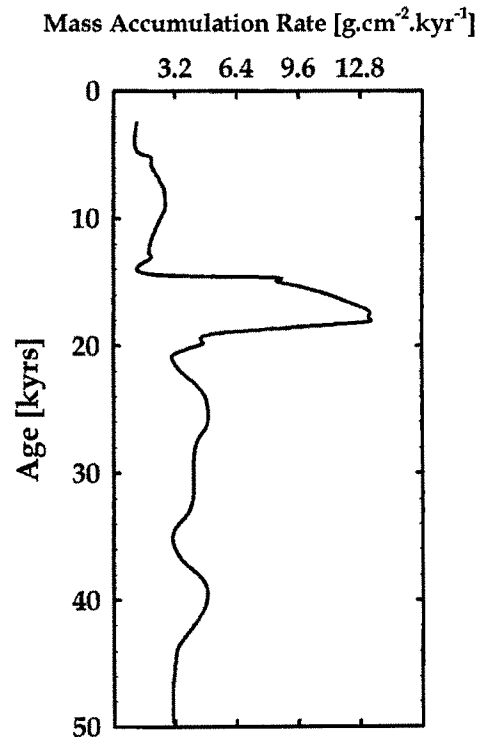


Fig. 5.3: Mass Accumulation Rate for the core 4032.

Following this, a consistent low MAR centering around $2 \text{ g.cm}^{-2}.\text{kyr}^{-1}$ persisted till around 2.5 kyr (Fig. 5.3).

Variation in Lithogenic Proxies

Sediment trap studies in the central Bay of Bengal show that the lithogenic flux is around $32 \text{ g.m}^{-2}.\text{day}^{-1}$ in shallow trap (995 m), and it

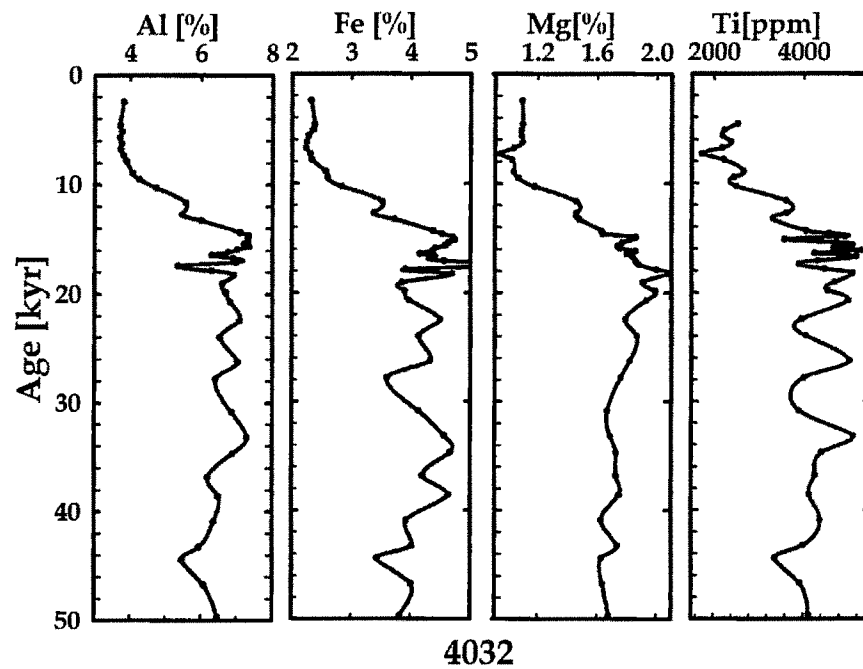


Fig. 5.4: Downcore variation of Al (%), Fe(%), Mg(%) and Ti(ppm) in the core 4032. In general, a slow decreasing pattern from 50 kyr to 14 kyr and a gradual decreasing pattern from 14 kyr to 7 kyr can be noticed.

almost doubled at $64 \text{ g.m}^{-2}.\text{day}^{-1}$ in the deep trap (2291 m) in the central Bay of Bengal during August, whereas during April–May, it increased marginally from $12 \text{ g.m}^{-2}.\text{day}^{-1}$ in shallow trap to $16 \text{ g.m}^{-2}.\text{day}^{-1}$ in the deep trap (Ramaswamy et al., 1997). Studies have shown that the lithogenic and the biogenic fluxes in the Bay of Bengal show identical patterns particularly during the southwest monsoon, which is attributed to the increased suspended load and increase in primary productivity facilitating efficient scavenging of the lithogenic particles (Ramaswamy et al., 1997). The

scavenging of the lithogenic particles is high during SW monsoon period due to a simultaneous increase in primary productivity and suspended load of the Bay of Bengal. Compared to this, discordance in lithogenic and biogenic flux was observed during winter monsoon, which is attributed to the reduction in fluvial discharge leading to the reduced lithogenic flux (Ramaswamy and Nair, 1994).

The concentration of the major elements as Al, Fe, Mg and Ti is used as a proxy for the continental terrigenous input to the oceans (Table 5.2; Goldberg and Arrhenius, 1958; Lisitsyn, 1972; Taylor and McLennan, 1985; Measures et al., 1986; Agnihotri et al., 2003). For example, Al belongs to the hydrolyzate elements and is not drawn into the biological cycle. Thus, its distribution in marine sediments reflects a terrigenous and volcanogenic source and is the second most widely distributed element (average concentration ~ 15%) in sedimentary deposits after silica (Lisitsyn, 1996; Dymond et al., 1997). Nature of distribution of Fe in ocean sediment is due to its participation in the biological cycle. In spite of this, Fe is associated both with sandy (proximal to ocean margins) and clayey fractions in pelagic realm (Skornyakova, 1970). In the equatorial zone, increased accumulation of Fe is observed in association with the fine grained sediments in coastal regions of Atlantic and Indian Oceans (Bostrom et al., 1973; Lisitsyn, 1996). The high concentration of Mg in marine sediments is associated with the basaltic rocks and thus its concentration can be used to identify the regions dominated by basaltic lithology. Additionally, it can also be contributed from the oceanic crust, and in few cases as terrigenous aeolian input (e.g. the Arabian Sea and the Indian Ocean; Lisitsyn, 1996). Ti and Fe are closely associated due to their identical ionic radii; however the latter is chemically stable, indicated by identical pattern of distribution (no grain size preference) in fluvial sediments (Lisitsyn, 1996).

The down core concentration variation of major elements (Al, Fe, Mg and Ti) in central Bay of Bengal (core-4032) shows a (i) consistent high values and low frequency fluctuations between 50 kyr and 14 kyr with an abrupt

Table: 5.2: Concentrations of Major and Trace elements in the bulk sediments of the core 4032

Core	Depth (cm)	Age (yrs)	Sr (ppm)	Cr (ppm)	Ba (ppm)	Mn (%)	Fe (%)	Mg (%)	Al (%)	Ca (%)
4032[0-2]	1	2454	726	44	729	0.16	2.3	1.10	3.8	23.4
4032[3-4]	3.5	4595	759	53	816	0.17	2.4	1.10	3.7	19.5
4032[4-5]	4.5	5137	745	57	865	0.19	2.4	1.09	3.8	19.5
4032[5-6]	5.5	5680	727	54	830	0.14	2.3	1.09	3.7	19.2
4032[6-7]	6.5	6222	735	56	854	0.18	2.3	1.10	3.8	18.7
4032[7-8]	7.5	6765	762	61	843	0.20	2.2	1.04	3.7	20.0
4032[8-9]	8.5	7307	715	60	649	0.22	2.3	0.95	3.8	20.2
4032[9-10]	9.5	7849	670	57	790	0.25	2.3	1.03	3.9	19.1
4032[11-12]	11.5	8934	646	67	706	0.37	2.6	1.04	4.1	17.6
4032[12-13]	12.5	9476	615	61	798	0.35	2.6	1.07	4.3	17.2
4032[13-15]	14	10290	538	59	707	0.40	2.8	1.18	4.7	16.0
4032[16-17]	16.5	11646	394	76	588	1.53	3.5	1.46	5.6	10.1
4032[18-19]	18.5	12731	448	77	695	2.31	3.4	1.46	5.5	12.0
4032[19-20]	19.5	13273	388	79	623	1.09	3.7	1.48	6.0	10.8
4032[21-22]	21.5	14358	277	91	487	0.49	4.4	1.63	7.1	6.8
4032[23-24]	23.5	14617	195	96	435	0.72	4.5	1.64	7.3	3.9
4032[25-26]	25.5	14877	242	99	582	2.23	4.7	1.86	7.3	4.7
4032[27-28]	27.5	15136	235	92	520	1.02	4.7	1.82	7.3	5.5
4032[29-30]	29.5	15395	239	88	511	0.57	4.6	1.77	7.2	5.4
4032[31-32]	31.5	15654	287	107	489	0.09	4.6	1.74	7.4	5.9
4032[33-34]	33.5	15914	286	102	502	0.07	4.4	1.75	7.0	6.4
4032[35-36]	35.5	16173	355	102	620	0.09	4.4	1.86	6.8	7.9
4032[37-38]	37.5	16432	388	94	650	0.10	4.2	1.80	6.3	8.7
4032[39-40]	39.5	16691	342	95	666	0.29	4.4	1.84	6.9	7.4
4032[42-43]	42.5	17080	302	101	553	0.08	4.6	1.86	7.0	7.0
4032[44-46]	45	17404	382	77	546	0.95	6.4	1.88	5.4	7.5
4032[48-49]	48.5	17858	359	92	606	0.08	3.9	2.00	6.3	8.8
4032[51-52]	51.5	18247	272	100	576	0.09	4.7	2.08	6.9	5.9
4032[54-55]	54.5	19031	322	99	535	0.07	3.9	1.91	6.6	7.5
4032[57-58]	57.5	19814	312	96	580	0.09	3.9	1.99	6.7	7.4
4032[60-61]	60.5	20720	313	100	562	0.10	4.0	1.93	6.8	7.6
4032[64-66]	65	22444	209	99	466	0.09	4.5	1.79	7.1	4.7
4032[68-70]	69	23977	309	93	538	0.10	4.1	1.87	6.5	7.5
4032[74-76]	75	26276	259	100	530	0.10	4.3	1.82	6.0	5.9
4032[78-80]	79	27809	373	92	582	0.10	3.6	1.76	6.4	9.3
4032[86-88]	87	30875	336	102	574	0.10	4.1	1.67	6.9	8.3
4032[92-94]	93	33174	265	107	439	0.10	4.6	1.69	7.3	5.8
4032[96-98]	97	34707	263	101	444	0.12	4.7	1.73	6.9	5.8
4032[102-104]	103	36824	356	90	556	0.13	4.2	1.73	6.2	8.8
4032[108-110]	109	38574	294	103	594	0.14	4.6	1.75	6.5	6.1
4032[116-118]	117	40908	366	97	602	0.11	3.9	1.63	6.4	8.8
4032[124-126]	125	43242	434	93	683	0.14	4.0	1.74	6.0	9.6
4032[128-130]	129	44409	497	95	711	0.13	3.4	1.63	5.5	10.9
4032[136-138]	137	46743	465	105	818	0.13	4.0	1.64	6.1	10.0
4032[146-148]	147	49660	397	107	708	0.11	3.8	1.68	6.5	9.0

Table 5.2 contd.

Core	Depth (cm)	Age (yrs)	Ni (ppm)	Co (ppm)	Zn (ppm)	Cu (ppm)	V (ppm)	Ti (ppm)
4032[0-2]	1	2454	--	--	--	--	--	--
4032[3-4]	3.5	4595	140	37	93	99	94	2535
4032[4-5]	4.5	5137	148	36	88	97	89	2245
4032[5-6]	5.5	5680	118	34	90	98	85	2192
4032[6-7]	6.5	6222	133	36	91	103	86	2379
4032[7-8]	7.5	6765	142	33	80	95	83	2183
4032[8-9]	8.5	7307	134	29	74	85	65	1735
4032[9-10]	9.5	7849	137	32	82	97	83	2222
4032[11-12]	11.5	8934	186	38	108	116	106	2666
4032[12-13]	12.5	9476	194	39	114	109	99	2447
4032[13-15]	14	10019	185	34	99	85	105	2503
4032[16-17]	16.5	11646	358	52	200	142	156	3616
4032[18-19]	18.5	12731	286	58	159	123	168	3621
4032[19-20]	19.5	13273	183	32	124	80	141	3322
4032[21-22]	21.5	14358	195	41	129	70	156	4052
4032[23-24]	23.5	14617	276	54	147	77	187	4575
4032[25-26]	25.5	14877	482	83	167	104	183	4924
4032[27-28]	27.5	15136	273	65	140	67	174	3582
4032[29-30]	29.5	15395	226	57	150	83	191	4726
4032[31-32]	31.5	15654	213	45	149	84	191	5066
4032[33-34]	33.5	15914	223	43	162	95	190	4660
4032[35-36]	35.5	16173	198	42	151	81	181	5276
4032[37-38]	37.5	16432	197	38	146	88	168	4247
4032[39-40]	39.5	16691	241	66	151	93	175	5175
4032[42-43]	42.5	17080	220	40	161	93	163	4309
4032[44-46]	45	17405	221	62	146	68	187	3905
4032[48-49]	48.5	17858	217	38	154	84	190	4471
4032[51-52]	51.5	18247	254	47	173	84	185	5086
4032[54-55]	54.5	19031	251	40	178	121	211	4694
4032[57-58]	57.5	19814	262	47	179	103	179	4546
4032[60-61]	60.5	20720	285	49	197	115	195	4994
4032[64-66]	65	22445	208	36	144	62	142	3961
4032[68-70]	69	23978	218	39	164	91	152	4065
4032[74-76]	75	26276	272	49	197	110	203	5024
4032[78-80]	79	27809	258	42	192	133	176	4023
4032[86-88]	87	30875	224	37	155	69	154	3912
4032[92-94]	93	33174	295	49	196	70	191	5104
4032[96-98]	97	34707	255	44	172	68	156	4412
4032[102-104]	103	36824	242	44	160	96	143	4258
4032[108-110]	109	38574	258	47	177	91	150	4134
4032[116-118]	117	40908	254	42	181	91	147	4375
4032[124-126]	125	43242	258	50	180	103	184	3993
4032[128-130]	129	44409	209	35	144	103	131	3376
4032[136-138]	137	46743	260	47	175	87	157	3924
4032[146-148]	147	49660	261	52	175	105	188	4118

decrease around 17 kyr in Al and Ti, (ii) a gradual decrease after 14 kyr which persisted till around 7 kyr and (iii) a consistently low values after 7 kyr till 2 kyr (Fig. 5.4). The association of Al with the lithogenically derived elements can serve as an indicator for Al content in opal which reflects the relative availability of iron and other trace nutrients (Dymond et al., 1997).

In case of the southern Bay of Bengal (core 4040), a high variability in the concentration of geochemical proxies is observed (Table 5.3). The down core variability indicates low frequency high magnitude fluctuations between 36 kyr and 3 kyr. A gradual increase after 36 kyr till 32 kyr followed by an abrupt decrease in Al, Fe and Mg around 30 kyr. This has been succeeded by an overall increase till around 22 kyr followed by a dip in the concentration of the above elements centering around 20 kyr (except for Mg). This was followed by an increase peaking around 14.5 kyr. After 14.5 kyr, a marginal decline in the geochemical proxies is noticed between 12.5 kyr to 10 kyr. After 10 kyr till 3 kyr, an increasing trend can be suggested though Mg and Ti show a decreasing trend (Fig.5.5).

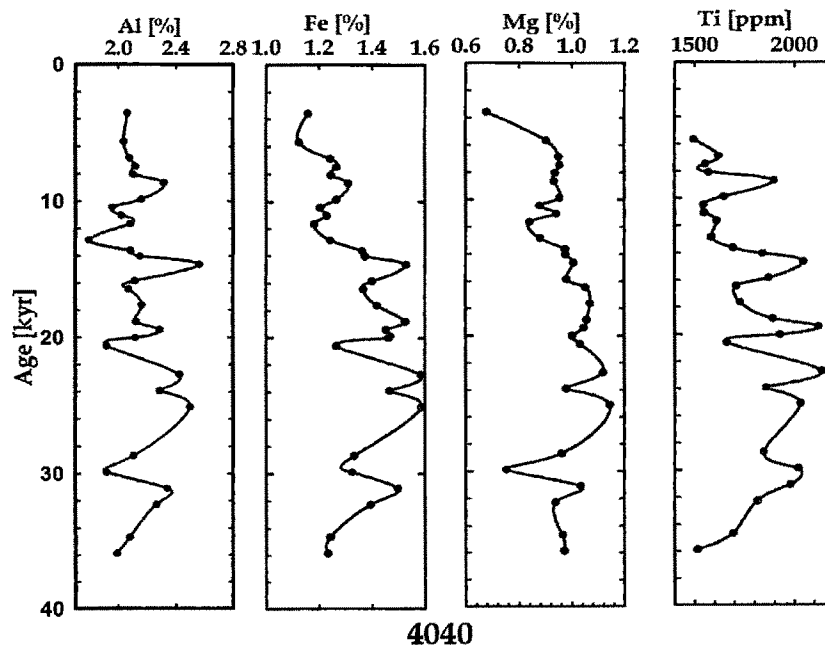


Fig. 5.5: Downcore variation of Al (%), Fe (%), Mg (%) and Ti (ppm) in the core 4040. Note, relatively high variability in their concentrations.

Table: 5.3: Concentrations of Major and Trace elements in the bulk sediments of the core 4040.

Core	Depth (cm)	Age (yrs)	Al (%)	Fe (%)	Mg (%)	Ca (%)	Sr (ppm)	Ba (ppm)	Ni (ppm)
4040[0-2]	1	3579	2.06	1.16	0.68	28.9	923	730	22
4040[4-5]	4.5	5671	2.04	1.12	0.90	16.6	1917	1530	85
4040[6-7]	6.5	6866	2.08	1.24	0.95	16.2	1890	1717	53
4040[7-8]	7.5	7464	2.12	1.27	0.95	16.5	1923	1680	71
4040[8-9]	8.5	8062	2.10	1.24	0.94	15.9	1811	1691	52
4040[9-10]	9.5	8659	2.32	1.31	0.93	15.6	1768	1699	73
4040[11-12]	11.5	9855	2.16	1.27	0.95	16.3	1847	1617	57
4040[12-13]	12.5	10453	1.96	1.20	0.88	15.7	1775	1580	52
4040[13-14]	13.5	11050	2.02	1.23	0.94	15.9	1829	1587	48
4040[14-15]	14.5	11648	2.08	1.18	0.84	15.8	1796	1460	68
4040[16-17]	16.5	12844	1.79	1.24	0.88	15.6	1753	1318	57
4040[17-18]	17.8	13621	2.08	1.36	0.97	15.8	1879	1423	90
4040[18-19]	18.5	14039	2.15	1.37	0.98	15.6	1873	1474	88
4040[19-20]	19.5	14637	2.56	1.53	1.01	16.0	1796	1473	147
4040[21-22]	21.5	15832	2.12	1.40	0.98	15.7	1766	1304	70
4040[22-23]	22.5	16430	2.07	1.37	1.05	15.6	1870	1273	55
4040[24-25]	24.5	17625	2.16	1.42	1.07	15.8	1845	1238	67
4040[26-27]	26.5	18821	2.12	1.52	1.06	15.7	1859	1233	49
4040[27-28]	27.5	19419	2.29	1.45	1.05	15.4	1786	1336	50
4040[28-29]	28.5	20016	2.12	1.46	1.00	14.9	1712	1137	50
4040[29-30]	29.5	20614	1.92	1.27	1.03	15.9	1840	1071	67
4040[32-34]	33	22706	2.42	1.58	1.12	15.5	1898	1225	58
4040[34-36]	35	23902	2.29	1.47	0.98	15.5	1832	1113	51
4040[36-38]	37	25097	2.50	1.59	1.14	15.6	1762	1231	61
4040[42-44]	43	28683	2.10	1.33	0.96	15.4	1872	1135	49
4040[44-46]	45	29879	1.92	1.33	0.75	14.5	1676	1171	51
4040[46-48]	47	31074	2.34	1.50	1.03	15.6	1806	1238	54
4040[48-50]	49	32270	2.26	1.39	0.94	15.8	1784	1291	63
4040[52-54]	53	34661	2.08	1.24	0.97	16.3	1751	1234	55
4040[54-56]	55	35856	1.99	1.23	0.97	16.2	1738	1214	56

Table 5.3 Contd.

Core	Depth (cm)	Age (yrs)	Co (ppm)	Cr (ppm)	Mn (ppm)	Zn (ppm)	Cu (ppm)	V (ppm)	Ti (ppm)
4040[0-2]	1	3579	16	20	648	--	--	--	--
4040[4-5]	4.5	5671	20	63	1369	92	10	55	1495
4040[6-7]	6.5	6866	21	73	1367	64	65	56	1622
4040[7-8]	7.5	7464	23	69	1443	65	64	55	1554
4040[8-9]	8.5	8062	21	70	1471	63	66	58	1571
4040[9-10]	9.5	8659	22	70	1612	88	108	66	1899
4040[11-12]	11.5	9855	20	68	1454	97	108	56	1646
4040[12-13]	12.5	10453	21	67	1703	61	64	53	1547
4040[13-14]	13.5	11050	20	71	1464	59	61	53	1548
4040[14-15]	14.5	11648	22	66	1370	92	88	55	1611
4040[16-17]	16.5	12844	21	70	1350	65	63	54	1585
4040[17-18]	17.8	13621	26	69	1901	68	64	62	1694
4040[18-19]	18.5	14039	26	73	2547	73	71	63	1841
4040[19-20]	19.5	14637	33	80	3848	115	113	74	2046
4040[21-22]	21.5	15832	60	74	2179	71	60	67	1872
4040[22-23]	22.5	16430	55	76	1408	69	54	62	1710
4040[24-25]	24.5	17625	62	86	1159	94	107	63	1729
4040[26-27]	26.5	18821	30	85	617	74	54	67	1893
4040[27-28]	27.5	19419	24	85	501	77	60	68	2121
4040[28-29]	28.5	20016	16	82	393	78	70	63	1928
4040[29-30]	29.5	20614	19	82	401	98	122	63	1662
4040[32-34]	33	22706	18	91	425	81	59	72	2138
4040[34-36]	35	23902	17	80	395	104	128	63	1860
4040[36-38]	37	25097	18	89	413	115	139	72	2032
4040[42-44]	43	28683	16	81	361	100	131	60	1846
4040[44-46]	45	29879	18	81	355	77	72	64	2020
4040[46-48]	47	31074	18	86	406	104	123	67	1981
4040[48-50]	49	32270	19	75	421	98	118	60	1816
4040[52-54]	53	34661	18	78	323	92	120	58	1694
4040[54-56]	55	35856	17	70	402	97	137	51	1514

To ascertain the variation in sediments flux in core 4032, the flux of the detrital proxies were calculated using the varying sedimentation rate and the moisture content. The average flux of Al, Fe, Mg and Ti was found to be near constant between 50 kyr till 20 kyr with a minor increase around 40 kyr. For example, Al and Fe varied between 15–25 $\text{g.cm}^{-2}.\text{kyr}^{-1}$, Mg 4–8 $\text{g.cm}^{-2}.\text{kyr}^{-1}$ and Ti 1–2 $\text{g.cm}^{-2}.\text{kyr}^{-1}$. After 20 kyr, all the lithogenic proxies show abrupt increases that persist till 14 kyr (Al and Fe 85–90 $\text{g.cm}^{-2}.\text{kyr}^{-1}$, Mg 28 $\text{g.cm}^{-2}.\text{kyr}^{-1}$ and Ti 6 $\text{g.cm}^{-2}.\text{kyr}^{-1}$). After 14 kyr till 2 kyr, overall a decrease in all proxies was seen (Fig. 5.6). In the absence of availability of moisture measurements for the core 4040, the fluxes could not be calculated for this

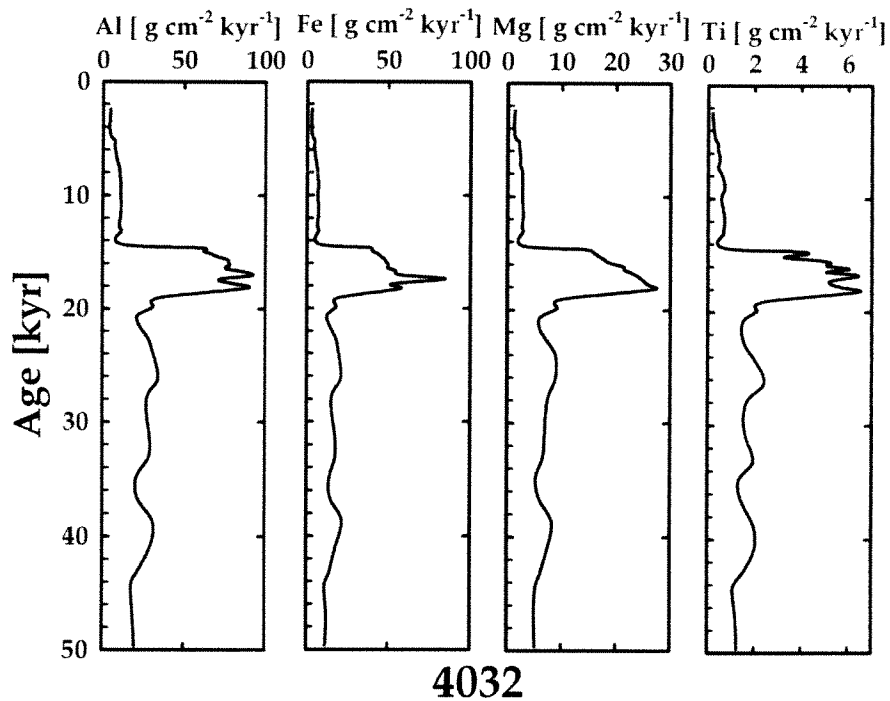


Fig. 5.6: Mass accumulation rate of lithogenic proxies for the core 4032. Abrupt increase from 20 kyr to 14 kyr indicates enhanced sediment flux.

The geochemical proxies were further weight normalized to Al in order to ascertain the temporal changes in sediment provenance for both central (4032) and southern (4040) Bay of Bengal cores (Figs. 5.7 and 5.8). The reason being, weighted ratios of Ti/Al and Mg/Al has been successfully used to infer changes in the aeolian contribution through time in the western and

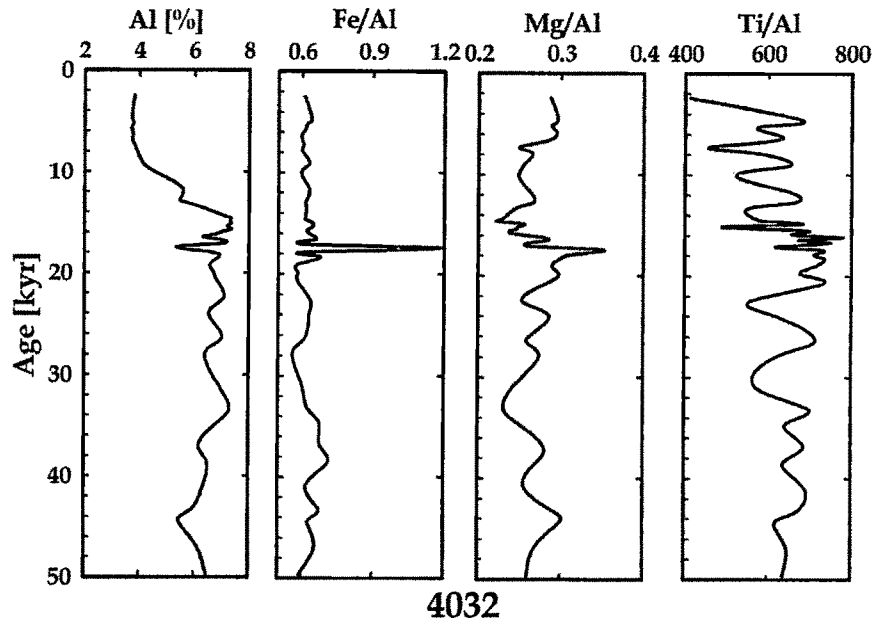


Fig. 5.7 Downcore variation of Al, Fe/Al, Mg/Al and Ti/Al in the core 4032

northwestern Arabian Sea (Sirocko et al., 1993; Reichart et al., 1997). However, in the case of southern Bay of Bengal (4040), a linear increase in Ti/Al ratio through time was attributed to increased denudation rates in Himalayan, maturation of Indian River systems and evolution of the southwest monsoon system (Nath et al., 1997; Timothy and Calvert, 1998).

The Fe/Al ratio in core 4032 remained almost constant (~ 0.6) except around 18 kyr where it sharply increases to 1. The Mg/Al ratio shows marginal fluctuation with an increase around 44 kyr and 18 kyr, following this, the ratio decreases till 12 kyr. After 12 kyr, a marginal increase is seen. In the case of Ti/Al, it can be suggested that there was an overall increase until around 18 kyr with prominent low values between ~ 34 kyr and ~ 22 kyr punctuated by an increase at ~ 26 kyr. After 18 kyr, an overall decrease with fluctuation till 2 kyr has been observed (Fig. 5.7). In the case of southern Bay of Bengal (4040), Fe/Al and Ti/Al ratios show an increasing trend from 36 kyr culminating around 30 kyr. After 30 kyr, Fe/Al show almost constant value

with minor fluctuation till 14 kyr. Following this, a marginal decrease till 1.5 kyr was seen. Similar trends are also observed in Mg/Al and Ti/Al (Fig. 5.8).

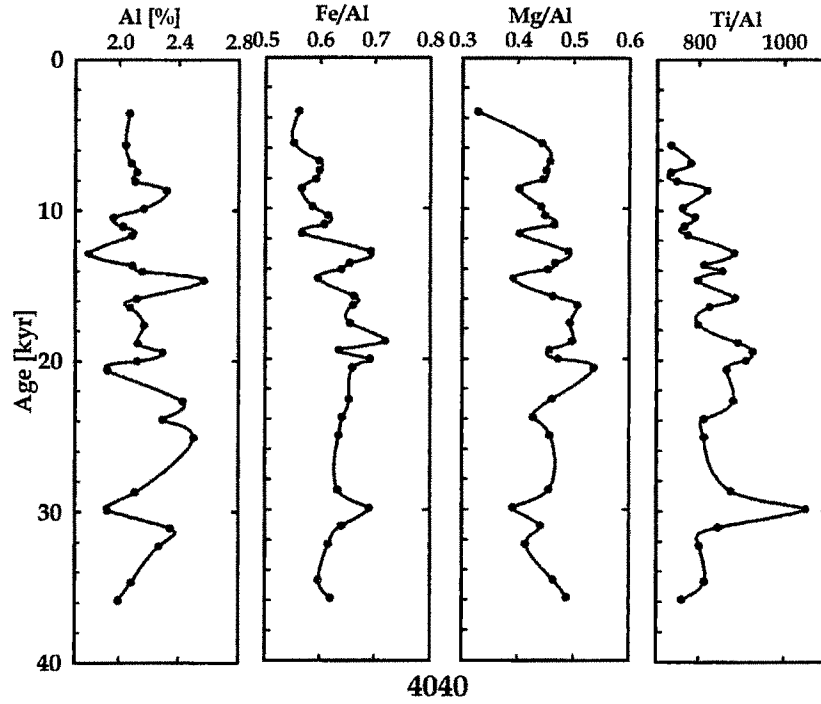


Fig. 5.8 Downcore variation of Al, Fe/Al, Mg/Al and Ti/Al in the core 4040.

Variation in Productivity Proxies

Palaeoproductivity is estimated using the biogenic remnants such as organic carbon, carbonate, opal, barium etc. Productivity in the Bay of Bengal is influenced by coastal upwelling along the east coast of India during SW monsoon (Shetye et al., 1991; Madhupratap et al., 2003; Kumar et al., 2004; Prassanna Kumar et al., 2007). The high freshwater flux from the Ganga and the Brahmaputra River in the northern region of the Bay of Bengal dampens the upwelling signatures. The primary productivity during December is marginally high (0.3 to 0.7 g.C.m⁻².day⁻¹) due to strengthened NE monsoon (October–November) that facilitates the supply of nutrients to the coastal waters. However, compared to this, the average surface productivity during SW monsoon (June–September) is relatively high which ranges from 51 to 113 mg.C.m⁻².day⁻¹ (Madhupratap et al., 2001; Gauns et al., 2005).

Carbonate, organic carbon, C/N ratio, $\delta^{13}\text{C}$, $\delta^{15}\text{N}$ along with Ca, Ba, and Sr and ratio of these elements normalized to Al were used as indicators of palaeoproductivity. The carbonate contribution in marine sediment (continental slope and pelagic oceans) is due to the growth of coccolithophores, foraminifera and pteropods. Concentration of phytoplanktons is governed by the presence of nutrients which can be of primary origin (from continent) or recycled by upwelling. In either case, variation in marine carbonate in principle would suggest strengthened monsoon conditions.

In core 4032, the carbonate concentration fluctuates around 20% between 50 kyr to ~14 kyr punctuated by frequent millennial scale low amplitude fluctuations (Table 5.4). After 14 kyr, a steady rise in carbonate content was observed that attains a maximum value of ~55% at the top dated

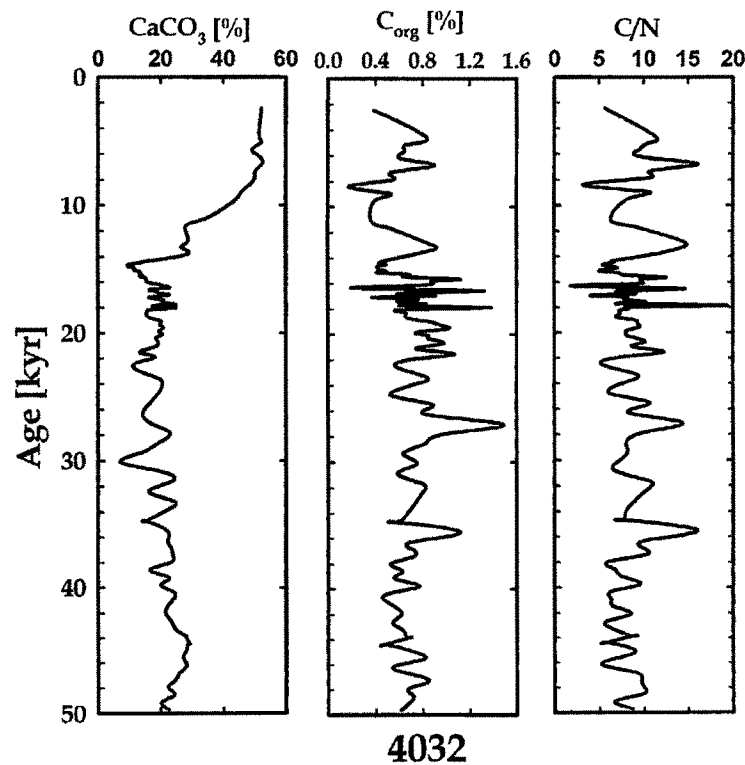


Fig. 5.9 Downcore variation of CaCO_3 , C_{org} and C/N in the core 4032

Table 5.4: Concentration of total carbon, organic carbon (C_{org}) and CaCO₃ along with C/N ratios in the core 4032

Core	Depth (cm)	Age (yrs)	CaCO ₃ (%)	Total C (%)	N (%)	C _{org} (%)	C/N
4032(0-2)	1	2454	52	6.7	0.07	0.39	5.7
4032(3-4)	3.5	4595	52	7.0	0.07	0.84	11.3
4032(4-5)	4.5	5137	52	6.9	0.06	0.66	10.6
4032(5-6)	5.5	5680	49	6.6	0.07	0.65	9.5
4032(6-7)	6.5	6222	52	6.8	0.06	0.62	9.8
4032(7-8)	7.5	6765	53	7.2	0.06	0.90	16.1
4032(8-9)	8.5	7307	50	6.6	0.05	0.53	10.8
4032(9-10)	9.5	7849	50	6.6	0.05	0.56	10.7
4032(10-11)	10.5	8392	49	6.0	0.05	0.17	3.1
4032(11-12)	11.5	8934	46	6.0	0.05	0.52	10.4
4032(12-13)	12.5	9476	44	5.7	0.05	0.40	8.3
4032(13-15)	14	10290	40	4.7	0.05	--	--
4032(15-16)	15.5	11104	34	4.4	0.06	0.37	6.4
4032(16-17)	16.5	11646	28	3.9	0.06	0.52	8.8
4032(18-19)	18.5	12731	29	4.3	0.06	0.82	14.1
4032(19-20)	19.5	13273	27	4.1	0.06	0.91	14.4
4032(20-21)	20.5	13816	29	4.1	0.06	0.67	11.4
4032(21-22)	21.5	14358	16	2.3	0.07	0.43	6.7
4032(22-23)	22.5	14488	14	2.1	0.07	0.49	6.7
4032(23-24)	23.5	14617	10	1.6	0.07	0.42	5.7
4032(24-25)	24.5	14747	10	1.6	0.07	0.42	5.7
4032(25-26)	25.5	14877	12	1.8	0.06	0.44	7.1
4032(26-27)	26.5	15006	11	1.9	0.08	0.49	5.9
4032(27-28)	27.5	15136	13	2.0	0.08	0.42	5.1
4032(28-29)	28.5	15265	13	2.3	0.10	0.68	6.8
4032(29-30)	29.5	15395	14	2.3	0.09	0.64	7.5
4032(30-31)	30.5	15525	13	2.4	0.09	0.76	8.8
4032(31-32)	31.5	15654	15	2.9	0.09	1.12	12.6
4032(32-33)	32.5	15784	15	2.7	0.09	0.91	10.1
4032(33-34)	33.5	15914	15	2.7	0.09	0.89	9.8
4032(34-35)	34.5	16043	17	2.9	0.09	0.87	9.7
4032(35-36)	35.5	16173	20	3.1	0.08	0.69	8.8
4032(36-37)	36.5	16302	21	2.7	0.11	0.20	--
4032(37-38)	37.5	16432	23	3.4	0.08	0.63	8.0
4032(38-39)	38.5	16562	17	3.3	0.09	1.33	14.7
4032(39-40)	39.5	16691	19	3.1	0.09	0.81	8.9
4032(40-41)	40.5	16821	19	2.9	0.09	0.61	7.2
4032(41-42)	41.5	16951	23	3.6	0.10	0.90	9.0
4032(42-43)	42.5	17080	20	2.8	0.09	0.37	4.0
4032(43-44)	43.5	17210	16	2.7	0.10	0.76	8.0
4032(44-46)	45	17404	21	3.1	0.07	0.58	7.8
4032(46-47)	46.5	17599	21	3.3	0.08	0.83	10.2
4032(47-48)	47.5	17728	25	3.6	0.08	0.62	7.4
4032(48-49)	48.5	17858	17	3.5	0.07	1.38	19.4
4032(49-50)	49.5	17988	25	3.8	0.09	0.80	9.4
4032(50-51)	50.5	18117	18	2.7	0.07	0.57	8.3
4032(51-52)	1.5	18247	16	2.5	0.09	0.65	7.3
4032(52-53)	52.5	18508	15	2.5	0.09	0.66	7.4
4032(53-54)	53.5	18769	1719.9	2.7	0.10	0.71	7.0

4032(54-55)	54.5	19031	19.6	3.27	0.10	0.88	9.1
4032(55-56)	55.5	19292	20.9	3.31	0.10	0.96	9.3
4032(56-57)	56.5	19553	19.3	3.52	0.11	1.01	9.5
4032(57-58)	57.5	19814	20.5	3.06	0.09	0.75	8.2
4032(58-59)	58.5	20076	18.5	3.30	0.11	0.84	8.0
4032(59-60)	59.5	20337	19.2	3.07	0.10	0.85	8.5
4032(60-61)	60.5	20720	17.6	3.28	0.10	0.98	10.2
4032(61-62)	61.5	21103	13.4	2.85	0.09	0.74	8.7
4032(62-63)	62.5	21486	18.2	2.68	0.09	1.07	12.3
4032(63-64)	63.5	21870	11.3	2.95	0.10	0.77	8.1
4032(64-66)	65	22444	15.9	1.92	0.11	0.57	5.3
4032(66-68)	67	23211	20.5	2.70	0.09	0.80	9.0
4032(68-70)	68.5	23786	19.1	3.24	0.09	0.78	8.5
4032(70-72)	71	24744	16.4	2.82	0.09	0.53	6.1
4032(72-74)	73	25510	14.3	2.87	0.08	0.89	10.8
4032(74-76)	75	26276	16.8	2.54	0.10	0.83	8.3
4032(76-78)	77	27043	23.0	3.51	0.10	1.49	14.3
4032(78-80)	79	27809	19.3	3.75	0.10	0.98	10.2
4032(80-82)	81	28576	13.9	3.13	0.10	0.82	8.1
4032(82-84)	83	29342	7.3	2.30	0.08	0.63	8.2
4032(84-86)	85	30108	21.0	1.63	0.11	0.75	7.1
4032(86-88)	87	30875	23.0	3.10	0.09	0.59	6.9
4032(88-90)	89	31641	16.1	3.55	0.07	0.79	10.6
4032(90-92)	91	32408	24.5	2.73	0.08	0.80	10.2
4032(92-94)	93	33174	21.1	2.37	0.09	--	--
4032(94-96)	95	33940	15.2	3.21	0.08	0.68	8.1
4032(96-98)	97	34707	21.9	2.40	0.08	0.58	7.8
4032(98-100)	99	35473	22.2	3.75	0.07	1.12	16.0
4032(100-102)	101	36240	23.3	3.38	0.07	0.72	10.7
4032(102-104)	103	36824	23.9	3.51	0.07	0.71	9.8
4032(104-106)	105	37407	22.8	3.59	0.07	0.72	10.3
4032(106-108)	107	37991	16.5	3.26	0.09	0.52	6.0
4032(108-110)	109	38574	22.7	2.61	0.09	0.63	6.8
4032(110-112)	111	39158	19.9	3.28	0.07	0.56	7.6
4032(112-114)	113	39741	24.1	3.16	0.08	0.77	9.6
4032(114-116)	115	40325	23.9	3.40	0.08	0.51	6.4
4032(116-118)	117	40908	21.9	3.35	0.08	0.48	6.4
4032(118-120)	119	41492	21.6	3.22	0.09	0.59	6.7
4032(120-122)	121	42075	23.4	3.20	0.07	0.61	8.6
4032(122-124)	123	42658	24.7	3.35	0.09	0.55	5.9
4032(124-126)	125	43242	28.1	3.60	0.10	0.64	6.5
4032(126-128)	127	43825	28.8	4.04	0.08	0.67	8.6
4032(128-130)	129	44409	28.1	3.96	0.08	0.51	6.2
4032(130-132)	131	44992	27.1	4.10	0.08	0.73	9.0
4032(132-134)	133	45576	28.3	4.05	0.11	0.80	7.3
4032(134-136)	135	46159	25.9	3.95	0.10	0.55	5.3
4032(136-138)	137	46743	24.7	3.80	0.08	0.69	8.9
4032(138-140)	139	47326	22.3	3.81	0.09	0.85	9.8
4032(140-142)	141	47910	24.4	3.35	0.07	0.68	10.0
4032(142-144)	143	48493	20.2	3.64	0.07	0.72	9.9
4032(144-146)	145	49077	22.5	3.10	0.10	0.68	6.7
4032(146-148.5)	147	49660		3.31	0.07	0.61	8.7

to 2.5 kyr (Fig. 5.9). Compared to this in core 4040, a gradual increase in carbonate concentration is observed after 40 kyr followed by a declining trend culminating around 30 kyr. Further, a marginal increase is noticed after 22 kyr with fluctuations followed by an increasing trend after 14 kyr which peak around 12.5 kyr. After 12.5 kyr, a marginal decline in carbonate concentration was observed which persists till 7 kyr. After 7 kyr till 3 kyr, it shows an increasing trend (Fig. 5.10).

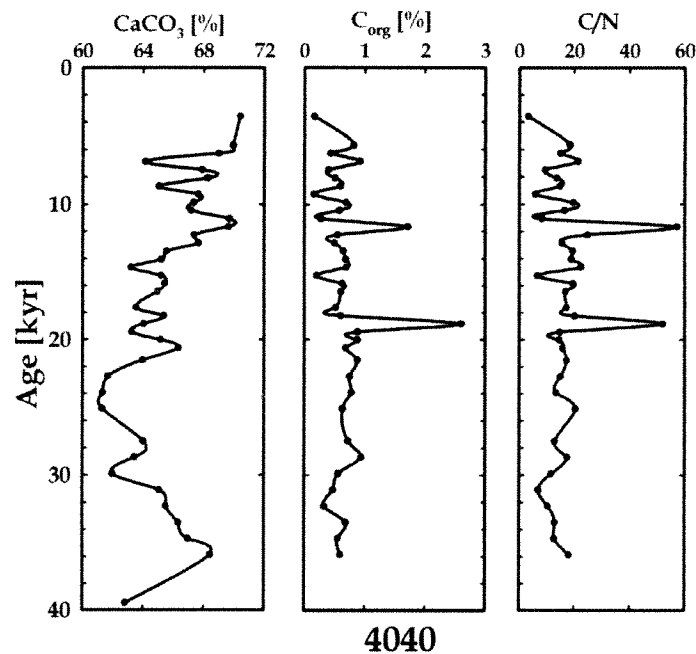


Fig. 5.10 Downcore variation of CaCO_3 , C_{org} and C/N in the core 4040

Though, there are several factors controlling the sedimentary organic carbon (C_{org}), it has still been extensively used to estimate palaeoproductivity (Agnihotri et al., 2003b; Bhushan et al., 2001; Galy et al., 2008). In the open ocean, only a small fraction of the organic matter produced in the upper ocean surface reaches the sea floor due to the degradation by microbial and chemical processes while it descends to the seafloor. However, on reaching the sea floor, early diagenetic reactions at sediment water interface makes it refractory and hence it gets preserved in the sediment record (Hartnett et al., 1998). Although, C_{org} in coastal regions can be used as a productivity indicator, the C_{org} content variation in the open ocean is due to its

preservation characteristics. In view of this, C_{org} has limited applicability as a potential productivity tracer in the open ocean (Emerson, 1985; Emerson and Hedges, 1988; Calvert and Pedersen, 1992; Paropkari et al., 1993; Canfield, 1994; Hartnett et al., 1998).

C_{org} in both the cores remained fairly constant (fluctuation between 0.5 to 1%) except for an increase around 35.5 kyr, 27 kyr and 18 kyr (core 4032) and around 20 kyr and 12 kyr (core 4040). During these periods, the C_{org} value is >1% (Table 5.5, Figs. 5.9 and 5.10). The carbon/nitrogen (C/N) ratio in the marine sediments is used to trace the source of organic carbon. For instance, the reported C/N ratio of phytoplankton and zooplankton is ~6, for freshly deposited organic matter, this ratio is ~10, while terrigenously (land derived) derived organic matter has ratios ranging from 20–200 (Meyers 1994, 1997). Overall the C/N ratio fluctuates between 5–10 suggesting a predominantly marine origin of the organic matter (overhead productivity). However, there are periods viz. 35.5 kyr, 27 kyr, 18 kyr, 13 kyr and 7 kyr (core 4032) and 20 kyr, 12 kyr (core 4040) when C/N ratio is greater than 10 (Figs. 5.9 and 5.10) suggesting a continental source. The $\delta^{13}C$ of the organic matter in marine sediments is used to identify the continental versus marine source of the organic matter. The marine organic matter $\delta^{13}C$ is around -19‰ , whereas for the continental origin it is around -26‰ (Table 5.6). The $\delta^{13}C$ of the organic matter in the northern Bay of Bengal (core 4032) is modulated by both overhead productivity and its subsequent enhanced transport to seafloor by adhering to the detrital particles from continental input (France–Lanord and Derry, 1994; Galy and France–Lanord, 2006; Galy et al., 2008). It is observed in core 4032 that during 42 kyr and 16 kyr, the $\delta^{13}C$ values fluctuated between -20‰ and -18‰ implying the dominance of marine origin material. After 16 kyr, depleted value of $\delta^{13}C$ ($<-22\text{‰}$) suggests a continental organic carbon contribution (Fig. 5.11).

The $\delta^{15}N$ of the C_{org} reflects the denitrification process in the marine sediments. The C_{org} undergoes microbial degradation through consumption of

Table 5.5: Concentration of total carbon, organic carbon (C_{org}) and CaCO₃ along with C/N ratios in the core 4040.

Core	Depth (cm)	Total C (%)	CaCO ₃ (%)	N (%)	C _{org} (%)	C/N
4040 [0-2]	1	8.6	70	0.05	0.16	3.3
4040 [4-5]	4.5	9.2	70	0.04	0.82	18.5
4040 [5-6]	5.5	8.7	69	0.03	0.43	15.0
4040 [6-7]	6.5	8.6	64	0.04	0.92	21.5
4040 [7-8]	7.5	8.6	68	0.04	0.40	9.5
4040 [8-9]	8.5	8.7	68	0.04	0.51	13.7
4040 [9-10]	9.5	8.4	65	0.04	0.59	14.9
4040 [10-11]	10.5	8.3	68	0.03	0.15	5.9
4040 [11-12]	11.5	8.8	67	0.04	0.69	19.7
4040 [12-13]	12.5	8.6	67	0.04	0.58	16.6
4040 [13-14]	13.5	8.6	70	0.03	0.28	8.4
4040 [14-15]	14.5	10.1	70	0.03	1.71	57.1
4040 [15-16]	15.5	8.6	67	0.02	0.55	24.9
4040 [16-17]	16.5	8.6	68	0.03	0.50	15.7
4040 [17-18]	17.5	8.5	66	0.03	0.65	19.6
4040 [18-19]	18.5	8.5	65	0.04	0.68	19.0
4040 [19-20]	19.5	8.3	63	0.03	0.69	22.4
4040 [20-21]	20.5	8.0	65	0.03	0.20	6.7
4040 [21-22]	21.5	8.5	65	0.03	0.63	19.6
4040 [22-23]	22.5	8.4	65	0.04	0.61	16.8
4040 [24-25]	24.5	8.1	64	0.03	0.52	17.2
4040 [26-27]	26.5	8.3	64	0.03	0.61	20.2
4040 [27-28]	27.5	10.2	63	0.05	2.60	52.0
4040 [28-29]	28.5	8.7	65	0.06	0.88	14.9
4040 [29-30]	29.5	8.8	66	0.06	0.88	14.7
4040 [30-32]	31	8.4	64	0.04	0.68	15.9
4040 [32-34]	33	8.3	62	0.05	0.88	17.3
4040 [34-36]	35	8.1	61	0.05	0.75	15.0
4040 [36-38]	37	8.1	61	0.06	0.78	13.5
4040 [40-42]	41	8.3	64	0.03	0.64	20.5
4040 [42-44]	43	8.3	63	0.06	0.73	13.0
4040 [44-46]	45	8.4	62	0.05	0.94	17.5
4040 [46-48]	47	8.4	65	0.05	0.56	11.7
4040 [48-50]	49	8.3	66	0.07	0.48	7.1
4040 [50-52]	51	8.3	66	0.03	0.33	10.6
4040 [52-54]	53	8.7	67	0.05	0.69	13.1
4040 [54-56]	55	8.8	68	0.04	0.56	13.0
4040 [60-62]	61	8.1	63	0.03	0.60	18.2

Table 5.6: $\delta^{13}\text{C}$ and $\delta^{15}\text{N}$ of the organic matter in the core 4032 from the Bay of Bengal.

Core	Depth (cm)	Age (yrs)	$\delta^{13}\text{C}$ (‰)	$\delta^{15}\text{N}$ (‰)
4032(0-2)	1	2000	-20.2	6.2
4032(3-4)	3.5	4876	-20.9	--
4032(7-8)	7.5	7050	-19.9	--
4032(11-12)	11.5	9224	-22.0	5.7
4032(16-17)	16.5	11941	-22.3	--
4032(21-22)	21.5	14658	-21.5	4.3
4032(23-24)	23.5	15280	-21.2	--
4032(27-28)	27.5	16522	-21.2	4.4
4032(31-32)	31.5	17764	-20.3	4.6
4032(35-36)	35.5	19007	-22.9	--
4032(39-40)	39.5	20248	-18.4	5.0
4032(44-46)	45	20869	-18.0	5.1
4032(53-54)	53.5	20869	-20.7	--
4032(60-61)	60.5	21532	-21.1	--
4032(64-66)	65	24512	-18.7	4.5
4032(72-74)	73	29148	-19.2	5.2
4032(82-84)	83	33899	-18.8	4.7
4032(92-94)	93	35059	-20.2	4.8
4032(102-104)	103	36295	-17.8	5.0
4032(112-114)	113	39372	-18.8	4.7
4032(124-126)	125	43065	-21.3	--
4032(128-130)	129	44295	-21.3	--
4032(136-138)	137	46755	-19.7	5.2
4032(146-148.5)	147	49834	-21.9	--

the dissolved oxygen while it's traverse through the water column. Enhanced overhead productivity results in depletion of the dissolved oxygen in the sub-surface waters causing an Oxygen Minimum Zone (200–1000 m) within the water column due to its consumption by C_{org} , as a result there is a reduction of nitrate to nitrite and finally to N_2 (Naqvi, 1994; Howell et al., 1997; Naqvi et al., 2006). This process of oxygen consumption by the settling C_{org} material is known as denitrification. The process of denitrification leads to an enrichment of $\delta^{15}N$ of the C_{org} with increasing denitrification (Schafer and Ittekkot, 1993; Altabet et al., 2002). The $\delta^{15}N$ values vary narrowly between 4 ‰ to 5.2 ‰ between 50 kyr to 14 kyr. After 14 kyr, a steady increase up to 6‰ indicates an intensification of the denitrification process (Fig. 5.11).

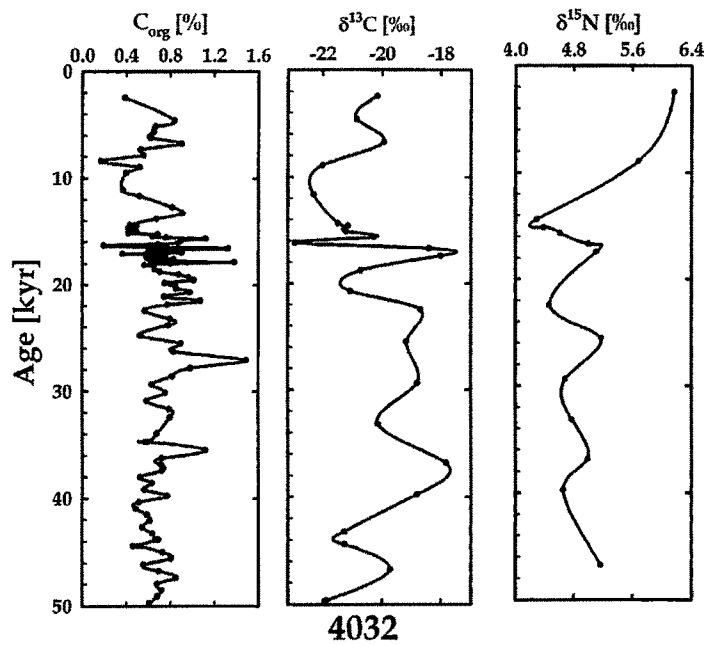


Fig. 5.11: Downcore variation of C_{org} and $\delta^{13}C$ and $\delta^{15}N$ of the organic matter in the core 4032.

Only 0.1 to 1% of the organic carbon produced in the surface waters is preserved in sediments (Berger et al., 1989), therefore, palaeoproductivity estimates based on organic carbon is fraught with uncertainties (Klump et al., 2000). In view of this, the variation in productivity based on organic carbon as

discussed above is further assessed using geochemical proxies as Ba, Ca and Sr, which are considered to be less affected by post depositional changes (Dymond et al., 1992; Schenau et al., 2001; Babu et al., 2002).

Barium is supplied to the seafloor by two main sources (i) within silicate lattice of terrigenous material and (ii) in association with organic matter as barite (Pattan et al., 2003). Ba enrichment is found in the sediments underneath the high biological productivity areas of coastal upwelling and in the equatorial divergent zones (Goldberg and Arrhenius, 1958). Barium is a useful proxy of surface ocean productivity in the overlying water column due to its high preservation factor as compared to its production (Bishop, 1988; Goldberg and Arrhenius, 1958; Schmitz, 1987). Algorithms have been developed to link biogenic barium accumulation in sediment to export production from water column (Dymond et al., 1992; Francois et al., 1995). Since the formation of barite is mechanically linked to biogenic material, biogenic Ba or Ba/Al ratio can be used as an indicator of surface productivity (Dymond, et al., 1992; Sirocko et al., 1996), provided the core location is free from reducing environment effects that can cause diagenetic dissolution (McManus et al., 1998). Both central and southern Bay of Bengal cores are raised from deep water, much below the denitrification zone (~ 200–700 m), and hence are less likely to be effected by reduction processes. The calcium in the cores is mostly derived from the overhead calcareous productivity of foraminifer species. Additionally, due to significant lithogenic flux in the Bay of Bengal, a fraction of Ca is likely to be associated with the dolomitic material brought along with the detrital material. Similarly, Sr with similar ionic radii gets incorporated in the calcareous material of the foraminifers and contributes for the major fraction of the Sr in sediments (Derry and France-Lanord, 1996). However, a significant fraction of Sr is expected to be associated with the silicate and the calcite fraction of the material delivered to the Bay of Bengal from various rivers (Krishnaswami et al., 1992; Bickle et al., 2005; Hohndorf et al., 2003).

The overhead productivity was ascertained using the variation in the concentration of Ba, Ca and Sr normalized to Al (Figs. 5.12 and 5.13). In core 4032, a marginal increase in Ca/Al, Ba/Al and Sr/Al is observed between 48 kyr to 42 kyr, followed by a consistent ratio (low) till around 14 kyr. After 14 kyr, a steady increase in all the proxies is observed which culminates around 7.5 kyr. After 7.5 kyr to 2 kyr, Ca/Al and Sr/Al show constant ratio (high), whereas, Ba/Al show a decreasing trend (Fig. 5.12).

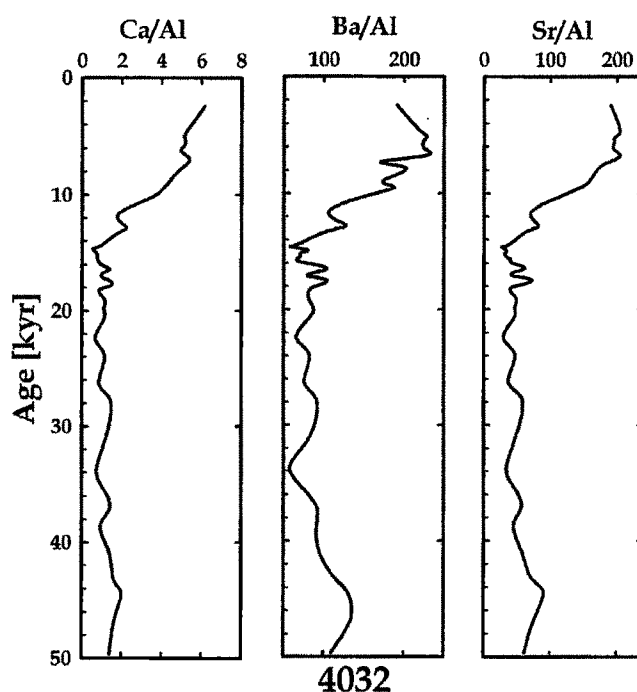


Fig. 5.12: Downcore variation of Ca/Al, Ba/Al and Sr/Al in the core 4032.

In core 4040, except for Ba/Al, both Ca/Al and Sr/Al show significant variability during 36 kyr and 4 kyr (Fig. 5.13). All the above proxies show a decreasing trend between 36 kyr to around 32 kyr, followed by an increase around 30 kyr. This increase is succeeded by an overall decreasing trend till 22 kyr. After 22 kyr, an abrupt increase is observed between 22 kyr and 20 kyr for Ca/Al and Sr/Al ratio, whereas, Ba/Al shows a marginal increasing trend. After 20 kyr, a general increase in all the proxies Ca/Al, Ba/Al and Sr/Al is observed with fluctuations with a sharp decline in all of them at 14.5 kyr. After 10 kyr, a declining trend is noticed with an abrupt decrease near 8.5

kyr followed by a marginal increase. However, in case of Ba/Al ratio, a gradual increase with minor fluctuations was observed after 20 kyr which continues till 4 kyr (Fig. 5.13).

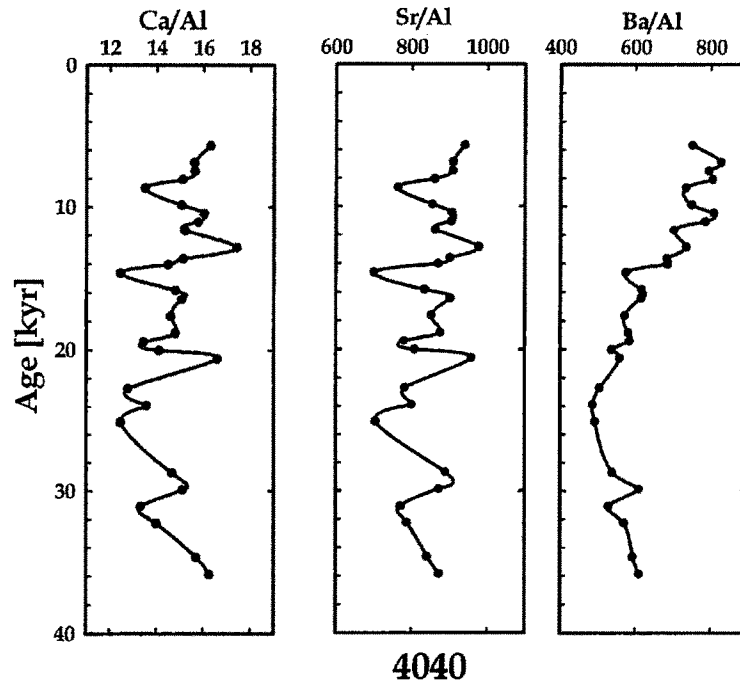


Fig. 5.13: Downcore variation of Ca/Al, Ba/Al and Sr/Al in the core 4040.

Variation in Trace Element Proxies

The trace elements in deep sea sediments have characteristically different composition as compared to the continental and near shore sediments. The deep-sea clays are enriched in certain trace elements (e.g. Mn, Cu) compared to the near shore and continental sediments (Chester and Hughes, 1969). The chemical composition of the deep sea is governed by the relative proportion of the minerals, pathways of its delivery in the marine environment, mechanism of its incorporation and sedimentation pattern (Wedepohl, 1960; Turekian and Wedepohl, 1961; Bostrom et al., 1973). Marine sedimentation is modulated by the rate of terrigenous flux (continental) and biogenic productivity variations. Post-depositional changes are governed by the ambient environmental conditions (changes in oxidizing conditions). For example, preservation of organic carbon was observed during reducing

conditions in the anoxic waters of the Oxygen Minimum Zone (OMZ) on the western continental slope of India (Sirocko et al., 2000; van der Weijden et al., 2006). The sediments in contact with OMZ have an absence of benthonic metazoan life due to oxygen depletion, eventually ceasing bioturbation and ultimately resulting in well preserved hydrogen-rich organic matter and have excellent hydrocarbon generation potential (Paropkari et al., 1993).

Unlike other open ocean regimes, the Bay of Bengal sediments provide a mixed signature of various proxies due to different processes operating in this region. The Bay of Bengal experiences temporal changes in the overhead productivity due to seasonally reversing monsoon system along with changes in the flux of detrital materials contributed by various rivers. Mn, Cr and V are redox sensitive elements which tend to migrate or get enriched in certain

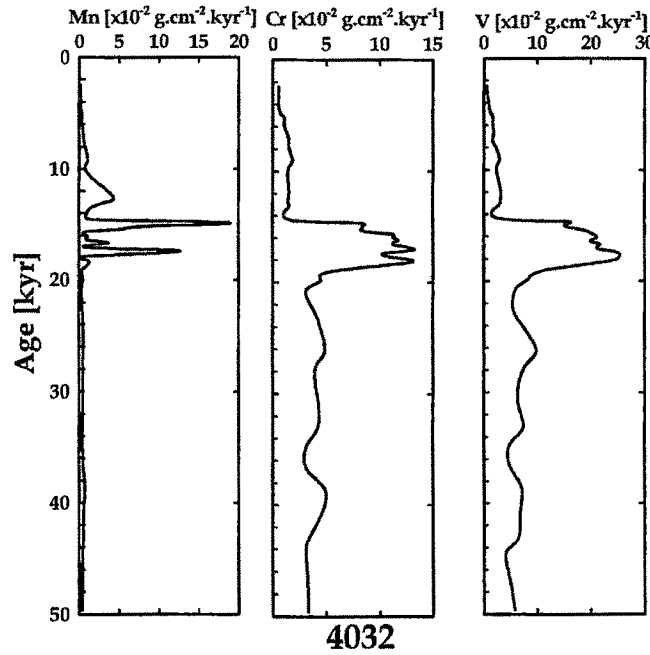


Fig. 5.14: Downcore variation of fluxes of redox sensitive elements in core 4032.

regions depending on the prevailing redox conditions governed either due to (i) changing overhead productivity (ii) varying sedimentation rates and/or (iii) changing bottom water conditions (Yadav, 1996; Chauhan and Rao., 1999; Chauhan, 2003). Redox sensitive elements thus provide information about the

changing bottom water conditions. However, if the trace elements are normalized to Al, the ratios would mimic the redox conditions caused due to the changing overhead productivity (Mangini et al., 2001). In core 4032, V and Cr show marginal variation in the fluxes between 50 kyr to 20 kyr (V 3–5 g.cm².kyr⁻¹ and Cr 5–10 g.cm².kyr⁻¹). Between 20 kyr and 14 kyr, these redox sensitive trace elements show significant increase in their fluxes. Compared to this, Mn shows only two distinct sharp peaks around 18 kyr and 14 kyr and

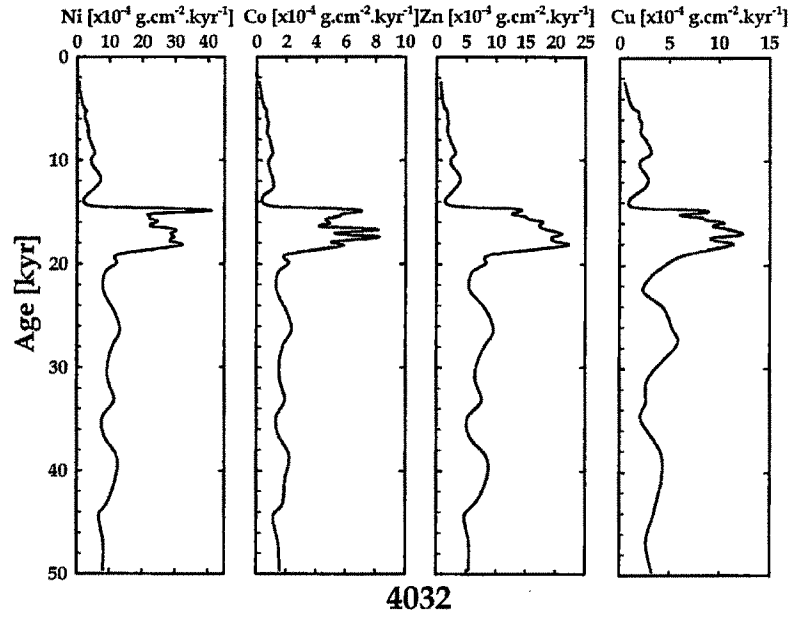


Fig 5.15: Downcore variation of fluxes of trace elemental proxies of Ni, Co, Zn and Cu in the core 4032

for the rest, it remains close to zero (Fig. 5.14). Similar trends are noticed in the fluxes of all the trace elements viz. Ni, Co, Zn and Cu measured in the core 4032 with a relatively constant flux during 50 kyr to 20 kyr and then sudden enhancement during 20 kyr to 14 kyr, but after 14 kyr all of them showed a decreasing trend (Fig. 5.15).

The redox proxies (V/Al and Cr/Al) when normalized to Al in core 4032, show a marginal increase between 50 kyr and 36 kyr. Cr/Al remain constant till 16 kyr followed by a decrease till 10 kyr. After 10 kyr, an increase till 7 kyr followed by a decreasing trend. V/Al broadly show an identical

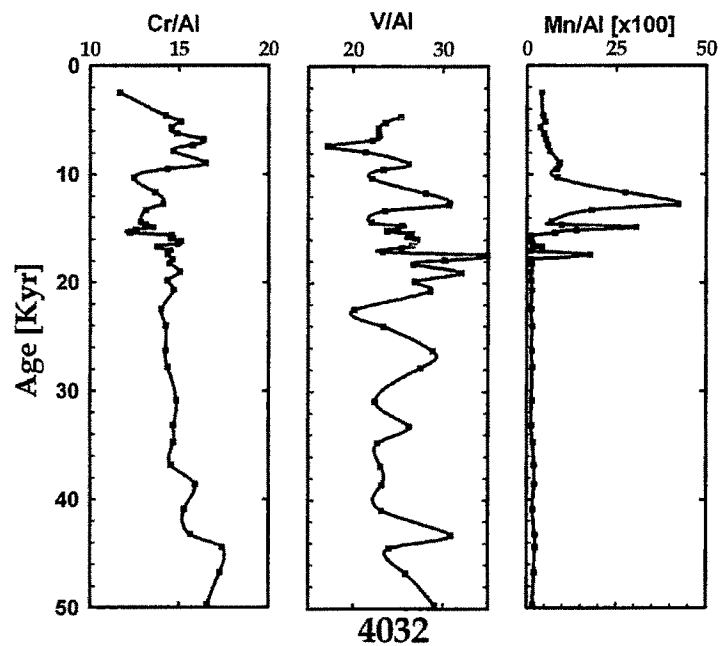


Fig. 5.16: Downcore variation of the redox sensitive elements normalized to Al for the core 4032.

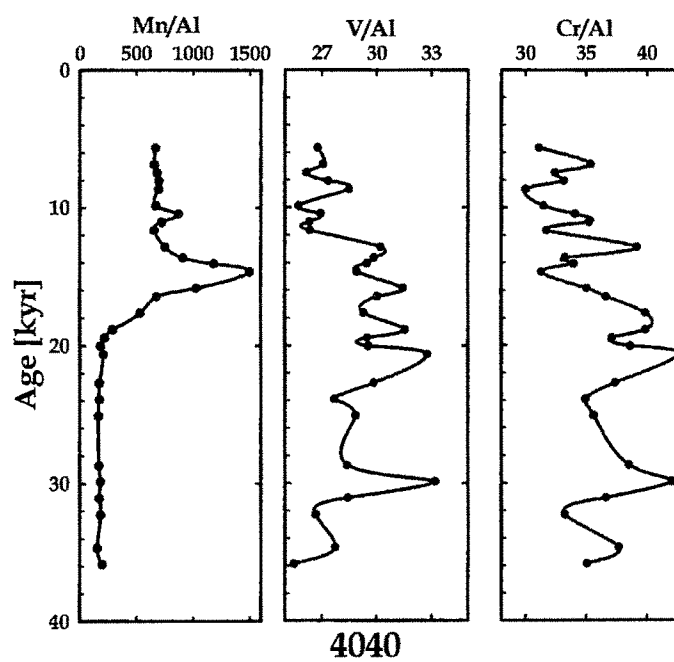


Fig. 5.17: Downcore variation of redox proxies normalised to Al in the core 4040.

pattern except for a prominent low around 22 kyr and a discernable increase during 20 kyr and 18 kyr. Whereas, Mn/Al shows a near zero

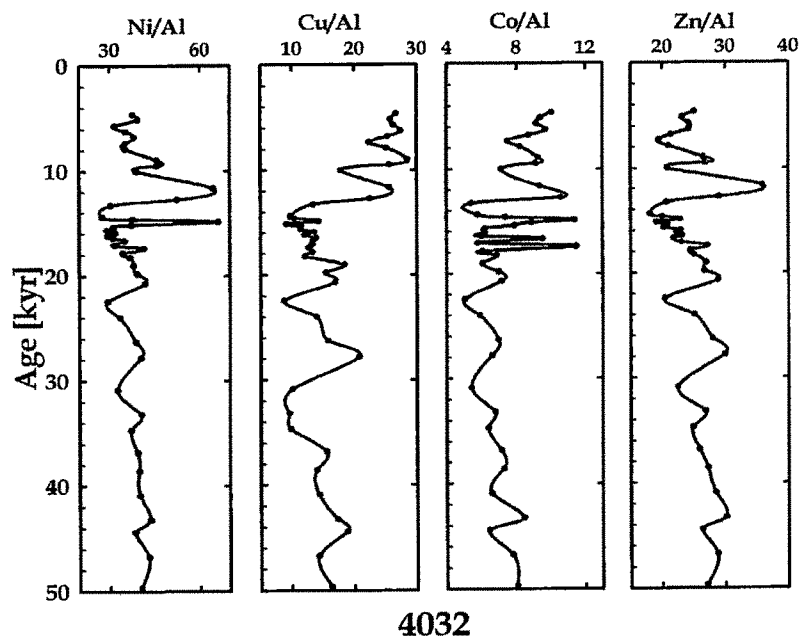


Fig. 5.18: Downcore variation of trace element proxies normalised to Al in the core 4032.

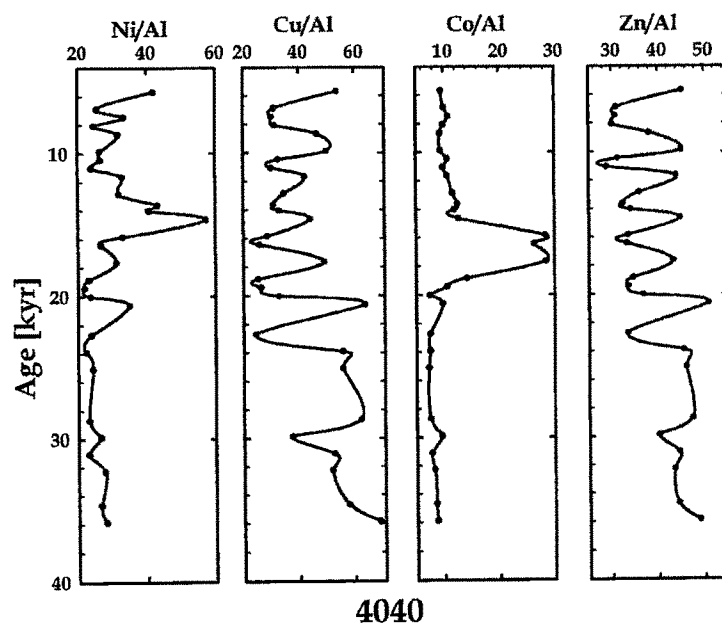


Fig. 5.19: Downcore variation of trace element proxies normalised to Al in the core 4040.

constant value through out, except for two enhanced peaks at 14 kyr and 16 kyr (Fig. 5.16).

In case of core 4040, an increasing trend between 35 kyr to 20 kyr followed by a continuous decreasing trend was observed for V/Al and Cr/Al, while Mn/Al shows a consistent low value till 19 kyr followed by a peak around 14 kyr (Fig. 5.17). When normalized with Al, Cu/Al, Co/Al and to some extent Zn/Al show an overall decreasing trend with fluctuations between 50 kyr and 20 kyr followed by an increase particularly after 14 kyr in core 4032. However, in case of Ni/Al the trend between 50 kyr and 20 kyr remains identical to that of other proxies but after 14 kyr and 10 kyr it shows a declining trend (Fig. 5.18). Similarly, an overall decreasing trend is observed in Cu/Al and Zn/Al in the core 4040 with major fluctuations and with significant enhancements at 20 kyr, 18–14 kyr and 9 kyr. Whereas, Ni/Al and Co/Al do not show any major fluctuations or trend, rather they are constant but show significant enhancement during the period 20–14 kyr (Fig. 5.19).

Strontium and Neodymium Isotopic Variations

The strontium and neodymium isotopic composition of the silicate fraction in the marine sediments preserve the record of provenance and hence that of environmental change (Raymo et al., 1988; Derry and France-Lanord, 1996, 1997; Colin et al., 1999; Burton and Vance, 2000; Clift et al., 2002; Frank, 2002). The sediments of the Bay of Bengal derive their origin to the Himalaya, Peninsular India and the Indo-Burman ranges. They have distinct Sr and Nd isotopic signatures typical to the source areas (France-Lanord et al., 1993; Singh and France-Lanord 2002; Colin et al., 2006). For example, the sediments of the G-B River system have high radiogenic $^{87}\text{Sr}/^{86}\text{Sr}$ values compared to that of the rivers draining the peninsular and Indo-Burman region. Among the G-B River system, the Ganga supplies sediments with high $^{87}\text{Sr}/^{86}\text{Sr}$ compared to the Brahmaputra. Similarly, the Nd isotopic composition of the sediments of the G-B River system (ϵ_{Nd} -12 to -18), Peninsular Rivers (-12 to -16) and Indo-Burman region (-8 to -11) are

completely distinct with enriched ϵ_{Nd} values for the Peninsular Rivers in the western Arabian Sea and that of Irrawaddy River draining through Arakan coast in the eastern Arabian Sea. Sr along with Nd isotopic composition measured in the silicate fraction of the surface sediments of the northern Bay of Bengal shows a strong influence of the G-B River system (Table 5.7; Bouquillon et al. 1990; Colin et al., 2006; Ahmad et al., 2005). Whereas, samples from the western Bay of Bengal show mixed signature of Sr and Nd isotopes derived mainly from the rivers draining the western continental margin of India (Colin et al., 1999). In case of the Andaman Sea sediments, low radiogenic Sr and more radiogenic ϵ_{Nd} , was found indicating contribution from the Irrawaddy River (Bouquillon et al., 1990; France-Lanord et al., 1993).

Table 5.7: $^{87}Sr/^{86}Sr$ and Sr concentration in the core 4032.

Core 4032	Depth (cm)	Age (yrs)	Sr (ppm)	$^{87}Sr/^{86}Sr$
0-1cm	0.5	2454	174	0.7172
5-6cm	5.5	5680	138	0.7165
16-17cm	16.5	11646	110	0.7178
21-22cm	21.5	14358	137	0.7160
25-26cm	25.2	14877	112	0.7175
31-32cm	31.5	15654	118	0.7172
35-36cm	35.5	16173	120	0.7183
39-40cm	39.5	16691	104	0.7187
42-43cm	42.5	17080	111	0.7183
51-52cm	51.5	18247	109	0.7186
55-56cm	55.5	19292	142	0.7159
64-66cm	65	22636	98	0.7190
74-76cm	75	26276	97	0.7187
78-80 cm	79	27809	120	0.7173
92-94 cm	93	33174	95	0.7184
108-110	109	38574	100	0.7187
116-118	117	40908	117	0.7179
124-126	125	43242	143	0.7164

Towards ascertaining the temporal changes in the provenance of the sediment, the silicate fraction of the sediments from the core 4032 (central Bay of Bengal) was analyzed for their Sr and Nd isotopic composition. With the same objective, the Nd isotopic composition of the sediments from the core 4040 was analysed in their silicate fraction at different depths. Selection of the sample was done on the basis of major variability observed in the proxies used for detrital flux. The measured $^{87}\text{Sr}/^{86}\text{Sr}$ in the sediments of the core 4032 varied

from 0.716 to 0.719 with majority of the $^{87}\text{Sr}/^{86}\text{Sr}$ values generally remained between 0.718–0.719.

Low $^{87}\text{Sr}/^{86}\text{Sr}$ values were

observed at 6 kyr, 14 kyr, 20 kyr, 28 kyr and 43 kyr (Fig. 5.20). A close correspondence between the detrital proxies and Sr isotopic variation is seen.

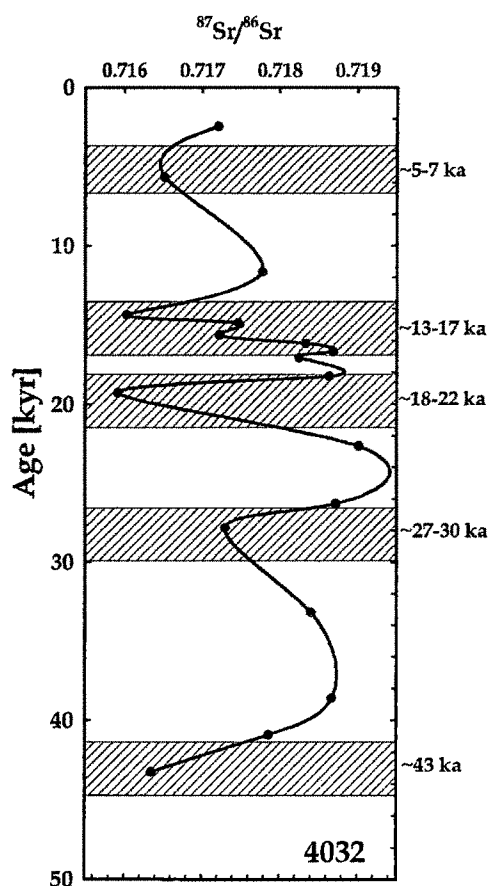


Fig. 5.20 Downcore variation of $^{87}\text{Sr}/^{86}\text{Sr}$ in the core 4032. Three prominent low $^{87}\text{Sr}/^{86}\text{Sr}$ ratios at 14, 20 and 43 kyr are observed.

The Nd isotopic composition (ϵ_{Nd}) in the sediments of the core 4032 varies between -10 and -8.9 with a general increasing pattern from 38 kyr to 20 kyr and subsequent decrease from 20 kyr to 12 kyr. There are three distinct events of increase in ϵ_{Nd} in core 4032 around 16 kyr, 20 kyr and 33 kyr. Out of these, a major increase is observed around 20 kyr (ϵ_{Nd} of -8.9) (Fig. 5.21). In core 4040, the Nd isotopic composition shows a gradual increase from 32 kyr (ϵ_{Nd} -10.5) and culminates around 20 kyr (ϵ_{Nd} -8.0). After 20 kyr, till 10 kyr a

decreasing trend of ϵ_{Nd} is noticed followed by a marginal increase from 10 kyr to 6 kyr (Fig. 5.22, Table 5.8).

Table: 5.8: ϵ_{Nd} and Nd concentration in the core 4032 and 4040.

Core: 4032

Depth (cm)	Age (years)	ϵ_{Nd}	Nd (ppm)
16-17	11646	-9.97	16.9
25-26	14876	-9.84	18.6
31-32	15654	-9.32	19.3
42-43	17080	-9.67	19.4
55-56	19292	-8.93	17.4
78-80	27809	-9.70	17.9
92-94	33173	-9.33	18.3
108-110	38574	-9.83	19.1

Core: 4040

Depth (cm)	Age (years)	ϵ_{Nd}	Nd (ppm)
4-5	5670	-11.01	13.7
11-12	9854	-11.17	13.8
14-15	11648	-9.68	15.1
21-22	15832	-9.21	18.1
26-27	18820	-8.11	18.9
32-34	22706	-8.51	21.1
44-46	29878	-9.07	19.9
48-50	32269	-10.48	15.7

Discussion

The G-B River system from the Himalayas, the Irrawaddy and Salween Rivers from the Indo-Burman ranges are the major contributors of terrigenous sediments to the Bay of Bengal. Studies have shown that sedimentation in the Bay of Bengal was modulated by glacio-eustatic sea level fluctuations, climate change and tectonic activity (Flood et al., 1995). Considering that the tectonic activity may be responsible for the long-term changes ($>10^5$ years) in sediment flux of riverine sediment (Schumm and Rea, 1995), climate change is largely responsible for variation in the sedimentation rate (Mulder and Syvitski, 1996). In view of this, the variation in sediment flux in the Bay of Bengal and the Andaman Sea can be used to reconstruct not only

the changing intensity of erosion and weathering in Himalayan and Burman regions (France-Lanord et al., 1993), but also towards reconstructing the past climatic conditions (Colin et al., 1999; Burton and Vance, 2000; Ahmed et al., 2005, 2008). For example, Colin et al. (1999) observed that between the Last Glacial Maximum (LGM) and Holocene a shift in the sea surface circulation pattern was invoked for the variation in detrital flux of G-B River system and western zone of Indo-Burman ranges (Colin et al., 1999). On a shorter time scale, variations in erosional patterns were directly related to the changes in monsoonal precipitation over the mountains. In recent studies, it has been demonstrated that sediment plumes originating from Irrawaddy River moves westwards during the northeast winter monsoon and eastwards during the southwest summer monsoon (e.g. Ramaswamy et al., 2004; Rao et al., 2005).

Sedimentation and Mass Accumulation Rates

In core 4032, it may be noted that there were significant variations in sedimentation rates during the last 50 kyr with a faster rate observed at ~ 20 kyr (Fig. 5.2). Similar observations have been made in the southeastern Arabian Sea indicating the post LGM enhanced sedimentation rates by a factor of 3–4 high compared to other periods during the past ~30 kyr (Agnihotri et al., 2001). The sedimentation rate at 4040 at the top of 90 East Ridge shows the least variation as it is located far off from the sediment source (Fig. 5.2).

In the central Bay of Bengal (core 4032), a discernable increase in sedimentation rate around 40 kyr was observed, this increase was also seen in the mass accumulation rate using major elements (Figs. 5.2 and 5.3). This period corresponds to the pluvial Marine Isotopic Stage-3 (MIS-3), with both marine and continental records indicating strengthened southwest monsoon conditions (Prell and Van Campo, 1986; Juyal et al., 2006). However, a prominent increase was observed in the mass accumulation rate after 20 kyr (post LGM) i.e. between 18 kyr and 14 kyr implying sediment mobilization that occurred during the transitional climatic condition following the LGM

(Goodbred Jr., 2003). The low sea level stand during the LGM led to the exposure of vast near coastal zone (Weber et al., 1997). As the climate began to ameliorate, these sediments were mobilized by increased runoff that probably outpaced the rising sea level. Weber et al. (1997) found sharp increase in terrigenous input around 15 kyr that continued till 12 kyr in the Bengal Fan which according to Goodbred Jr. (2003) is the first evidence for a post LGM revival of the Ganga dispersal system. After 14 kyr, the sea began to inundate a broad area of Bengal basin as the sea level rose to around 55 m below the present level by around 11 kyr. Consequently, majority of the sediment began to trap far inland causing a significant drop in the sedimentation rate on the upper Bengal Fan (Weber et al., 1997). This is indicated by significant decrease in sedimentation and mass accumulation rates after 14 kyr in the central Bay of Bengal (Fig. 5.3). However, compared to this, the southern Bay of Bengal (core 4040) shows a monotonous sedimentation rate except between 17 kyr and 15 kyr, when a marginal increase is observed. In the southern Bay of Bengal (core 4040), it is expected that major sedimentation variability would not be discernible due to its distal location from the influence of continental input and being on the top of the 90 East Ridge (Fig. 5.2).

Due to highly varying sedimentation rates in the Bay of Bengal, it is expected that the region experienced severe excursions in climate during the last ~50 kyr both due to sediment flux and overhead productivity. The Mass Accumulation Rates (MAR) calculated for the core 4032 reveals an interesting aspect of the changes in sedimentation and subsequently MAR (Fig. 5.3). The MAR in the Bay of Bengal was 3–5 g.cm⁻².kyr⁻¹ during 50 kyr till Last LGM. Around 17.5 kyr, a sudden enhanced MAR of ~13 g.cm⁻².kyr⁻¹ was observed. This can only be explained by enhanced sedimentation post LGM bringing loads of sediments locked in the estuarine regions and from the exposed coastal zone (Agnihotri et al., 2003). Since, the sedimentation in the Bay of Bengal is controlled by the riverine input, enhanced monsoon conditions leads to large fresh water discharge. Thus, transitions from glacial–interglacial periods, wherein large sediment load is delivered to the

Bay due to enhanced freshwater flux, brings in sediments from the exposed coastal zones post LGM with low sea level.

Lithogenic Proxies

The detrital proxies measured in 4032 were also measured in core 4040, located in the southern Bay of Bengal. The down core variation of the concentration of the lithogenic proxies (Al, Fe, Mg and Ti) in both the cores shows decreasing trends after LGM (Figs. 5.4 and 5.5). Increased concentration in detrital proxies is expected due to the intensification of Southwest Summer monsoon (SWSM) during the post LGM. However, with the SWSM intensification, it is likely to have enhanced productivity that may cause a relative decrease in the concentrations of detrital proxies. Towards this, the location of core 4040, which is away from the direct influence of riverine fluxes, would respond to both changes in the detrital and overhead productivity (biogenic flux). With increasing distance from the coast, the sediment cores are expected to restore the productivity variations more efficiently than detrital variations. Sediment trap studies have showed that annual rain rates of particulate matter for lithogenic material decrease from north to south in the Bay of Bengal, and remained almost same for the carbonate and opal and high for C_{org} for northern and Central Bay of Bengal and slightly lower at the southern Bay of Bengal (Ramaswamy and Nair, 1994). This is clearly reflected in the Fe/Al, Mg/Al and Ti/Al ratios in core 4040 during the last ~36 kyr (Fig. 5.8). Although, these proxies do not show drastic changes, the variation suggests periodic changes in productivity as well as changes in the source of sediments during the glacial–interglacial transition. A general decrease in the ratios of detrital proxies since last the LGM to present is indicative of source variation with increasing productivity or intensification of the SW monsoon (Figs. 5.7 and 5.8). This decrease is due to an increase of biogenic component leading to a relative decrease in the detrital component (Al), finally resulting in an overall decrease of the ratios of detrital proxies. The last deglaciation was characterized by an increased

terrigenous input during 15700–14800 yr, and this is attributable to an early strengthening of summer monsoon activity in the region. Similarly, a remarkable increase in kaolinite content with reduced chlorite and illite was attributed to enhanced Holocene precipitation during 8800–6400 BP (Thamban et al., 2002).

Major elemental variation in the central Bay of Bengal shows a consistent increase between 50 kyr and 14 kyr. The reason being the period between 50 kyr and 30 kyr is considered as pluvial MIS-3 when the southwest monsoon was enhanced. Hence, it is expected that during this period (barring the short term instability) an overall increase in these elements should have been observed. This would imply that after MIS-3, sediment flux was influenced probably by the stronger northeast winter monsoon. There are evidences to suggest that the Bay of Bengal experienced enhanced winter monsoon (Sarkar et al., 1990; Tiwari et al., 2006). After 14 kyr, decreasing trend in major elements could be interpreted as due to the deposition of continental flux at the continental margins and deltas because of rising sea level.

Compared to this, in the southern Bay of Bengal, a weakened monsoon condition can be inferred around 30 kyr, followed by a distinct enhancement till 22 kyr. Around LGM, an overall decrease in overhead productivity suggests decreasing strength of the southwest monsoon. The monsoon appears to improve and peak around 14 kyr and 9 kyr. Similar patterns are also observed in the lithogenic proxies.

A rather detailed picture of monsoon variability emerges from the C/N ratio. In the central Bay of Bengal, terrigenous input giving rise to increased C/N ratios (>10) was attributed to enhanced monsoon conditions at about 35.5 kyr, 27 kyr (latter part of MIS-3), 18 kyr, 17 kyr, 13 kyr (post LGM) and 7 kyr (early Holocene) (Fig. 5.9). In the southern Bay of Bengal (location less modulated by small variations in detrital discharge), two

prominent periods of enhanced detrital input viz. 20 kyr and 12 kyr. After 20 kyr, a stepwise improvement in the monsoon can be suggested by the gradual increase in carbonate concentration. The sharp increase in C_{org} and C/N ratios after 20 kyr and 12 kyr is indicative of sediment mobilization during the transitional climatic condition following the LGM (Goodbred Jr., 2003; Fig. 5.10).

Biogenic Proxies

Stable isotopic analyses of organic carbon ($\delta^{13}C$) data from the central Bay of Bengal (core 4032) indicate dominance of marine organic matter between 50 kyr and 20 kyr, which thus implies a limited continental organic contribution. This could be due to the burial of organic matter in deltaic sediments during periods of enhanced monsoon condition at least during the MIS-3. However, after LGM, it can be suggested that the central Bay of Bengal began to receive organic carbon from the G-B River system due to low sea stand after LGM and the beginning of Holocene. The $\delta^{15}N$ of the C_{org} is expected to show effects of denitrification in case of anoxicity of bottom waters in the sediments (Altabet et al., 1999; Sarkar et al., 2000). The $\delta^{15}N$ values, however, do not show any large scale variation indicative of denitrification process in the region and range from 4–6‰ (Fig. 5.11). However, a close correlation of $\delta^{15}N$ with productivity is noticed in the downcore variation of the core (Banakar et al., 2005). The increase in $\delta^{15}N$ of the C_{org} during the Holocene signifies a period of high productivity causing enhanced denitrification within the subsurface waters, which is also reflected in its variation (Thamban et al., 2001; Agnihotri et al., 2003a). The $\delta^{15}N$ during the same period indicates reduced denitrification followed by enhanced denitrification process (Ganeshram et al., 2002).

A more robust proxy for palaeoproductivity are the ratios of Ca/Al, Ba/Al and Sr/Al. In the present case, only Ba/Al shows some variability which appears to be consistent with the proxies discussed above (Babu et al., 2002; Winkler et al., 2005). For example, a high ratio between 50 kyr

and 35 kyr (MIS-3) accords well with the monsoon induced enhanced productivity in the central Bay of Bengal (Fig. 5.12). Following this, a consistent low value till 18 kyr suggests a weakened productivity phase, after 15 kyr a stepwise increase in productivity implies gradual strengthening of the monsoon as observed in the carbonate variation. In the southern Bay of Bengal, though data are scanty below 30 kyr, based on the trends noticed it can be speculated that prior to 30 kyr (MIS-3), the region experienced enhanced productivity and after 30 kyr and prior to 20 kyr, a decrease in monsoon can be suggested (Agnihotri et al., 2003a). However, interestingly Ca/Al and Sr/Al shows an increase in productivity around 20 kyr (LGM), and this can be attributed to the enhanced northeast wind driven productivity in the southern Bay of Bengal. After 20 kyr, Ba/Al suggests a stepwise strengthening of the productivity implying a re-establishment of the southwest monsoon. Here, it is worth mentioning that a discernable low value around 8.5 kyr in all the three proxies indicates temporary weakening of the monsoon. Given the dating uncertainty, this could as well correspond to a short lived 8.2 kyr cooling event observed in the northern latitudes (Alley et al., 1993, 1997).

The Bay of Bengal is a region known for its rather high sedimentary input compared to any other oceanic region of the world due to several rivers draining into it which bring in a tremendous sediment load. During LGM, studies have shown that sediment input was reduced due to the locking of sediments in the continental margins and in the upper reaches of Himalaya (Goodbrød Jr., 2003). It was after the LGM, major flux of continental input was observed as indicated by the enhancement of lithogenic fluxes (Fig. 5.6). During such transitional periods increased organic carbon burial efficiency has been observed by (Galy and France-Lanord 2006; Galy et al., 2008). This is amply demonstrated by increase in fluxes of the redox sensitive elements viz. Mn, V and Cr after 20 kyr and 14 kyr in the central Bay of Bengal (Fig. 5.14). Near identical patterns with variability has also been observed in the

ratios of the above elements in the southern Bay of Bengal (Figs. 5.16 and 5.17).

Provenance Variation using Strontium and Neodymium Isotopes

Strontium in the Bay of Bengal sediments is deposited in both carbonate and silicate phases. In the carbonate phase, Sr is either associated with the carbonaceous overhead surface productivity or with the detrital carbonate component brought along with the rivers. While in the silicate fraction, strontium is mainly associated with detrital clay. The sediment with high radiogenic Sr to the Bay of Bengal is mainly contributed by the Himalayan Rivers compared to the other rivers draining the peninsular India and the Indo-Burman region. (Palmer and Edmond, 1989, 1992; Edmond, 1992; Krishnaswami et al., 1992 France-Lanord et al., 1993). On the contrary, the ϵ_{Nd} values of the sediments supplied by the peninsular rivers are either comparable or enriched compared to the Himalayan Rivers with low $^{87}Sr/^{86}Sr$. Hence, isotopic variation in the sediments of the Bay of Bengal can be inferred in terms of changes in the source of sediments and their transport pathways (Colin et al., 1999; Walter et al., 2000).

Colin et al. (1999) identified three end members responsible for the sedimentary distribution of $^{87}Sr/^{86}Sr$ in the Bay of Bengal. They are the Ganga River ($^{87}Sr/^{86}Sr \approx 0.735$ and $\epsilon_{Nd} \approx -15$), Irrawaddy River (≈ 0.713 , ≈ -11) and the Arakan coast (≈ 0.716 , -7.0). To ascertain the end member values of $^{87}Sr/^{86}Sr$ and ϵ_{Nd} of different possible sources for the sediments of the Bay of Bengal, Sr and Nd isotopic analyses was carried out for the bed sediments of the Ganga, Mahanadi, Godavari and Krishna at the river mouth. The Sr and Nd isotopic composition of river bed sediments of Ganga shows $^{87}Sr/^{86}Sr$ value of 0.76 and ϵ_{Nd} of -16, for the Mahanadi river the values are 0.755 and -17, for the Godavari river it is 0.72 and -14 and for the Krishna river the values are 0.72 and -12.

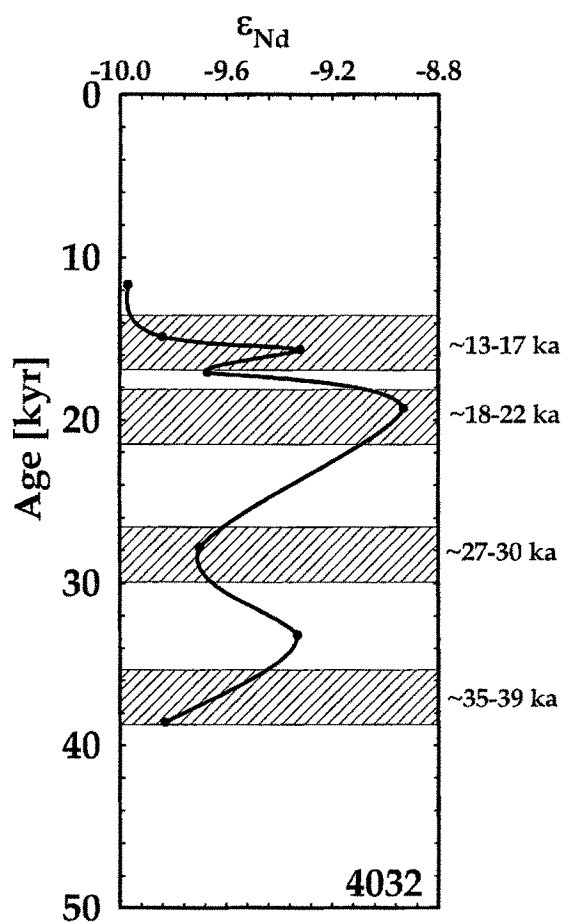
Dispersion of sediment in the Bay of Bengal is influenced by the strengthening or weakening of the Southwest Summer Monsoon (SWSM) and Northeast Winter Monsoon (NEWM). During the winter monsoon, East India Coastal Current (EICC) flow moves southeastwards (during October to January period) whereas during the summer monsoon, the EICC flow direction changes to northeastward (February to September) (Tomczack and Godfrey, 1994).

The northern and the western Bay of Bengal receive sediments predominantly from G-B River system with minor contribution from the Irrawaddy River, which drains into the Andaman Sea. The Southwest monsoon is a major source of water for the G-B River system which has a larger catchment area. In comparison, the Irrawaddy river catchment is very small and the discharge is dependent on the winter monsoon precipitation. The high $^{87}\text{Sr}/^{86}\text{Sr}$ ratio (0.718–0.719) in these sediments is attributed to the Himalayan source sediments. The Irrawaddy river drains into the Andaman Basin and during the winter months the sediment input to the Bay of Bengal is prominent as the EICC moves southeastward. Recent studies has demonstrated that sediment plumes originating from Irrawaddy river moves westwards during the Northeast Winter Monsoon and eastwards during the Southwest Summer Monsoon (e.g. Ramaswamy et al., 2004; Rao et al., 2005). Therefore, together with the circulation pattern and low $^{87}\text{Sr}/^{86}\text{Sr}$ ratio around 43 kyr, 28 kyr, 20 kyr, 14 kyr and 6 kyr (Fig. 5.20) indicates a significant contribution from the Irrawaddy river system through the Arakan coast during weakened southwest monsoon. The higher $^{87}\text{Sr}/^{86}\text{Sr}$ ratio during the intervening periods is attributed to the high discharge and increased sediment flux from the Himalaya region during enhanced southwest monsoon (Fig. 5.20). Alternatively, the $^{87}\text{Sr}/^{86}\text{Sr}$ ratio can also be altered if the sediment provenance within Himalayan range changes from the Higher Himalayan Crystalline (HHC) which have low $^{87}\text{Sr}/^{86}\text{Sr}$ values compared to the Lesser Himalayan Crystalline (LHC) rocks (Jacobsen et al., 2002; Singh et al., 2008). Studies on glaciations patterns in the Himalayas suggest that during periods

of weak southwest monsoon, Higher Himalaya regions were snow covered (Owen et al., 2005). In view of this, it is reasonable to assume that sediment supply from the HHC with low $^{87}\text{Sr}/^{86}\text{Sr}$ ratio would have been reduced and the dominant sediments supply was from the LHC with a high $^{87}\text{Sr}/^{86}\text{Sr}$ ratio. The above scenario seems to be less likely for the simple reason that in such situations high $^{87}\text{Sr}/^{86}\text{Sr}$ ratio should have been preserved around 20 kyr (LGM), which has not been observed here. The other possible source of material with low $^{87}\text{Sr}/^{86}\text{Sr}$ ratio could have been from the peninsular rivers ($^{87}\text{Sr}/^{86}\text{Sr}$ ratio ~ 0.715 - 0.725) (Ahmad et al., 2005). In the present study (Chapter-4), it has been demonstrated that $^{87}\text{Sr}/^{86}\text{Sr}$ ratio of surface sediment in the Bay of Bengal near the eastern coast of India range from 0.715 to 0.720 suggesting significant influence by G-B River system, almost masking the affect of peninsular rivers even in the near coastal regions.

The low $^{87}\text{Sr}/^{86}\text{Sr}$ represent periods of weakened SWSM at the expense of strengthened NEWM leading to enhanced supply of low radiogenic $^{87}\text{Sr}/^{86}\text{Sr}$ from the Irrawaddy River along the Arakan coast through the southeastward movement of EICC. In order

to attest to this hypothesis, Nd isotopic composition



(ϵ_{Nd}) in the silicate fraction of select sediment samples from the two cores were analysed. The ϵ_{Nd} in the core 4032 varies from -10 to -8.9 and in core 4040 from -11 to -8. The high ϵ_{Nd} values in core 4032 at 20 kyr are -8.9 and -9.4 corresponding to 16 kyr and 34 kyr, respectively (Fig. 5.21). In core 4040, however, the only high of ϵ_{Nd} of -8.0 corresponds to 20 kyr (Fig. 5.22). Such high values of ϵ_{Nd} have not been observed in the sediments of the other major rivers draining into the Bay of Bengal (Galy and France-Lanord, 2001; Colin et al., 1999). However, the highest ϵ_{Nd} measured in the Irrawaddy river is at the river's mouth in the Andaman Sea where the value is -11 and there is no data available for ϵ_{Nd} in the suspended sediments of the Irrawaddy river. It is thus probable that the western fan of the Irrawaddy river is a likely candidate for the high radiogenic ϵ_{Nd} to the Bay of Bengal. Singh and France-Lanord (2002) observed very high values of ϵ_{Nd} (-6.9 and -8.4) in the sediments of the eastern tributaries of Brahmaputra (Dibang and Dhansiri) draining through the Trans Himalayan plutonic belt and Indo-Burman ranges. A similar lithology is found in the Irrawaddy river basin. Considering the above, it is speculated at this stage (due to lack of suspended load data) that the Irrawaddy river is probably the source of more radiogenic ϵ_{Nd} into the Bay of Bengal. Based on the above premise, it is suggested that during

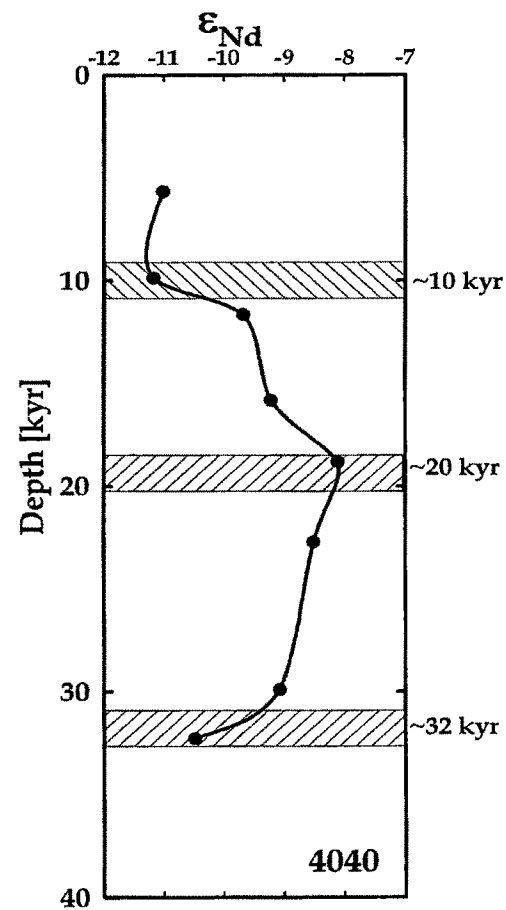


Fig.5.22 Downcore variation of ϵ_{Nd} in the silicate fraction of the sediments from the core 4040. Note, the lowest ϵ_{Nd} of -8.0 at 20 kyr

LGM, strengthened NEWM high sediment flux from the Arakan coast was routed through the Irrawaddy river to the eastern Bay of Bengal.

Together with the Sr and the Nd isotopic variations as seen in the two sediment cores, it can be inferred that during LGM the SWSM was weaker with a correspondingly strengthened NEWM. Based on other geochemical proxies and Nd isotopic variation, amelioration of the NEWM can be suggested from 32 kyr to 20 kyr. However, from 20 kyr (LGM) to 10 kyr, amelioration of the SWSM is clearly discernible.

Regional and Global Correlations

The physical, biological and chemical environment of the Bay of Bengal is closely linked to the variation in the summer and winter monsoon systems of the Indian subcontinent (Shetye et al., 1993). The monsoonal system of the Indian Ocean as a whole is one of the major atmospheric components of the tropical climate patterns where there are large seasonal variations with intensive rainfall during summer. During the northern winter, dry cold winds from the Asian continent flows off shore (McGregor and Nieuwolt, 1998). The monsoonal cycle dominates the fluvial runoff of one of the world's largest rivers systems viz. the Ganga and Brahmaputra system, which drains most of the Himalayas and the northern Indian subcontinent. Himalayan rivers are typically characterized by very high topography particularly on the southern Himalayan flank (boundary between the Lesser and Higher Himalaya). This front receives the major blast of the southwest monsoon resulting in intense physical erosion of the area (Seeber and Gortniz, 1983). Within the Himalayan basin, modern accumulation of eroded material represents a very minor reservoir compared to the Bay of Bengal (Bengal fan). In view of this, changes in sedimentation rate, geochemistry and isotopic proxies used in the present study enable us to reconstruct the variation in monsoon intensity during the last 50 kyr (Henderson, 2002). Three major climatic excursions as recorded in the sediment cores suggests enhanced monsoon during MIS-3 (between 50 kyr and 30 kyr), a weakening of the monsoon around LGM

(dated to 20 kyr) and a post glacial strengthening of the monsoon (after 20 kyr and 10 kyr). Within these periods, low frequency and low amplitude fluctuations have been recorded. It is observed that around 14 kyr, all proxies indicate enhanced summer monsoon conditions. Continental record from India, though limited, corroborates well with these observations. For example, during the MIS-3 valley glaciers receded in Central Himalaya suggest improved monsoonal condition. In the Central Ganga plain, Thar desert, western and Central India, regional flood plain aggradation and pedogenesis during the MIS-3 (50 kyr and 30 kyr) are attributed to an enhanced phase of monsoon activity (Kale and Rajaguru, 1987; Andrews et al, 1998, Singh et al., 1999; Srivastava et al., 2001; Jain and Tandon, 2003; Juyal et al., 2006). Considering the duration (<60 kyr and 30 kyr) and regional nature of this event, it was suggested that southwest monsoon was probably similar to or wetter than today (Juyal et al., 2006).

Gradual initiation of the weakening of monsoon is interpreted based on the decrease in mass accumulation rate, and productivity that began after 30 kyr and continued till around 20 kyr (LGM). In Himalaya, less extensive valley glaciation during this period was attributed to the weakening of the southwest monsoon (Benn and Owen, 1998; Pant et al., 2006). The Lesser Central Himalayan lake sediments suggest an arid phase between 25.6 kyr and 21.5 kyr (Kotlia et al., 1997; 2000). In the southern margin of the Thar desert, evidence suggests that the summer monsoon began to dwindle after 30 kyr and peak aridity appeared around 20 kyr (Juyal et al., 2003 and 2006). After 20 kyr, an abrupt increase in mass accumulation rate (after 20 kyr and 14 kyr) suggests mobilization of the sediments in the Himalaya region after the recession of valley glaciers (Goodbred Jr., 2003). In the Higher Central Himalaya after 20 kyr, deposition of sand in otherwise varve dominated lakes was attributed to post LGM warming (Juyal et al., 2004). Sinha et al. (2005) based on oxygen isotopic variation in a stalagmite collected from Timta cave in western Himalaya show multi-decadal monsoon variability between 15.2 kyr and 11.7 kyr. According to them, a progressive depletion in oxygen

isotope value between 15.2 kyr to 14.3 kyr is due to the strengthening of monsoon intensity and the addition of ^{16}O to the ocean by melting of Himalayan ice sheets.



In the Bay of Bengal and the Andaman Sea cores, study based on the magnetic grain size and CIA variations show prominent cooling events (weak monsoon) around 21 kyr and 14 kyr punctuated by a marginal improvement in monsoon (Colin et al., 1998). This is further corroborated by Kudrass et al. (2001) suggesting enriched oxygen isotope value and relatively high salinity around 21 kyr and 14 kyr which they attributed to the reduced hydrological discharge from Himalayan regions. Similarly, in the Arabian Sea sediments the percentage change in *G. Bulloides* around 14.5 kyr is attributed to an abrupt increase in monsoon strength (Overpeck et al., 1996). Based on the organic carbon variation, in the northeastern Arabian Sea, Schulz et al. (1998) have suggested weak monsoon periods around 23 kyr and 15 kyr, whereas the intervening period (between 23 kyr and 15 kyr) were identified as strengthened monsoon conditions. Based on the above, it can be suggested that multi-millennial climatic variability accords reasonably well with the continental and marine records obtained in earlier study. This would imply that climate variability reconstructed from the Bay of Bengal core responded to a regional climatic system.

In core 4032, only two distinct events of low productivity are noticed at 12 kyr and 14.6 kyr coinciding with H0 and H1 respectively. H0 event was also seen in 4040 but was bit dampened in 4032 (Fig. 5.12). But H0 and H1 events are clearly discernible in the Bay of Bengal with decreased productivity thereby indicating its strength and its effect in low latitudes. Most of other high or low productivity events seem to have been masked in 4032 by the high detrital component at this location. Additionally, both the cores, in all their biogenic proxies show continuous increase from LGM to present reflecting intensification of SW monsoon during the last 20 kyr. The periods of strengthened monsoon conditions can be noticed from events such as high

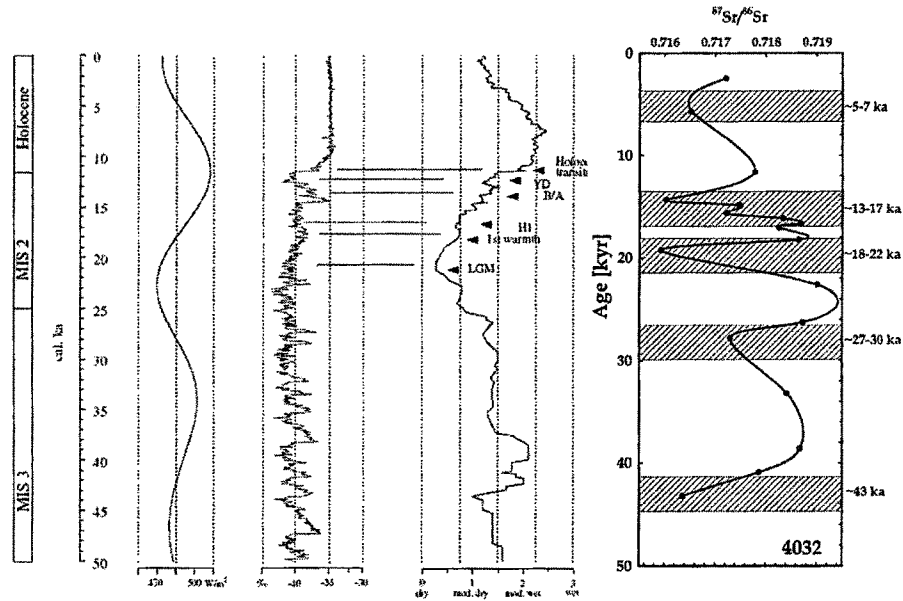


Fig. 5.23: Comparison of $^{87}\text{Sr}/^{86}\text{Sr}$ with solar insolation and mean effective moisture (Herszschuh et al., 2006). Note, synchronous variation of $^{87}\text{Sr}/^{86}\text{Sr}$ with solar insolation and moisture indicative of global correlation of the Bay of Bengal climate.

productivity. There are evidences for rapid changes in climate during LGM in tropical Atlantic (Hughen et al., 1996).

An important observation made during the present study is the implication of $^{87}\text{Sr}/^{86}\text{Sr}$ ratio and ϵ_{Nd} towards reconstructing the summer and winter monsoon variability provided the cores are strategically selected. It has been demonstrated that periods of winter rainfall are associated with low $^{87}\text{Sr}/^{86}\text{Sr}$ ratio and high ϵ_{Nd} and vice versa (Fig. 5.23). Synchronous variation in solar insolation, mean effective moisture and $^{87}\text{Sr}/^{86}\text{Sr}$ in the core 4032 is observed. The dry period corresponds to low $^{87}\text{Sr}/^{86}\text{Sr}$ is indicative of low detrital discharge from the G-B River system, which coincides with low solar insolation (Herszschuh, 2006).

Continental and marine records discussed above show near synchronous changes in monsoon variability during the last 50 kyr. Such changes have been attributed to coupled global and local processes (Gasse

and Van Campo, 1994; Prell and Kutzbach, 1987, 1992). For example, coherency between low-latitude monsoonal climate variability and rapid temperature fluctuations as observed in the Greenland ice record during the last glacial stage provides a link to climate in geographically distinct parts of the world (Schulz, et al., 1998; Rashid et al., 2007). Schulz et al. (1998) have demonstrated that during the north Atlantic interstadials, monsoon induced biological productivity was high in the northeastern Arabian sea whereas periods of low productivity was associated with high latitude atmospheric cooling and the injection of melt water into the North Atlantic basin. Zonneveld et al. (1997) suggested that the connectivity between the North Atlantic climate and summer monsoon is likely to be atmospheric. According to Colin et al. (1998), any changes in the boundary conditions of high latitudes should modify the amount and timing of cold air transported towards the south, which in turn influences the formation and development of the low surface pressure above the Tibetan Plateau. A westerlies–swinging model was proposed by Fang et al. (1999) to demonstrate the climatic connectivity between northern latitude and Asian monsoon variability. According to their model, during high-insolation periods (interglacials/interstadials) strong low pressure develops over Tibet (Tibetan low), as a result of which westerlies stay north of the Tibetan Plateau causing enhancement of the summer monsoon through northward propagation of moisture laden winds and the converse happens during the low-insolation periods. Recent studies have shown that during the intensified monsoon phases in the late Pleistocene and Holocene time, moisture migrated into the high arid part of the northwest Himalaya which in turn enhanced the sediment flux compared to the present day weaker monsoon condition (Bookhagen et al., 2005b).

Climatic Periodicities from Proxies

The solar radiation reaching the earth surface has been varying with time and shows periodicity in its variation with the solar insolation cycles. These variations in the total solar irradiance result in global changes in the climate (Milankovich, 1920; Imbrie, 1985; Haigh, 2001). While solar irradiance

supplies the periodic forcing, the coupled ENSO–monsoon anomalies provide the amplification for these signals to appear in climate archives (Higginson et al., 2004). The Earth’s climate system is highly sensitive to extremely weak perturbations in the Sun’s energy output on the centennial to millennial time scales. The apparent solar response was robust in the North Atlantic even as early Holocene (Bond et al. 2001). These changes in the climate are stored in proxies stored in various repositories. The marine sediments are one such repository which preserves these signatures. The short term climatic oscillations are obliterated in the marine records due to bioturbation of the sediments by the burrowing animals. Additionally, it becomes difficult to retrieve short-term fluctuations as the deep-sea sediments are deposited at slower rates of 1–10 cm/kyr.

In this study, from the undisturbed record of detrital and biogenic proxies from two cores in the Bay

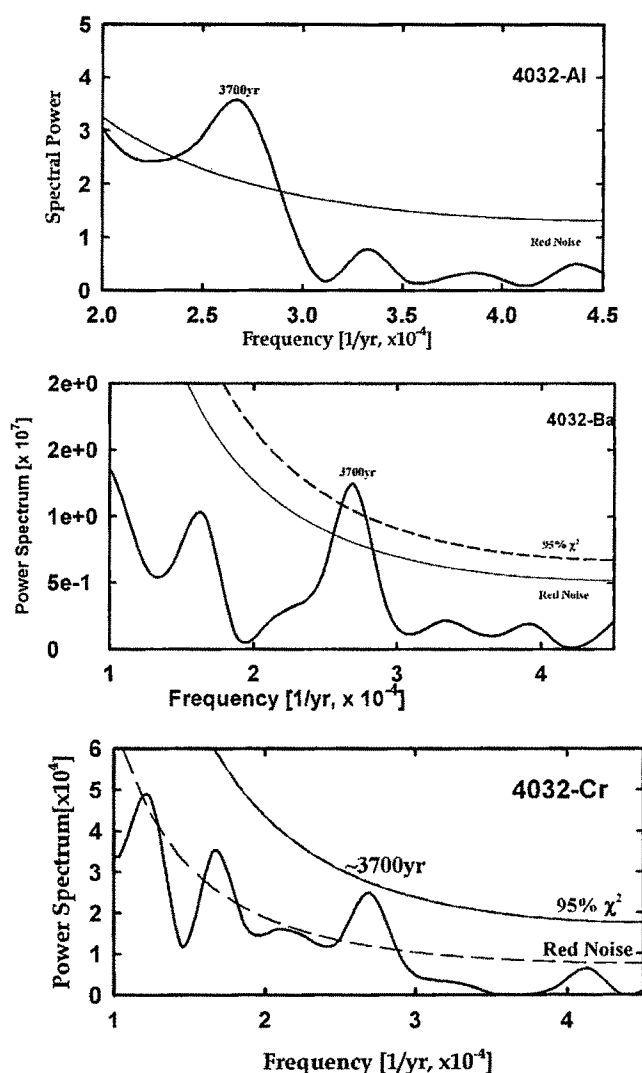


Fig. 5.24: Periodicities observed in the core 4032 in various proxies. Note 3.7 kyr periodicity prominent in all the proxies.

of Bengal (4032 and 4040), some of these millennial scale periodicities of climatic oscillations are derived by Fourier analyses of these data. Leuschner and Sirocko (2003) based on high-resolution record of upwelling and dust flux from the western Arabian Sea found resemblance to an insolation-based Indian Summer Monsoon Index. The insolation forcing in the low latitudes directly controls atmospheric processes in the African, Indian and Asian Monsoon, responsible for huge amount of trans-equatorial water vapour and therefore latent heat transport. The millennial-scale variability of the monsoonal

climate is noticed at periodicities near 100, 1450, 1750 and 2300 yrs (Agnihotri et al., 2002; Leuschner and Sirocko, 2003).

To ascertain the forcing factors responsible for the cyclic fluctuations in the lithogenic and biogenic proxies in cores 4032 and 4040, spectral analysis was performed

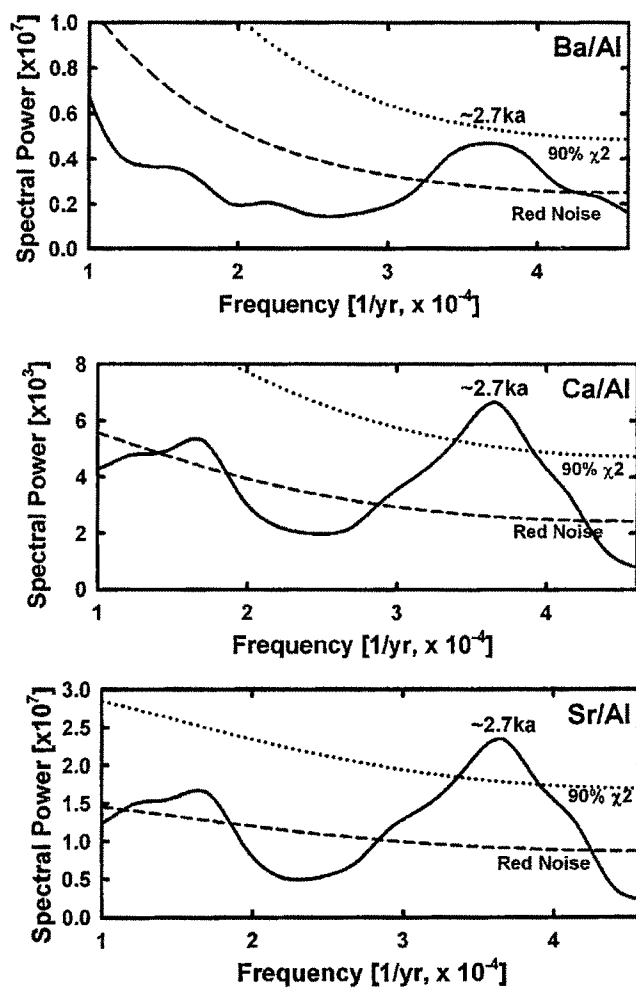


Fig. 5.25: Periodicities observed in the core 4040 in productivity proxies. Note 2.7 kyr periodicity prominent in all the proxies.

using the standard methods (Schulz and Stattegger, 1997; Schultz et al., 1998; Schulz and Mudelsee, 2000) applicable for geochemical data for unevenly spaced time series data (Figs 5.24, 5.25, 5.26). This method determines a theoretical red noise level and a false alarm level based on first order autoregressive (AR1) process algorithm. False alarm level is the maximum spectral amplitude expected if the time series would have been generated by AR1 process. Spectral peaks with amplitudes less than the theoretical red

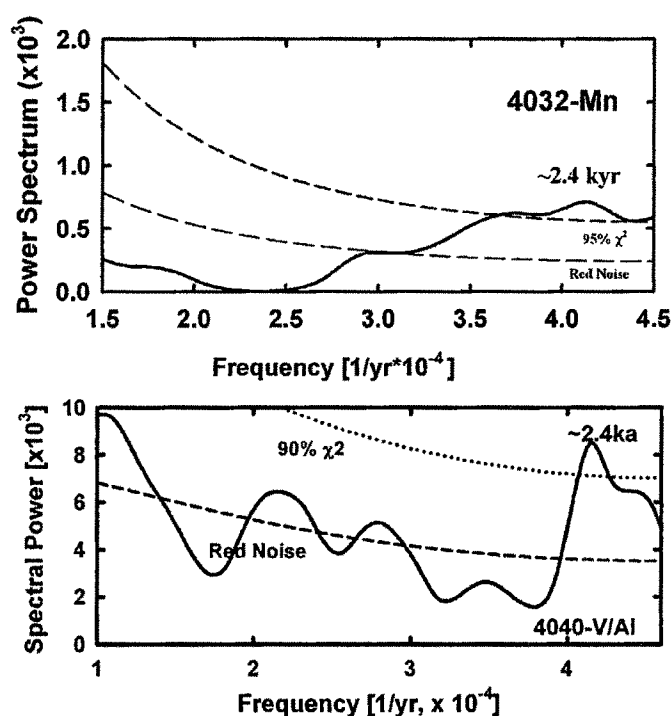


Fig. 5.26.: Periodicities observed in the core 4032 for Mn and V/Al. Note 2.4 kyr periodicity prominent in all the proxies.

noise level are rejected and exceeding or close to the false alarm level (above 80 to 95% confidence level) indicate non-AR1 component and are considered "significant".

The spectral analysis of the detrital, productivity and redox sensitive proxies were carried out in both the cores 4032 and 4040 (Fig. 5.24, 5.25 and Fig. 5.26). Three dominant periodicities of 2.4, 2.7 and 3.7 kyr are noticed in various proxies in both the cores. The 2.5, 2.77 and 3.95 kyr periodicities have

been confirmed to be of solar origin of insolation cycles from speleothem records (Stoykova et al., 2008). The synchronous retrieval of various periodicities indicates solar forcing of climate and its variations in the Bay of Bengal with these cycles. High resolution records can provide much more conclusive evidence for these periodicities. The solar influence on monsoon activity is not due to a change in radiative heating in the troposphere, rather, originates from the stratosphere through modulation of the upwelling in the equatorial troposphere, which produces a north-south seesaw of convective activity over the Indian Ocean sector, during summer. High precipitation over Arabia and India, thus, occurs during high solar activity (Kodera 2004).

Chapter-VI

SUMMARY AND CONCLUSIONS

The present study was aimed to address three important aspects of the northern Indian Ocean viz. the surface water circulation in the Arabian Sea, the pattern of surface sediment dispersion, and the palaeoclimatic reconstruction using sediment core samples of the Bay of Bengal.

As a part of ocean circulation studies (air-sea exchange of CO_2) in the Arabian Sea, several profiles of water column in the Arabian Sea were investigated for hydrographic parameters and radiocarbon content of the dissolved inorganic carbon (Broecker et al., 1985; Bhushan et al., 2000; Dutta, 2001). ^{14}C measurements were made in the water column of the Arabian Sea and the equatorial Indian Ocean to assess the temporal variations in bomb ^{14}C distribution and its inventory. In the present study, four GEOSECS stations were reoccupied (three in the Arabian Sea and one in the equatorial Indian Ocean) to discern the temporal variation in the water column inventories of bomb radiocarbon. It is observed that the sites investigated show increased penetration of bomb ^{14}C along with a decrease in its surface water activity. This indicates that during the last two decades since GEOSECS, vertical mixing has led to a deeper penetration of ^{14}C in the water column, while the surface activity has decreased probably due to an overall decrease in the atmospheric ^{14}C concentration.

The radiocarbon distribution in the water column in the top 1000 m is found to be modulated by the vertical mixing rates. Based on the available bomb ^{14}C inventories of the atmosphere and the water column, the air-sea exchanges of CO_2 were fitted in a box model (Oeshger et al., 1975, Broecker et

al., 1980) to obtain the vertical mixing rate/upwelling rates. The upwelling rates derived by model simulation of bomb ^{14}C depth profile ranged from 3-9 m yr^{-1} (Bhushan et al., 2008). The western Arabian Sea areas experiencing high wind-induced upwelling have yielded higher upwelling rates (5-9 m yr^{-1}). However, the upwelling rate estimates of the GEOSECS stations were higher than obtained for the same location during this study after two decades. This is attributed to reduced ^{14}C gradient compared to that during the GEOSECS sampling expedition.

The spatial and temporal variability in the Bay of Bengal sedimentation pattern is governed by the physical erosion of the drainage areas of major rivers that contribute to the terrigenous flux predominantly influenced by the SWSM activity with a smaller supplementary contribution resulting from the effect of the NEWM. In addition to this continental source, an appreciable contribution results from the overhead biological productivity.

The geochemical indicators for detrital proxies show a decreasing trend from the coast to the open ocean regions, implying decreasing continental influence as a function of distance from the coast. This accords well with the observation made by earlier workers (e.g. Rao and Kessarkar, 2001; Rao et al., 2005). Similar trends are also noticed in C_{org} that can be attributed to a better preservation in the proximal areas (mainly due to enhanced sedimentation) rather than enhanced productivity.

The Sr and Nd isotopic composition of the Bay of Bengal sediments carry the imprint of the source areas (provenance) from where the materials have been derived. Though, the Bay of Bengal receives sediment from both Himalayan and peninsular rivers, it is however the G-B River system that has an overwhelming effect.

In the northern Bay of Bengal, the high $^{87}\text{Sr}/^{86}\text{Sr}$ (0.725–0.735) and low ϵ_{Nd} (-18 to -12) of the surface sediments indicate a strong G-B River system

influence. However, samples from the western Bay of Bengal show mixed signatures of Sr and Nd isotopes mainly derived from the rivers draining the eastern continental margin of India, viz. the Mahanadi, Godavari, Krishna and Cauvery Rivers. The low radiogenic $^{87}\text{Sr}/^{86}\text{Sr}$ and high radiogenic ϵ_{Nd} in surface sediments from the Andaman Sea points signifies from the Irrawaddy River.

Two gravity cores collected from the central and southern Bay of Bengal were analysed for geochemical and isotopic proxies to reconstruct the climatic history during the last 50 kyr. Considering that the sediment flux is intimately associated with the tectonic and climatic variability (monsoon), the sedimentary archive in the Bay of Bengal provides a rare opportunity to reconstruct the past climatic (Gupta and Thomas, 2003) and tectonic activity (Metivier and Gaudemer, 1999).

In the central Bay of Bengal (core 4032), a discernable increase in the sedimentation rate around 40 kyr is observed. A prominent increase is also observed in the mass accumulation rate after 20 kyr (post LGM) i.e. between 18 kyr and 14 kyr implying sediment mobilization during the transitional climatic condition following the LGM (Goodbred Jr., 2003). In the southern Bay of Bengal (core 4040) a monotonous sedimentation rate is seen except between 17 kyr and 15 kyr, when a marginal increase is observed.

In the central Bay of Bengal, a general decrease in the ratios of detrital proxies since the last LGM to the present is indicative of source variation with a corresponding increase in productivity due to the intensification of the SW monsoon. This is attributed to the increase of biogenic component leading to relative decrease in the detrital component. The high ratio of biogenic proxies (Ba/Al, Sr/Al) between 50 kyr and 35 kyr suggests a monsoon induced enhanced productivity. After 35 kyr and till 18 kyr consistent low values of biogenic proxies are interpreted as a weakening of the monsoon activity.

However, after 15 kyr a stepwise increase in productivity indicates a gradual strengthening of the monsoon.

In the southern Bay of Bengal, the increasing trend in productivity proxies prior to 30 kyr indicates strengthened monsoon activity prior to 30 kyr. A declining trend observed after 30 kyr suggests a decrease in monsoon intensity. However, in the southern Bay of Bengal Ca/Al and Sr/Al ratios show an increase in productivity around 20 kyr (LGM) that can be attributed to an enhanced northeast wind driven productivity. After 20 kyr, Ba/Al suggests a stepwise strengthening of the productivity implying re-establishment and dominance of the southwest monsoon. It is worth mentioning here that a discernable low value around 8.5 kyr in all the three proxies indicate temporary weakening of the monsoon. This could as well correspond to a short lived cooling event dated to 8.2 kyr in the northern latitude (Alley et al., 1992, 1997).

The higher $^{87}\text{Sr}/^{86}\text{Sr}$ ratio (0.718-0.719) obtained in sediments of the southern Bay of Bengal is attributed to the Himalayan source sediments, whereas for the Irrawaddy sediments the $^{87}\text{Sr}/^{86}\text{Sr}$ ratio is ~ 0.713 and for that of the Arakan Coast it is 0.716 (Colin et al., 1999). The Irrawaddy River primarily drains into the Andaman Basin and during winters the sediment input from the Irrawaddy River to the Bay of Bengal is more prominent as the EICC moves southeastward (Shetye et al., 1996).

It has been observed that during periods of strengthened NEWM, the low $^{87}\text{Sr}/^{86}\text{Sr}$ contribution is from the Irrawaddy River, whereas during enhanced SWSM periods, the Himalayan source became dominant as indicated by the high $^{87}\text{Sr}/^{86}\text{Sr}$ ratio. This is further indicated by the Nd isotopic composition (ϵ_{Nd}) in the silicate fraction of the select sediment samples of the two cores. The high ϵ_{Nd} values recorded in the core from the central Bay of Bengal at 34 kyr, 20 kyr and 16 kyr, and in the southern Bay of Bengal core at around 20 kyr is interpreted as strengthened NEWM, during

which more radiogenic ϵ_{Nd} was contributed by the Irrawaddy River system. In the absence of suspended sediment data from the Irrawaddy River, the above interpretation should be treated as a working hypothesis for future investigation.

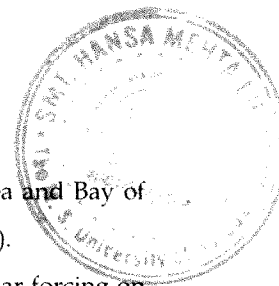
Conclusions

The following inferences can be drawn from the present study:

- 1) The upwelling rates determined for the Arabian Sea and the Equatorial Indian Ocean stations ranged from 3-9 m yr⁻¹ which is low when compared to the GEOSECS stations. High upwelling rates obtained correspond to the western region of the Arabian Sea, which is known for high wind induced upwelling. The atmospheric ¹⁴C concentration has almost stabilized since about a decade leading to the reduced gradient of ¹⁴C, which could be the reason for lower estimates of upwelling rates.
- 2) Lithogenic proxies in the surface sediments show a progressive decrease from the coast to the open ocean. This is attributed to the reduction in detrital sediment flux and an increase in the biogenic flux.
- 3) The observed decreasing trend in C_{org} from the coast to the open sea suggests a better preservation of C_{org} in coastal regions of the Bay of Bengal that is probably due to enhanced continental sediment flux.
- 4) Increased sediment flux in the Bay of Bengal occurred during the transitional climatic condition between the Last Glacial Maximum (LGM) and Holocene and this is attributed to the combination of low sea level, exposed coastal zone, and the strengthening of SWSM.
- 5) A general decrease in the ratios of detrital proxies since LGM to the present is due to increased productivity as a result of gradual strengthening of the SWSM.

- 6) The low $^{87}\text{Sr}/^{86}\text{Sr}$ ratios and enhanced ϵ_{Nd} values represent periods of weakened SWSM at the expense of a strengthened NEWM. It is due to an enhanced NEWM with the supply of low radiogenic $^{87}\text{Sr}/^{86}\text{Sr}$ from the Irrawaddy River (along the Arakan coast). In addition, the western fan of the Irrawaddy River along the Arakan Coast is suggested to be a likely contributor for high radiogenic ϵ_{Nd} during periods of enhanced NEWM.
- 7) Based on the Sr and the Nd isotopic variations, it is inferred that NEWM began to strengthened after 30 kyr and culminating at about 20 kyr. However after 20 kyr to 10 kyr a progressive strengthening of the SWSM is observed.
- 8) Three dominant periodicities of 2.4, 2.8 and 3.7 kyr noticed in the lithogenic and biogenic proxies are synchronous to the well known insolation cycles of 2.5, 2.77 and 3.95 kyr of solar origin. This indicates the influence of solar forcing in modulating the climate in the Bay of Bengal and parts of the northern Indian Ocean.

REFERENCES



- Agnihotri, R., "Chemical and Isotopic Studies of Sediments from the Arabian Sea and Bay of Bengal", *Ph.D Thesis*, Mohanlal Sukhadia University, Udiapur, India (2001).
- Agnihotri, R., Dutta, K., Bhushan, R. and Somayajulu, B.L.K., "Evidence for Solar forcing on Indian monsoon during the last millennium", *Earth and Planetary Science Letters*, **198**, 521-527 (2002).
- Agnihotri, R., Bhattacharya, S.K., Sarin, M.M. and Somayajulu, B.L.K., "Changes in surface productivity and the subsurface denitrification during the Holocene: A multiproxy study from the eastern Arabian Sea", *The Holocene*, **135**, 701-713 (2003a).
- Agnihotri, R., Sarin, M.M., Somayajulu, B.L.K., Jull, A.J.T. and Burr, G.S., "Late-Quaternary biogenic productivity and organic carbon deposition in the eastern Arabian Sea", *Palaeogeography Palaeoclimatology Palaeoecology*, **197**, 43-60 (2003b).
- Ahmad S. M., Anil Babu G., Padmakumari V. M., Dayal A. M., Sukhija B. S., and Nagabhushanam P. "Sr, Nd isotopic evidence of terrigenous flux variations in the Bay of Bengal: Implications of monsoons during the last ~34,000 years", *Geophysical Research Letters*, **32**(22), 1-4 (2005).
- Ahmad S. M., Anil Babu G., Padmakumari V. M., and Raza, W., "Surface and deep water changes in the northeast Indian Ocean during the last 60 ka inferred from the carbon and oxygen isotopes of planktonic and benthic foraminifera", *Palaeogeography Palaeoclimatology Palaeoecology*, **262**, 182-188 (2008).
- Alley, R.B., Meese, D.A., Shuman, C.A. Gow, A.J., Taylor, K.C., Grootes, P.M., White, J.W.C., Ram, M., Waddington, E.D., Mayewski, P.A., Zienlinski, G.A., "Abrupt increase in Greenland snow accumulation at the end of the Younger Dryas" *Nature*, **362**, 527-529 (1993).
- Alley, R.B., Mayewski, P.A., Sowers, T., Stuiver, M., Taylor, K.C. and Clark, P.U., "Holocene climatic instability: A prominent, widespread event 8200 yr ago", *Geology*, **25**(5), 483-486 (1997).
- Altabet, M.A., Pilskaln, C., Thunell, R., Pride, C., Sigman, D., Chavez, F. and Francois, R., "The nitrogen isotope biogeochemistry of sinking particles from the margin of the Eastern North Pacific", *Deep-Sea Research I*, **46**, 655-679 (1999).
- Altabet, M.A., Higginson, M.J. and Murray, D.W., "The effect of millennial-scale changes in Arabian Sea denitrification on atmospheric CO₂", *Nature*, **415**, 159-162 (2002).

- Amin, B.S., Likhite, S.D., Radhakrishnamurthy, C. and Somayajulu, B.L.K., " Susceptibility, stratigraphy and palaeomagnetism of some deep Pacific Ocean cores, " *Deep Sea Research*, **19**, 249-252, (1972).
- Andrews, J.E., Singhvi, A.K. Kailath, A.J., Kuhn, R., Dennis, P.F., Tandon, S.K. and Dhir, R.P., "Do Stable Isotope Data from Calcrete Record Late Pleistocene Monsoonal Climate Variation in the Thar Desert of India?" *Quaternary Research*, **50**(3), 240-251, (1998).
- Babu, C.P., Brumsack, H.-J., Schnetger, B. and Bottcher, M.E., "Barium as a productivity proxy in continental margin sediments: A study from the eastern Arabian Sea", *Marine Geology*, **184**, 189-206 (2002).
- Banakar, V.K., Oba, T., Chodankar, A.R., Kurmato, T., Yamamoto, M. and Minagawa, M., "Monsoon related changes in sea surface productivity and water column denitrification in the Eastern Arabian Sea during the last glacial cycle", *Marine Geology*, **219**, 99-108, 2005.
- Bard E., Arnold M., Ostlund H. G., Maurice P., Monfray P., and Duplessy J. C., "Penetration of bomb radiocarbon in the tropical Indian Ocean measured by means of accelerator mass spectrometry", *Earth & Planetary Science Letters*, **87**, 379-389 (1988).
- Bard, E., Arnold, M., Toggweiler, J.R., Maurice, P. and Duplessy, J.C., "Bomb ^{14}C in the Indian Ocean measured by accelerator mass spectrometry: oceanographic implications", *Radiocarbon*, **31**(3), 510-522 (1990).
- Bender, M., T. Sowers, M.L. Dickson, J. Orchardo, P.M. Grootes, P.A. Mayewski, and D.A. Meese, "Climate correlations between Greenland and Antarctica during the past 100,000 years", *Nature*, **372**, 663-666 (1994).
- Benn, D. and Owen, L. A., "The role of the Indian summer monsoon and the mid-latitude westerlies in Himalayan glaciation: review and speculative discussion", *Journal of Geological Society of London*, **155**, 353-363 (1998).
- Berger, W.H., Smetacek, V.S. and Wefer, G., "Ocean productivity and paleoproductivity—an overview", In: W.H. Berger, V.S. Smetacek and G. Wefer, Editors, *Productivity of the Ocean Present and Past*, 1989, Wiley, New York, 1-34 (1989).
- Bhushan, R., Somayajulu, B.L.K., Chakraborty, S. and Krishnaswami, S., "Radiocarbon measurements in the Arabian Sea water column: Temporal variations since two decades after GEOSECS and CO_2 air-sea exchange rates", *Journal of Geophysical Research*, **105**(C6), 14273-14282 (2000).
- Bhushan, R., Chakraborty, S. and Krishnaswami, S., "Physical Research Laboratory (Chemistry): Radiocarbon Date List CH-1", *Radiocarbon*, **36**, 251-256, (1994).

- Bhushan, R., Dutta, K., Mulsow, S., Povinec, P.P. and Somayajulu, B.L.K., "Distribution of natural and man-made radionuclides during reoccupation of GEOSECS Stations 413 and 416 in the Arabian Sea: Temporal change" *Deep-Sea Research II*, **50**, 2777-2784 (2003).
- Bhushan, R., Dutta, K. and Somayajulu, B.L.K., "Concentrations and burial fluxes of organic and inorganic carbon on the eastern margins of the Arabian Sea", *Marine Geology*, **178**, 95-113 (2001).
- Bhushan, R., Krishnaswami S. and Somayajulu, B.L.K., "¹⁴C in air over the Arabian Sea", *Current Science*, **73**(3), 273-276 (1997).
- Bhushan, R., Dutta, K. and Somayajulu, B.L.K., "Estimates of the upwelling rates in the Arabian Sea and the equatorial Indian Ocean", *Journal of Environmental Radioactivity*, in press (2008).
- Bickle M. J., Chapman H. J., Bunbury J., Harris N. B. W., Fairchild I. J., Ahmad T., and Pomies C. (2005) Relative contributions of silicate and carbonate rocks to riverine Sr fluxes in the headwaters of the Ganges. *Geochimica et Cosmochimica Acta* **69**(9), 2221-2240.
- Bishop, J.K.B., "The barite-opal-organic carbon association in oceanic particulate material", *Nature*, **332**, 341-343, (1988).
- Bond, G. et al., "Evidence for massive discharges of icebergs into the North Atlantic ocean during the last glacial period", *Nature*, **360**, 245-249 (1992).
- Bond, G.C. and Lotti, R., "Iceberg discharges into the north-Atlantic on millennial time scales during the last glaciation", *Science*, **267**(5200), 1005-1010, (1995).
- Bond, G., Kromer, B., Beer, J., Muscheler, R., Evans, M.N., Showers, W., Hoffmann, S., Lotti-Bond, R., Hajdas, I. and Bonani, G., "Persistent solar influence on North Atlantic climate during the Holocene", *Science*, **294**, 2130-2136 (2001).
- Bookhagen, B., Thiede, R.C. and Strecker, M.R., "Abnormal monsoon years and their control on erosion and sediment flux in the high, arid northwest Himalaya", *Earth and Planetary Science Letters*, **231**, 131-146 (2005).
- Bostrom, K., Kraemer, T. and Gartner, S., "Provenience and accumulation rates Opaline Silica, Al, Ti, Fe, Mn, Cu, Ni and Co in Pacific Pelagic sediments", *Chemical Geology*, **11**, 123-148 (1973).
- Bouquillon, A., France-Lanord, C., Michard, A. and Tiercelin, J-J, "Sedimentology and isotopic chemistry of the Bengal fan sediments: The denudation of the Himalaya", *Proceedings of the Ocean Drilling Program, Scientific Results*, **116**, 43-58, (1990).

- Broecker, W.S., Peng, T.-H. and Stuiver, M., 1978. An estimate of the upwelling rate in the equatorial Atlantic based on the distribution of bomb radiocarbon. *Journal of Geophysical Research*, **83**(C12): 6179-6186.
- Broecker, W.S., Toggweiler, J.R. and Takahashi, T., "The Bay of Bengal – A major nutrient source for the deep Indian Ocean", *Earth and Planetary Science Letters*, **49**, 506-512 (1980).
- Broecker, W.S., Peng, T.-H., Ostlund, G. and Stuiver, M., "The distribution of bomb radiocarbon in the ocean", *Journal of Geophysical Research*, **90**, 6953-6970 (1985).
- Broecker, W.S. and Peng, T.-H., "Stratospheric contribution to the global bomb radiocarbon inventory: model versus observation", *Global Biogeochemical Cycles*, **8**, 377-384 (1994).
- Broecker, W.S., Sutherland, S., Smethie, W., Peng, T.-H. and Ostlund, G., "Oceanic radiocarbon: separation of the natural and bomb components", *Global Biogeochemical Cycles*, **9**, 263-288 (1995).
- Burton, K.W. and Vance, D., "Glacial-interglacial variations in the neodymium isotope composition of seawater in the Bay of Bengal recorded by planktonic foraminifera", *Earth and Planetary Science Letters*, **176**, 425-441 (2000).
- Canfield D. E., "Factors influencing organic carbon preservation in marine sediments", *Chemical Geology*, **114**, 315-329, (1994).
- Calvert S. E. and Pedersen T. F., "Organic carbon accumulation and preservation in marine sediments: How important is anoxia?" In *Productivity, Accumulation and Preservation of Organic Matter in Recent and Ancient Sediments*, 231-263 (1992).
- Carpenter, J.H., "The Chesapeake Bay Institute. Technique for the Winkler oxygen method. *Limnology Oceanography*, **10**, 141-143 (1965).
- Chakraborty, S., "Environmental significance of isotope and trace elemental variations in banded corals, Environmental significance of isotopic and trace elemental variations in banded corals" *Ph.D Thesis*, M.S. University of Baroda, 141 (1993).
- Chakraborty, S., Ramesh, R. and Krishnaswami, S., "Air-sea exchange of CO₂ in the Gulf of Kutch, northern Arabian Sea based on bomb-carbon in corals and tree rings", *Proceedings-Indian Academy of Sciences, Earth & Planetary Sciences*, 329-340 (1994).
- Chauhan, O.S. and Gujar, A.R., "Surficial clay mineral distribution on the southwestern continental margin of India : Evidence of input from the Bay of Bengal", *Continental Shelf Research*, **16**(3), 321-333 (1996).
- Chauhan, O.S. and Rao, Ch.M., "Influence of sedimentation on enrichment of manganese and growth of ferromanganese micronodules, Bengal Fan, India", *Marine Geology*, **161**, 39-47 (1999).

- Chauhan, O.S., "Geochemistry of ferromanganese micronodules and associated Mn and trace metals diagenesis at high terrigenous depositional site of middle fan region, Bay of Bengal", *Deep-Sea Research II*, **50**, 961-978, (2003).
- Chauhan, O.S., "Past 20,000-year history of Himalayan aridity: Evidence from oxygen isotope records in the Bay of Bengal", *Current Science*, **84**(1), 90-93 (2003).
- Chauhan, O.S., Patil, S.K. and Suneethi, J., "Fluvial influx and weathering history of the Himalayas since Last Glacial Maxima – isotopic, sedimentological and magnetic records from the Bay of Bengal", *Current Science*, **87**(4), 509-515 (2004).
- Chauhan, O.S., Rajawat, A.S., Pradhan, Y., Suneethi, J. and Nayak, S.R., "Weekly observations on dispersal and sink pathways of the terrigenous flux of the Ganga-Brahmaputra in the Bay of Bengal during NE monsoon", *Deep Research II*, **52**, 2018-2030 (2005).
- Chester, R. and Hughes, M.J. "The trace element geochemistry of a North Pacific pelagic core", *Deep sea Research*, **13**, 627-634 (1969).
- Clift, P. D., Lee, J.I., Hildebrand, P., Shimizu, N., Layne, G. D., Blusztajn, J., Blum, J. D., Garzanti, E., and Khan, A. A., "Nd and Pb isotope variability in the Indus River system: Implications for sediment provenance and crustal heterogeneity in the Western Himalaya", *Earth and Planetary Science Letters*, **200**, 91-106 (2002).
- Clemens S C and Prell W L, "One million year record of summer monsoon winds and continental aridity from the Owen Ridge (site 722), Northwest Arabian Sea", In: *Proceedings of the Ocean Drilling Program, Scientific Results*, **117** (eds) W L Prell, N Niitsuma, et al. (Texas: College Station) 365–388 (1991).
- Coleman, J.M., "Brahmaputra River: Channel processes and sedimentation", *Sediment Geology*, **3**, 129-239 (1969).
- Colin, C., Kissel, C., Blamart, D. and Turpin, L., "Magnetic properties of sediments in the Bay of Bengal and the Andaman Sea : Impact of rapid North Atlantic Ocean climatic events on the strength of the Indian monsoon", *Earth and Planetary Science Letters*, **160**, 623-635 (1998).
- Colin C., Turpin L., Bertaux J., Desprairies A., and Kissel C., "Erosional history of the Himalayan and Burman ranges during the last two glacial-interglacial cycles". *Earth and Planetary Science Letters* **171**(4), 647-660 (1999).
- Colin, C., L. Turpin, D. Blamart, N. Frank, C. Kissel, and S. Duchamp, "Evolution of weathering patterns in the Indo-Burman Ranges over the last 280 kyr: Effects of sediment provenance on $^{87}\text{Sr}/^{86}\text{Sr}$ ratios tracer", *Geochemistry Geophysics Geosystems*, **7**(3), Q03007, doi:10.1029/2005GC000962 (2006).

- Cullen, J.L. "Microfossil evidence for changing salinity patterns in the Bay of Bengal over the last 20,000 years", *Paleogeography Paleoclimatology Paleoecology*, **35**, 315–356 (1981).
- Curray, J.R., "Sediment volume and mass beneath the Bay of Bengal", *Earth and Planetary Science Letters*, **125**, 371–383 (1994).
- Currie, R.I., Fisher A.E. and Hargreaves, P.M., "Arabian Sea Upwelling", *The Biology of the Indian Ocean*, B. Zeitzschel (ed.), Chapman and Hall Ltd., 37–52 (1973).
- Dalai, T.K., Krishnaswami, S. and Kumar, A., "Sr and $^{87}\text{Sr}/^{86}\text{Sr}$ in the Yamuna River System in the Himalaya: Sources, fluxes and controls on Sr isotopic composition", *Geochimica et Cosmochimica Acta*, **67(16)**, 2931–2948 (2003).
- Dansgaard, W., Johnsen, S.J., Clausen, H.B., Dahl-Jensen, D., Gundestrup, N.S., Hammer, C. U. Hvidberg, C. S., Steffensen, J. P., Sveinbjnsdottir, A. E., Jouzel, J. and Bond G., "Evidence for general instability of past climate from a 250-kyr ice-core record" *Nature*, **364**, 218 – 220 (1993).
- Das, A., S. Krishnaswami, and A. Kumar, "Sr and $^{87}\text{Sr}/^{86}\text{Sr}$ in rivers draining the Deccan Traps (India): Implications to weathering, Sr fluxes, and the marine $^{87}\text{Sr}/^{86}\text{Sr}$ record around K/T", *Geochemistry Geophysics Geosystems*, **7**, Q06014, doi:10.1029/2005GC001081 (2006).
- Degens, E.T., "Geochemistry of Sedimentary Formations", Russian Translation, Mir, Moscow (1967).
- Derry, L.A., "Neogene growth of the sedimentary organic carbon reservoir", *Paleoceanography*, **11(3)**, 267–275 (1996).
- Derry, L.A. and France-Lanord, C., "Neogene Himalayan weathering history and river $^{87}\text{Sr}/^{86}\text{Sr}$: Impact on the marine Sr record", *Earth and Planetary Science Letters*, **142**, 59–74 (1996).
- Derry, L. A., and C. France-Lanord, "Himalayan weathering and erosion fluxes: Climate and tectonic controls, in Tectonic Uplift and Climate Change", edited by W. F. Ruddiman, 289–312, Springer, New York (1997).
- Dickens, A.F., Gelinas, Y., Masiello, C.A., Wakeham, S. and Hedges, J.I., "Reburial of fossil organic carbon in marine sediments", *Nature*, **427**, 336–339 (2004).
- D.O.E., "Handbook of methods for the analysis of the various parameters of the carbon dioxide system in seawater", version 1.0, edited by A.G. Dickson and C. Goyet (1991).
- Dube, S.K., Rao, A.D., Sinha, P.C. and Jain, I., "Implications of climatic variations in the fresh water outflow on the wind-induced circulation of the Bay of Bengal", *Atmospheric Environment*, **29(16)**, 2133–2138 (1995).

- Duplessy, J.C., "Glacial to interglacial contrasts in the northern Indian Ocean", *Nature*, **295**, 495–498 (1982).
- Dupre, B., Viers, J., Oliva, P., Fortune, J.P., Braun, J.J., Martin, F. and Robian, H., "The effect of organic matter on chemical weathering in the tropics", *Mitt. Geol-Palaont. Inst., Univ. Hamburg*, **82**, 35-38(1999).
- Dutta, K., "Study of marine processes in the Northern Indian Ocean using radiocarbon" *Ph.D. Thesis*, M.S. University of Baroda, Vadodara, India (2001).
- Dutta, K., Bhushan, R. and Somayajulu, B.L.K., " ΔR correction values for the Northern Indian Ocean.", *Radiocarbon*, **43(2)**, 483-488 (2001).
- Dutta, K., Bhushan, R. and Somayajulu, B.L.K., "Rapid vertical mixing in deep waters of the Andaman Sea", *The Science of the Total Environment*, **384(1-3)**: 401-408, (2007).
- Dutta, K., Bhushan, R., Somayajulu, B.L.K. and Rastogi, N., "Interannual Variation of Atmospheric $\Delta^{14}C$ over the Northern Indian Ocean", *Atmosphere Environment*, **40(24)**, 4501-4512 (2006).
- Dymond J., Suess E., and Lyle M., "Barium in deep-sea sediment: a geochemical proxy for paleoproductivity", *Paleoceanography*, **7(2)**, 163-181 (1992).
- Dymond, J., Collier, R., McManus, J., Honjo, S. and Manganini, S., "Can the aluminium and titanium contents of ocean sediments be used to determine the paleoproductivity of the oceans", *Paleoceanography*, **12(4)**, 586-593 (1997).
- Edmond, J.M., "Himalayan tectonics, weathering processes, and the strontium isotope record in marine limestones" *Science* **258**, 1594-1597 (1992).
- Eigenheer, A. and Quadfasel, D., "Seasonal variability of the Bay of Bengal circulation inferred from TOPEX/Poseidon altimetry", *Journal of Geophysical Research*, **105(C2)**, 3243-3252 (2000).
- Emerson S., "Organic carbon preservation in marine sediments" *The carbon cycle and atmospheric CO₂: natural variations Archean to present. Chapman conference papers, 1984*, 78-87 (1985).
- Emerson, S. and Hedges, J.I., "Processes controlling the organic carbon content of open ocean sediments", *Paleoceanography*, **3(5)**, 621-634 (1988).
- Esbensen, S.K. and Kushnir, Y., "The heat budget of the global ocean: An atlas based on estimates from surface marine observations, The Heat Budget of the Global Ocean", *An Atlas Based on Estimates from Surface Marine Observations* (1981).
- Fang, X. M., Ono, Y., Fukusawa, H., Tian, P. B., Li, J. J., Hong, G. D., Oi, K., Tsukamoto, S., Torii, M., Mishima, T., "Asian summer monsoon instability during the past 60,000

- years: magnetic susceptibility and pedagogic evidence from the western Chinese Loess Plateau", *Earth Planetary Science Letters*, **168**, 219–232 (1999).
- Flood, R. D., Piper, D. J.W., and Klaus, A., "Proceedings of the OceanDrilling Program, Initial reports, Volume 155: College Station, Texas", *Ocean Drilling Program*, 1233, (1995).
- France-Lanord C., Derry L., and Michard A., "Evolution of the Himalaya since Miocene time: isotopic and sedimentological evidence from the Bengal Fan", *Himalayan Tectonics*, 603-621 (1993).
- France-Lanord C. and Derry L. A., " $\delta^{13}\text{C}$ of organic carbon in the Bengal Fan: source evolution and transport of C3 and C4 plant carbon to marine sediments", *Geochimica et Cosmochimica Acta* **58**(21), 4809-4814 (1994).
- France-Lanord, C. and Derry, L.A., "Organic carbon burial forcing of the carbon cycle from Himalayan erosion", *Nature*, **390**, 65-68 (1997).
- Francois, R., Honjo, S., Manganini, S.J. and Ravizza, G.E., "Biogenic barium fluxes to the deep sea: Implications for paleoproductivity reconstruction", *Global Biogeochemical Cycles*, **9**(2), 289-303 (1995).
- Frank, M., "Radiogenic Isotopes : Tracers of Past Ocean Circulation and Erosional Input", *Reviews of Geophysics*, **40**, 1-38 (2002).
- Frerichs, W.E., "Pleistocene-Recent Boundary and Wisconsin Glacial Biostratigraphy in the Northern Indian Ocean", *Science*, **159** (3822):1456-1458 (1968).
- Galy, A., C. France-Lanord and L.A. Derry, "The Late Oligocene-Early Miocene Himalayan belt constraints deduced from isotopic compositions of Early Miocene turbidites in the Bengal Fan", *Tectonophysics*, **260**, 109–118 (1996).
- Galy A. and France-Lanord C., "Weathering processes in the Ganges-Brahmaputra basin and the riverine alkalinity budget", *Chemical Geology* **159**(1-4), 31-60 (1999).
- Galy, A., France-Lanord, C. and Derry L.A., "The strontium isotopic budget of Himalayan rivers in Nepal and Bangladesh", *Geochimica et Cosmochimica Acta*, **63** (13-14), 1905–1925 (1999).
- Galy A. and France-Lanord C., "Higher erosion rates in the Himalaya: Geochemical constraints on riverine fluxes", *Geology*, **29**(1), 23-26 (2001).
- Galy V. and France-Lanord C., "Particulate organic carbon transport during Himalayan erosion", *Geochimica et Cosmochimica Acta*, **70**(18, Supplement 1), A191 (2006).
- Galy V., France-Lanord C., and Lartiges B., "Loading and fate of particulate organic carbon from the Himalaya to the Ganga-Brahmaputra delta", *Geochimica et Cosmochimica Acta*, **72**(7), 1767-1787 (2008).

- Ganeshram, R.S., Pedersen, T.F., Calvert, S.E. and Francois, R., "Reduced nitrogen fixation in the glacial ocean inferred from changes in marine nitrogen and phosphorus inventories", *Nature*, **415**, 156-159 (2002).
- Gasse F. & Van Campo E., "Abrupt post-glacial climate events in west Asia and North Africa monsoon domains", *Earth Planetary Science Letters*, **126**, 435-456 (1994).
- Gauns, M., Madhupratap, M., Ramaiah, N., Jyothibabu, R., Fernandes, V., Paul, J.T. and Prasanna Kumar, S., "Comparative accounts of biological productivity characteristics and estimates of carbon fluxes in the Arabian Sea and the Bay of Bengal", *Deep Sea Research II*, **52**, 2003-2017 (2005).
- George M. D., Dileep Kumar M., Naqvi S. W. A., Banerjee S., Narvekar P. V., de Sousa S. N., and Jayakumar D. A., "A study of the carbon dioxide system in the northern Indian Ocean during premonsoon", *Marine Chemistry*, **47**(3-4), 243-254 (1994).
- Goldberg, E.D. and Griffin, J.J., "The sediments of the northern Indian Ocean", *Deep Sea Research*, **17**, 513-537 (1970).
- Goldberg, E.D. and Arrhenius G.O.S., "Chemistry of Pacific pelagic sediments", *Geochimica et Cosmochimica Acta*, **13**(2-3), 153-198, 199-212 (1958).
- Goldstein, S.J. and Jacobsen, S.J., "The Nd and Sr isotopic systematics of river-water dissolved material: Implications for the sources of Nd and Sr in seawater", *Chemical Geology: Isotope Geoscience section*, **66**(3-4), , 245-272 (1987).
- Goodbred Jr. S. L. and Kuehl S. A., "Holocene and modern sediment budgets for the Ganges-Brahmaputra river system: Evidence for highstand dispersal to flood-plain, shelf, and deep-sea depocenters", *Geology*, **27**(6), 559-562 (1999).
- Goodbred, S. L., "Response of the Ganges dispersal system to climate change: a - source-to-sink view since the last interstadial", *Sedimentary Geology*, **162**, 83-104 (2003).
- GRIP Members, "Climate instability during the last interglacial period recorded in the GRIP ice core" *Nature*, **364**, 203-207 (1993).
- Grootes, P.M., M. Stuiver, J.W.C. White, S.J. Johnsen, and J. Jouzel., "Comparison of oxygen isotope records from the GISP2 and GRIP Greenland ice cores", *Nature*, **366**, 552-554 (1993).
- Grumet N. S., Guilderson T. P., and Dunbar R. B. "Meridional transport in the Indian Ocean traced by coral radiocarbon", *Journal of Marine Research*, **60**(5), 725-742 (2002a).
- Grumet N. S., Guilderson T. P., and Dunbar R. B. "Pre-bomb radiocarbon variability inferred from a Kenyan coral record", *Radiocarbon*, **44**(2), 581-590 (2002b).

- Gupta, A K and Thomas, E., "Initiation of Northern Hemisphere glaciation and strengthening of the northeast Indian monsoon: Ocean Drilling Program Site 758, eastern equatorial Indian Ocean", *Geology*, **31**, 47-50 (2003).
- Haigh, J.D., Climate variability and the influence of the Sun", *Science*, **294**, 2109-2111 (2001).
- Hartnett, H.E., Keil, R.G., Hedges, J.I. and Devol, A.H., "Influence of oxygen exposure time on organic carbon preservation in continental margin sediments", *Nature*, **39**, 572-574 (1998).
- Hedges, J.I., Baldock, J.A., Ge'linas, Y., Lee, C., Peterson, M. and Wakeham, S.G., "Evidence for non-selective preservation of organic matter in sinking marine particles", *Nature*, **409**, 801- 804 (2001).
- Heinrich, H., "Origin and consequences of cyclic ice rafting in the Northeast Atlantic Ocean during the past 130,000 years", *Quaternary Research*, **29**(2), 142-152 (1988).
- Henderson, G.M., "New oceanic proxies for paleoclimate", *Earth and Planetary Science Letters*, **203**, 1-13 (2002).
- Herzschuh, U., " Paleo-moisture evolution in monsoonal Central Asia during the last 50,000 years", *Quaternary Science Reviews*, **25**, 163-178 (2006).
- Heusser, L.E., and Sirocko, F., "Millennial pulsing of environmental change in southern California from the past 24 k.y.: a record of Indo-Pacific ENSO events" *Geology*, **25**, 243-246 (1997).
- Higginson, M.J., Altabet, M.A., Wincze, L., Herbert, D. and Murray, D.W., "A solar (irradiance) trigger for millennial-scale abrupt changes in the southwest monsoon?", *Paleoceanography*, **19**, PA3015, 1-18 (2004).
- Hohndorf A., Kudrass H. R., and France-Lanord C. "Transfer of the Sr isotopic signature of the Himalayas to the Bay of Bengal", *Deep-Sea Research Part II: Topical Studies in Oceanography*, **50**(5), 951-960 (2003).
- Howden, S.D. and Murtugudde, R., "Effects of river inputs into the Bay of Bengal", *Journal of Geophysical Research*, **106**(C9), 19825-19843 (2001).
- Howell, E.A., Doney, S.C., Fine, R.A. and Olson, D.B., "Geochemical estimates of denitrification in the Arabian Sea and the Bay of Bengal during WOCE", *Geophysical Research Letters*, **24**(21), 2549-2552 (1997).
- Hughen, K.A., Overpeck, J.T., Peterson, L.C. and Trumbore, S., "Rapid climate changes in the tropical Atlantic region during the last deglaciation", *Nature*, **380**, 51-59 (1996).
- Hua, Q. and Barbetti, M., "Review of tropospheric bomb ¹⁴C data for carbon cycle modeling and age calibration purposes" *Radiocarbon*, **46**(3): 1273-1298 (2004).

- Imbrie, J., "A theoretical framework for the Pleistocene ice ages" *Journal of the Geological Society of London*, **142**(3), 417-432 (1985).
- Ittekkot, V., Nair, R.R., Honjo, S., Ramaswamy, V., Bartsch, M., Manganini, S. and Desai, B.N., "Enhanced particle fluxes in Bay of Bengal induced by injection of fresh water", *Nature*, **351**, 385-387 (1991).
- Jacobson, A.D., Blum, J.D. and Walter, L.M., "Reconciling the elemental and Sr isotope composition of Himalayan weathering fluxes: insights from the carbonate geochemistry of stream waters", *Geochimica et Cosmochimica Acta*, **66**(19), 3417-3429 (2002).
- Jain, M., Tandon, S. K., "Fluvial response to Late Quaternary climate changes, western India", *Quaternary Science Reviews* **22**, 2223-2235 (2003).
- Johnson, K.M., King, A.E. and Sieburth, J. M., "Coulometric TCO₂ analyses for marine studies: an introduction", *Marine Chemistry*, **16**, 61-82 (1985).
- Juyal, N., Kar, A., Rajaguru, S.N., Singhvi, A.K., "Luminescence chronology of aeolian deposition during the Late Quaternary on the southern margin of Thar Desert, India" *Quaternary International*, **104**, 87-98 (2003).
- Juyal, N., Pant, R.K., Basavaiah, N., Yadava, M.G., Saini, N.K. and Singhvi, A.K. (2004) Climate and seismicity in the Higher Central Himalaya during the last 20 ka: evidences from Garbayang basin, Uttaranchal, India", *Palaeogeography Palaeoclimatology Palaeoecology*, **213**, 315-330 (2004)
- Juyal, N., Chamyal, L.S., Bhandari, S., Bhushan, R. and Singhvi, A.K., "Continental records of the southwest monsoon during the last 130ka: Evidence from the southern margin of the Thar Desert, India", *Quaternary Science Reviews*, **25**, 2632-2650 (2006).
- Kale, V.S. and Rajaguru, S.N., "Late Quaternary alluvial history of the Northwestern Deccan upland region", *Nature*, **325**, 612-614 (1987).
- Kamesh Raju, T. Ramprasad, P.S. Rao, B. Ramalingeswara Rao and J. Varghese, "New insights into the tectonic evolution of the Andaman basin, northeast Indian Ocean" *Earth Planetary Science Letters*, **221**, 145-162 (2004).
- Kennett, E. J. and R. Toumi, "Himalayan rainfall and vorticity generation within the Indian summer monsoon", *Geophysical Research Letters*, **32**(4): 1-4 (2005).
- Kessarkar, P.M., Rao, V.P., Ahmad, S.M., Patil, S.K., Anil Kumar, A., Anil Babu, G., Chakraborty, S. and Soundar Rajan, R., "Changing sedimentary environment during the Late Quaternary: Sedimentological and isotopic evidence from the distal Bengal Fan", *Deep Sea Research I*, **52**(9), 1591-1615 (2005).

- Klump, J., Hebbeln, D. and Wefer, G., "The impact of sediment provenance on barium-based productivity estimates", *Marine Geology*, **169**(3-4), Pages 259-271 (2000).
- Kodera, K., "Solar influence on the Indian Ocean Monsoon through dynamical processes", *Geophysical Research Letters*, **31**, L24209, 1-4 (2004).
- Kolla V. and Biscaye P. E., "Clay mineralogy and sedimentation in the eastern Indian Ocean", *Deep Sea Research and Oceanographic Abstracts*, **20**(8), 727-728 (1973).
- Kolla, V. and Coumes, F., "Morpho-acoustic and sedimentologic characteristics of the Indus Fan", *Geo-Marine Letters*, **3**, 133-140 (1984).
- Kolla V., Henderson L., and Biscaye P. E., "Clay mineralogy and sedimentation in the western Indian ocean", *Deep Sea Research and Oceanographic Abstracts*, **23**(10), 949-961 (1976a).
- Kolla V., Moore D. G., and Curran J. R., "Recent bottom-current activity in the deep western Bay of Bengal", *Marine Geology*, **21**(4), 255-270 (1976b).
- Kolla, V., Bé, A.W.H. and Biscaye, P.E., "Calcium carbonate distribution in the surface sediments of the Indian Ocean", *Journal of Geophysical Research*, **81** (C15), 2605-2616, 1976.
- Kolla V., Ray P. K., and Kosteki J. A., "Surficial sediments of the Arabian Sea", *Marine Geology*, **41**(3-4), 183-204 (1981).
- Kolla V. and Rao N. M., "Sedimentary sources in the surface and near-surface sediments of the Bay of Bengal", *Geo-Marine Letters*, **10**(3), 129-135 (1990).
- Kotlia, B.S., Bhalla, M.S., Sharma, C., Rajagopalan, G., Ramesh, R., Chauhan, M.S., Mathur, P.D., Bhandari, S., Chacko, S.T., "Palaeoclimatic conditions in the upper Pleistocene and Holocene Bhimtal-Naukuchiatal lake basin in south-central Kumaun, North India", *Palaeogeography, Palaeoclimatology Palaeoecology*, **130**, 307-322 (1997).
- Kotlia, B.S., Sharma, C., Bhalla, M.S., Rajagopalan, G., Subrahmanyam, K., Bhattacharyya, A., Valdiya, K.S., "Palaeoclimatic conditions in the late Pleistocene Wadda Lake, eastern Kumaun Himalaya (India)", *Palaeogeography Palaeoclimatology Palaeoecology*, **162**, 105-118 (2000).
- Krishnaswami, S., Trivedi, J.R., Sarin, M.M., Ramesh, R. and Sharma, K.K., "Strontium isotopes and rubidium in the Ganga-Brahmaputra river system: Weathering in the Himalaya, fluxes to the Bay of Bengal and contributions to the evolution of oceanic $^{87}\text{Sr}/^{86}\text{Sr}$ ", *Earth and Planetary Science Letters*, **109**, 243-253 (1992).
- Krishnaswami, S. and Nair, R.R., "JGOFS (India) - Introduction", *Current Science*, 831-905 (1996).

- Kudrass H. R., Hofmann A., Doose H., Emeis K., and Erlenkeuser H., "Modulation and amplification of climatic changes in the Northern Hemisphere by the Indian summer monsoon during the past 80 k.y." *Geology*, **29**(1), 63-66 (2001).
- Kuehl, S.A., Levy, B.M., Moore, W.S. and Allison, M.A., "Subaqueous delta of the Ganges-Brahmaputra river system", *Marine Geology*, **144**, 81-96 (1997).
- Kumar S. P., Nuncio M., Narvekar J., Kumar A., Sardesai S., De Souza S. N., Gauns M., Ramaiah N., and Madhupratap M., "Are eddies nature's trigger to enhance biological productivity in the Bay of Bengal?", *Geophysical Research Letters* **31**(7), L07309 1-5 (2004).
- Lal D., "Biogeochemistry of Arabian Sea", *Proceedings of Indian Academy of Sciences- Earth and Planetary Sciences*, **103** (1994).
- Lasseby, K.R., Manning, M.R. and O'Brien, B.J., "An overview of Oceanic Radiocarbon: Its inventory and dynamics", *Aquatic Science*, **3**(2-3): 117-146 (1990).
- Leuschner, D.C. and Sirocko, F., "Orbital insolation forcing of the Indian Monsoon- a motor for global climate changes", *Palaeogeography Palaeoclimatology Palaeoecology*, **197**, 83-95 (2003).
- Lisitsyn, A.P., "Sedimentation in the World Ocean", Banta Press, Tulsa, (1972).
- Lisitsyn, A.P., *Oceanic Sedimentation : Lithology & Geochemistry*, 192-230 (1996).
- Madhupratap, M., Gopalakrishnan, T.C., Haridas, P., Nair, .K.C., "Mesozooplankton biomass, composition and distribution in the Arabian Sea during fall intermonsoon: implications of oxygen gradients", *Deep-Sea Research II*, **48**, 145-1368 (2001).
- Madhupratap M., Gauns M., Ramaiah N., Prasanna Kumar S., Muraleedharan P. M., de Sousa S. N., Sardesai S., and Muraleedharan U., "Biogeochemistry of the Bay of Bengal: physical, chemical and primary productivity characteristics of the central and western Bay of Bengal during summer monsoon", *Deep Sea Research Part II: Topical Studies in Oceanography Bay of Bengal*, **50**(5), 881-896 (2003).
- Mallik T. K., "Shelf sediments of the Ganges delta with special emphasis on the mineralogy of the western part, Bay of Bengal, Indian Ocean", *Marine Geology* **22**(1), 1-32 (1976).
- Mangini, A., Jung, M. and Laukenmann, S., "What do we learn from peaks of uranium and of manganese in deep sea sediments?", *Marine Geology*, **177**, 63-78 (2001).
- McGregor, G.R. and Nieuwolt, S., "Tropical Climatology: An Introduction to the Climates of the Low Latitudes", Book, Publisher: John Wiley & Sons Inc; 2nd edition, 339pp. (1998).
- McManus J., Berelson W. M., Klinkhammer, G. P., Johnson, K. S., Coale, K. H., Anderson R. F., Kumar N., Burdige D. J., Hammond D. E., Brumsack H. J., McCorkle D. C., and

- Rushdi A., "Geochemistry of barium in marine sediments: Implications for its use as a paleoproxy", *Geochimica et Cosmochimica Acta*, **62**(21-22), 3453-3473 (1998).
- Measures, C.I., Edmond, J.M., Jickells, T.D., "Aluminium in the North West Atlantic", *Geochimica et Cosmochimica Acta*, **50**, 1423-1429 (1986).
- Métivier, G., "Stability of output fluxes of large rivers in South and East Asia during the last 2 million years: implications on floodplain processes", *Basin Research*, **11**(4), 293-303 doi:10.1046/j.1365-2117.1999.00101.x (1999).
- Meybeck, M., "Concentrations and fluxes of major elements in solution to the oceans", *Review of Geological Dynamic Geographic Physics*, **21**, 215-246, (1979).
- Meyers, P., "Preservation of elemental and isotopic identification of Sedimentary organic matter", *Chemical Geology*, **144**, 289-302 (1994).
- Meyers, P., "Organic geochemical proxies of paleoceanographic, paleolimnologic, and paleoclimatic processes", *Organic Geochemistry*, **27**, 213-250 (1997).
- Milankovich, M., "Théorie mathématique des phénomènes thermiques produits par la radiation Solaire" Paris, Gauthier-Villars (1920).
- Milliman, J.D. and Meade R.H., "World wide delivery of sediments river sediment to the oceans", *Journal of Geology*, **91**, 1-21 (1983).
- Milliman, J.D. and Syvitski, J.P.M., "Geomorphic/Tectonic control of sediment discharge to the ocean: the importance of small mountainous rivers", *Journal of Geology*, **100**, 525-544 (1992).
- Mulder, T. and Syvitski J.P.M., "Climatic and morphologic relationships of rivers. Implications of sea level fluctuations on river loads", *Journal of Geology* **104**, 509-523 (1996).
- Naidu, P.D. and Malmgren, B.A., "Quaternary carbonate record from the equatorial Indian Ocean and its relationship with productivity changes", *Marine Geology*, **161**, 49-62 (1999).
- Naidu, P.D. and Malmgren, B.J., "A high-resolution record of late Quaternary upwelling along the Oman Margin, Arabian Sea based on planktonic foraminifera", *Paleoceanography*, **11**(1), 129-140 (1996).
- Naidu, P.D., "Postglacial Indian Ocean", *Encyclopedia of Quaternary Sciences*, Elsevier, 1831-1839 (2007).
- Nair, R.R., Ittekkot, V., Manganini, S.J., Ramaswamy, V., Haake, B., Degens, E.T., Desai, B.N. and Honjo, S., "Increased particle flux to the deep ocean related to monsoons", *Nature*, **338**, 749-751 (1989).

- Naqvi S. W. A., "Denitrification processes in the Arabian Sea", *Proc. Ind. Acad. Sci.*, **103**, pp. 181-202 (1994).
- Naqvi, S.W.A., Shailaja, M.S., Dipeep Kumar, M. and Sengupta, R., "Respiration rates in subsurface waters of the northern Indian Ocean: Evidence for low decomposition rates of organic matter within the water column in the Bay of Bengal", *Deep Research Research II*, **43(1)**, 73-81 (1996).
- Naqvi, S.W.A., "Chemical oceanography", *The Indian Ocean: A perspective*. eds. by: SenGupta, R.; Desa, Ehrlich, Oxford & IBH; New Delhi (India): **1**; 159-236 (2001).
- Naqvi S. W. A., Naik H., Pratihary A., D'Souza W., Narvekar P. V., Jayakumar D. A., Devol A. H., Yoshinari T., and Saino T., "Coastal versus open-ocean denitrification in the Arabian Sea", *Biogeosciences* **3(4)**, 621-633 (2006).
- Narvekar, P.V., Bhushan, R. and Somayajulu, B.L.K., "Ascertaining depths for samples from hydrographic casts without CTD", *Journal of Marine and Atmospheric Research*, **1**, 33-37 (1997).
- Nath, B. N., Bau, M., Rao, B.R. and Rao, Ch.M., "Trace and rare earth elemental variation in Arabian Sea sediments through a transect across the oxygen minimum zone", *Geochimica et Cosmochimica Acta*, **61**, 2375-2388 (1997).
- Nath, B.N., "Geochemistry of sediments", *The Indian Ocean: A perspective*. eds. by: Sengupta, R.; Desa, Ehrlich, Oxford & IBH; New Delhi (India): **2**, 645-689 (2001).
- Nydal, R. and Lovseth, K., "Tracing bomb ^{14}C in the atmosphere 1962-1980", *Journal of Geophysical Research*, 3621-3642 (1983).
- Nydal, R. and Lovseth, K., "Carbon-14 Measurements in the Atmospheric CO_2 from Northern and Southern Hemispheric Sites", 1962-1993 (1996).
- Oeschger, H., Siegenthaler, U., Schlotterer, U. and Gugelmann, A., "A box diffusion model to study the carbon dioxide in nature" *Tellus*, **27**: 168-192 (1975).
- Okubo A., Obata H., Nozaki Y., Yamamoto Y., and Minami H., " ^{230}Th in the Andaman Sea: Rapid deep-sea renewal", *Geophysical Research Letters*, **31**, 1-5 (2004).
- Ostlund, H.G., Oleson, R. and Brescher, R., "GEOSECS Indian Ocean radiocarbon and tritium results (Miami)", *Tritium Lab Data Report*, **9** (1980).
- Overpeck, J., Anderson, D., Trumbore, S., Prell, W., "The southwest monsoon over the last 18000 years", *Climate Dynamics*, **12**, 213-225 (1996).
- Owen, L.A., Finkel, R.F., Barnard, P.L., Haizhou, M., Asahi, K., Caffee, M.W. and Derbyshire, E., "Climatic and topographic controls on the style and timing of Late Quaternary glaciation throughout Tibet and the Himalaya defined by ^{10}Be

- cosmogenic radionuclide surface exposure dating", *Quaternary Science Reviews*, **24**(12-13), 1391-1411, 2005.
- Palmer, M.R. and Edmond, J.M., "The strontium isotope budget of the modern ocean", *Earth and Planetary Science Letters*, **92**(1), 11-26 (1989).
- Palmer, M.R. and Edmond, J.M., "Controls over the strontium isotope composition of river water", *Geochimica et Cosmochimica Acta*, **56**(5), 2099-2111 (1992).
- Pant, R.K., Juyal, N., Basavaiah, N. and A.K. Singhvi, "Late Quaternary glaciation and seismicity in the Higher Central Himalaya: evidence from Shalang basin (Goriganga), Uttarakhand", *Current Science*, **90**, 1500-1505 (2006).
- Paropkari, A.L., Babu, C.P. and Mascarenhas, A., "A critical evaluation of depositional parameters controlling the variability of organic carbon in Arabian Sea sediments", *Marine Geology*, **107**, 213-226 (1992).
- Paropkari, A.L., Babu, C.P. and Mascarenhas, A., "New evidence for enhanced preservation of organic carbon in contact with oxygen minimum zone on the western continental slope of India", *Marine Geology*, **111**, 7-13 (1993).
- Pattan, J.N. and Shane, P., "Excess aluminum in deep sea sediments of the Central Indian Basin", *Marine Geology*, **161**, 247-255 (1999).
- Pattan J. N., Masuzawa T., Naidu P. D., Parthiban G., and Yamamoto M. (2003) Productivity fluctuations in the southeastern Arabian Sea during the last 140 ka. *Palaeogeography, Palaeoclimatology, Palaeoecology*, **193**(3-4), 575-590.
- Peng, T.-H., Key, R.M. and Ostlund, H.G., "Temporal variations of bomb radiocarbon inventory in the Pacific Ocean", *Marine Chemistry*, 3-13 (1998).
- Pierson-Wickmann, A.-C., Reisberg, L. and France-Lanord, C., "Os-Sr-Nd results from sediments in the Bay of Bengal: Implications for sediment transport and the marine Os record", *Paleoceanography*, **16**(4), 435-444 (2001).
- Prasanna Kumar S., Muraleedharan P. M., Prasad T. G., Gauns M., Ramaiah N., de Souza S. N., Sardesai S., and Madhupratap M. "Why is the Bay of Bengal less productive during summer monsoon compared to the Arabian Sea?" *Geophysical Research Letters* **29**(24), 88-1 (2002).
- Prasanna Kumar S., Nuncio M., Ramaiah N., Sardesai S., Narvekar J., Fernandes V., and Paul J. T., "Eddy-mediated biological productivity in the Bay of Bengal during fall and spring intermonsoons", *Deep Sea Research Part I: Oceanographic Research Papers*, **54**(9), 1619-1640 (2007).
- Prell, W.L., Van Campo, E., "Coherent response of Arabian Sea upwelling and pollen transport to late Quaternary monsoonal winds", *Nature*, **323**, 526-528 (1986).

- Prell W. L., Hutson W. H., Williams D. F., Be A. W. H., Geitzenauer K., and Molfino B., "Surface circulation of the Indian Ocean during the last glacial maximum, approximately 18,000 yr B.P", *Quaternary Research* **14**(3), 309-336 (1980).
- Prell, W.L. and Kutzbach, J.E., "Monsoon variability over the past 150,000 years", *Journal of Geophysical Research*, **92**(D7), 8411-8425 (1987).
- Prell, W.L. and Kutzbach, J.E., "Sensitivity of the Indian monsoon to forcing parameters and implications for its evolution", *Nature*, **360**, 647-652 (1992).
- Qasim, S.Z., "Biological productivity of the Indian Ocean", *Indian Journal of Marine Sciences*, 122-137 (1977).
- Qasim, S.Z., 1982, "Oceanography of the northern Arabian Sea", *Deep Sea Research Part A. Oceanographic Research Papers*, **29**(9): 1041-1068.
- Rai, S.K. and Singh, S.K., "Temporal variation in Sr and $^{87}\text{Sr}/^{86}\text{Sr}$ of the Brahmaputra: Implications for annual fluxes and tracking flash floods through chemical and isotope composition", *Geochemistry Geophysics Geosystems*, **8**(8), doi:10.1029/2007GC001610 (2007).
- Ramamurty, M. and Shrivastava, P.C., "Clay minerals in the shelf sediments of the northeastern part of the Bay of Bengal", *Marine Geology*, **33**, M21-M32 (1979).
- Ramaswamy V. and Nair R. R., "Fluxes of material in the Arabian Sea and Bay of Bengal - sediment trap studies", *Proceedings - Indian Academy of Sciences, Earth & Planetary Sciences* **103**(2), 189-210 (1994).
- Ramaswamy V., Nair R. R., Manganini S., Haake B., and Ittekkot V., "Lithogenic fluxes to the deep Arabian sea measured by sediment traps", *Deep Sea Research Part A. Oceanographic Research Papers*, **38**(2), 169-184 (1991).
- Ramaswamy, V., Rao, P. S., Rao, K. H., Srinivasa Rao, S.T.N. and Raiker, V., "Tidal influence on suspended sediment distribution and dispersal in the northern Andaman Sea and Gulf of Martaban", *Marine Geology*, **208**(1), 33-42 (2004).
- Ramaswamy, V., Vijay Kumar, B., Parthiban, G., Ittekkot, V. and Nair, R.R., "Lithogenic fluxes in the Bay of Bengal measured by sediment traps", *Deep Sea Research II*, **44**(5), 793-810 (1997).
- Ramesh, R., Ramanathan, A.L., Ramesh, S., Purvaja, R. and Subramanian, V., "Distribution of rare earth elements and heavy metals in the surficial sediments of the Himalayan river system", *Geochemical Journal*, **34**, 295-319 (2000).
- Rao, P.S., Ramaswamy, V. and Thwin, S., "Sediment texture, distribution and transport on the Ayeyarwady continental shelf, Andaman Sea", *Marine Geology*, **216**, 239-247 (2005).

- Rao, V.P. and Nath, B.N., "Nature, distribution and origin of clayminerals in grain size fractions of sediments from manganese nodule field, Central Indian Ocean Basin" *Indian Journal of Marine Science*, 17, 202-207 (1988).
- Rao, V. P., "Clay mineral distribution in the continental shelf sediments from Krishna to Ganges River mouth, east coast of India", *Indian Journal of Marine Sciences*, 20(1), 7-12 (1991).
- Rao, V.P. and Kessarkar, P.M., "Geomorphology and Geology of the Bay of Bengal and the Andaman Sea", *The Indian Ocean : A Perspective - Volume 2*, Ed. R.S. Gupta and E. Desa, A.A. Balkema Publishers, 817-868 (2001)
- Rashid, H., Flower, B.P., Poore, R.Z. and Quinn, T.M., "A ~25 ka Indian Ocean monsoon variability record from the Andaman Sea", *Quaternary Science Reviews*, 26, 2586-2597 (2007).
- Raymo, M.E., W.F. Ruddiman, and P.N. Froelich, "Influence of late Cenozoic mountain building on ocean geochemical cycles", *Geology*, 16, 649-653 (1988).
- Reichert G. J., den Dulk M., Visser H. J., van der Weijden C. H., and Zachariasse W. J., "A 225 kyr record of dust supply, paleoproductivity and the oxygen minimum zone from the Murray Ridge (northern Arabian Sea)", *Palaeogeography, Palaeoclimatology, Palaeoecology*, 134(1-4), 149-169 (1997).
- Rengarajan, R., Sarin, M.M., Somayajulu, B.L.K. and Suhasini, R., "Mixing in the surface waters of the western Bay of Bengal using ^{228}Ra and ^{226}Ra ", *Journal of Marine Research*, 60, 255-279 (2002).
- Rhein, M., L. Stramma, and O. Plahn, Tracer signals of the intermediate layers of the Arabian Sea, *Geophys. Res. Lett.*, 24, 2561-2564, 1997.
- Rixen, T., Ittejjot, V., Haake-Gaye, B. and Schafer, P., "The influence of the SW monsoon on the deep-sea organic carbon cycle in the Holocene", *Deep-Sea Research II*, 47, 2629-2651 (2000).
- Rodolfo, K.S., "Sediments of the Andaman Basin, Northeastern Indian Ocean", *Marine Geology*, 7, 371-402 (1969).
- Roonwal, G.S., Glasby, G.P. and Chugh, R., "Mineralogy and geochemistry of surface sediments from the Bengal Fan, Indian Ocean", *Journal of Asian Earth Sciences*, 15(1), 33-41 (1997).
- Sarin, M.M., Borole, D.V. and Krishnaswami, S., "Geochemistry and geochronology of sediments from the Bay of Bengal and the equatorial Indian Ocean", *Proc. Indian Acad. Sci.*, 88A(2), 131-154 (1979).

- Sarin, M.M., Krishnaswami, S., Dilli, K., Somayajulu, B.L.K. and Moore, W.S., "Major ion chemistry of the Ganga-Brahmaputra river system: Weathering processes and fluxes to the Bay of Bengal", *Geochimica et Cosmochimica Acta*, 53, 997-1009 (1989).
- Sarkar, A., Ramesh, R., Bhattacharya, S.K. and Rajagopalan, G. "Oxygen isotope evidence for stronger winter monsoon current during the last glaciation" *Nature* 343, 549–551 (1990).
- Sarkar, A., Bhattacharya, S.K. and Sarin, M.M., "Geochemical evidence for anoxic deep water in the Arabian Sea during the last glaciation", *Geochimica et Cosmochimica Acta*, 57, 1009-1016 (1993).
- Sarkar, A., Ramesh, R., Somayajulu, B.L.K., Agnihotri, R., Jull, A.J.T. and Burr, G.S., "High resolution Holocene monsoon record from the eastern Arabian Sea", *Earth and Planetary Science Letters*, 171, 209-218 (2000).
- Sarma, V.V. S.S., Kuma, M.D. and George M.D., "The central and eastern Arabian Sea as a perennial source of atmospheric carbon dioxide", *Tellus*, Sec. B, 50, 179-184 (1998).
- Schafer P. and Ittekkot V., "Seasonal variability of $\delta^{15}\text{N}$ in settling particles in the Arabian sea and its palaeogeochemical significance", *Naturwissenschaften*, 80, 511-513 (1993).
- Schenau S. J., Prins M. A., De Lange G. J., and Monnin C., "Barium accumulation in the Arabian Sea: controls on barite preservation in marine sediments", *Geochimica et Cosmochimica Acta*, 65(10), 1545-1556 (2001).
- Schmitz, B., "Barium, equatorial high productivity, and the northward wandering of the Indian continent", *Paleoceanography*, 2, 63–77 (1987).
- Schott, F.A., and McCreary, J.P. Jr., "The monsoon circulation of the Indian Ocean", *Progress in Oceanography*, 51, 1-123 (2001).
- Schulz, H., von Rad, U. and Erlenkeuser, H., "Correlation between Arabian Sea and Greenland climate oscillations of the past 100,000 years", *Nature*, 393, 54-57 (1998).
- Schulz M. and Mudelsee M., "REDFIT: Estimating red-noise spectra directly from unevenly spaced paleoclimatic time series", *Comp. Geosci.*, (2000).
- Schulz M. and Stattegger K., "SPECTRUM: Spectral analysis of unevenly spaced paleoclimatic time series", *Computers and Geosciences*, 23, 929-945 (1997).
- Schumm S.A. and David K. Rea, "Sediment yield from disturbed earth systems", *Geology*, 23(5), 391-394; DOI: 10.1130/0091-7613 (1995).
- Seeber, L., and V. Gornitz, "River profiles along the Himalayan arc as indicators of active tectonics" *Tectonophysics*, 92, 335-467, doi:10.1016/0040-1951(83)90201-9 (1983).

- SenGupta R., Moraes C., George M. D., Kureishy T. W., Noronha R. J., and Fondekar S. P., "Chemistry and hydrography of the Andaman Sea" In *Indian Journal of Marine Sciences*, **10**, 228-233 (1981).
- Sengupta et al., "In: Recent Geoscientific studies in the Bay of Bengal and Andaman Sea", *Geological Survey of India Special Publication*, **29**, 201-207 (1992).
- Shetye S. R., Shenoi S. S. C., Gouveia A. D., Michael G. S., Sundar D., and Nampoothiri G., "Wind-driven coastal upwelling along the western boundary of the Bay of Bengal during the southwest monsoon", *Continental Shelf Research*, **11**(11), 1397-1408 (1991).
- Shetye S. R., Gouveia A. D., Shenoi S. S. C., Sundar D., Michael G. S., and Nampoothiri G., "The western boundary current of the seasonal subtropical gyre in the Bay of Bengal", *Journal of Geophysical Research*, **98**(C1), 945-954 (1993).
- Shetye, S.R., Gouveia, A.D. and Shenoi, S.S.C., "Circulation and water masses of the Arabian Sea", *Proceedings - Indian Academy of Sciences, Earth & Planetary Sciences*, 107-123 (1994).
- Shetye S. R., Gouveia A. D., Shankar D., Shenoi S. S. C., Vinayachandran P. N., Sundar D., Michael G. S., and Nampoothiri G., "Hydrography and circulation in the western Bay of Bengal during the northeast monsoon", *Journal of Geophysical Research C: Oceans*, **101**(C6), 14011-14025 (1996).
- Siddiquie, H.N., "Recent sediments of the Bay of Bengal", *Marine Geology*, **5**, 249-291 (1967).
- Singh S. K., Trivedi J. R., Pande K., Ramesh R., and Krishnaswami S., "Chemical and Strontium, Oxygen, and Carbon Isotopic Compositions of Carbonates from the Lesser Himalaya: Implications to the Strontium Isotope Composition of the Source Waters of the Ganga, Ghaghara, and the Indus Rivers", *Geochimica et Cosmochimica Acta*, **62**(5), 743-755 (1998).
- Singh, I. B., Sharma, S., Sharma, M., Srivastava, P. Rajagopalan, G., "Evidence of human occupation and humid climate of 30 ka in the alluvium of southern Ganga Plain." *Current Science*, **76**, 1022-1026 (1999).
- Singh, S.K. and France-Lanord, C., "Tracing the distribution of erosion in the Brahmaputra watershed from isotopic compositions of stream sediments", *Earth and Planetary Science Letters*, **202**, 645-662 (2002).
- Singh S. K., Reisberg L., and France-Lanord C., "Re-Os isotope systematics of sediments of the Brahmaputra River system", *Geochimica et Cosmochimica Acta* **67**(21), 4101-4111 (2003).

- Singh S. K., Kumar A., and France-Lanord C., "Sr and $^{87}\text{Sr}/^{86}\text{Sr}$ in waters and sediments of the Brahmaputra river system: Silicate weathering, CO_2 consumption and Sr flux", *Chemical Geology*, **234**(3-4), 308-320 (2006).
- Singh, S. K., S. Rai, and S. Krishnaswami, "Sr and Nd isotopes in river sediments from the Ganga Basin: Sediment Provenance and Spatial Variability in Physical Erosion", *Journal of Geophysical Research*, doi:10.1029/2007JF000909, in press (2008).
- Sinha, A., Cannariato, K.G., Stott, L.D., Li, C.H., You, C.F., Cheng, H., Edwards, R.L., Singh, I.B., "Variability of Southwest Indian summer monsoon precipitation during the Bølling-Ållerød", *Geology*, **33**, 813-816 (2005).
- Sirocko, F., Sarnthein, M., Erlenkeuser, Land, H., Arnold, M., Duplessy, J.C., "Century-scale events in monsoonal climate over the past 24,000 years", *Nature*, **364**, 321-324 (1993).
- Sirocko F., Garbe-Schonberg D., McIntyre A., and Molino B., "Teleconnections between the subtropical monsoons and high-latitude climates during the last deglaciation", *Science*, **272**, 526-529 (1996).
- Sirocko, F., Schonberg, D.G. and Devey, C., "Processes controlling trace element geochemistry of Arabian Sea sediments during the last 25,000 years", *Global and Planetary Change*, **26**, 217-303 (2000).
- Skornyakova, N.S., "Dispersed iron and manganese in Pacific sediments", In: *Tikhiiy Okean*, t. VI (The Pacific Ocean, 6), Nauka, Moscow (1970).
- Somayajulu B.L.K., Bhushan, R., Sarkar, A., Burr, G.S. and Jull, A.J.T., "Sediment deposition rates on the continental margins of the eastern Arabian Sea using ^{210}Pb , ^{137}Cs and ^{14}C ", *The Science of the Total Environment*, **237/238**, 429-429 (1999).
- Somayajulu, B.L., Yadav, D.N. and Sarin, M.M., "Recent sedimentary records from the Arabian Sea", *Proceedings of Indian Academy of Sciences (Earth Planetary Sciences)*, **103**(2), 315-327 (1994).
- Somayajulu, B.L.K., Bhushan, R. and Narvekar, P.V., " $\Delta^{14}\text{C}$, ΣCO_2 and Salinity of the Western Indian Ocean deep waters : Spatial and Temporal variations", *Geophysical Research Letters*, **26**(18), 2869-2872 (1999).
- Somayajulu, B.L.K., Martin, J.M., Eisma, D., Thomas, A.J., Borole, D.V. and Rao, K.S., "Geochemical studies in the Godavari, India", *Marine Chemistry*, **43**, 83-93 (1993).
- Somayajulu, B.L.K., Rengarajan, R. and Jani, R.A., "Geochemical cycling in the Hooghly estuary, India", *Marine Chemistry*, **79**, 171-183 (2002).
- Srivastava, P., Juyal, N., Singhvi, A.K., Wasson, R.J. and Bateman, D., "Luminescence chronology of river adjustment and incision of Quaternary sediments in the alluvial plain of Sabarmati River, north Gujarat, India", *Geomorphology* **36**, 217-229 (2001).

- Stoykova, D.A., Y.Y. Shopov, D. Garbeva, L.T. Tsankov, and C.J. Yonge, "Origin of the climatic cycles from orbital to sub-annual scales", *Journal of Atmospheric and Solar-Terrestrial Physics*, **70**, 293-302 (2008).
- Stuiver M. and Polach H. A., "Discussion: Reporting of ^{14}C data", *Radiocarbon*, **19**, 355-363 (1977).
- Stuiver M., " ^{14}C distribution in the Atlantic Ocean. *Journal of Geophysical Research*", **85**(C5): 2711-2718 1980.
- Stuiver, M. and Ostlund, H.G., "GEOSECS Indian Ocean and Mediterranean radiocarbon", *Radiocarbon*, 1-29 (1983).
- Stuiver, M., Braziunas, T.F., Becker, B. and Kromer, B., "Climatic, solar, oceanic, and geomagnetic influences on late-glacial and Holocene atmospheric $^{14}\text{C}/^{12}\text{C}$ change", *Quaternary Research*, **35**, 1-24 (1991).
- Stuiver, M., P.M. Grootes, and T.F. Braziunas., "The GISP2 $\delta^{18}\text{O}$ climate record of the past 16,500 years and the role of the sun, ocean and volcanoes", *Quaternary Research* **44**, 341-354 (1995).
- Stuiver M., Reimer P. J., Bard E., Beck J. W., Burr G. S., Hughen K. A., Kromer B., McCormac G., Van Der Plicht J., and Spurk M., "INTCAL98 radiocarbon age calibration, 24,000-0 cal BP", *Radiocarbon*, **40**, 1041-1083 (1998a).
- Stuiver M., Reimer P. J., and Braziunas T. F., "High-precision radiocarbon age calibration for terrestrial and marine samples", *Radiocarbon*, **40**, 1127-1151 (1998b).
- Stummeyer, J., Marchig, V. and Knabe, W., "The composition of suspended matter from Ganges-Brahmaputra sediment dispersal system during low sediment transport season", *Chemical Geology*, **185**, 125-147 (2002).
- Subramanian, V., "Mineralogical input of suspended matter by Indian rivers into the adjacent areas of the Indian Ocean", *Marine Geology*, **36**, M29-M34 (1980).
- Subramanian, V., Van'T Dack, L. and Van Grieken, R., "Chemical composition of river sediments from the Indian sub-continent", *Chemical Geology*, **48**, 271-279 (1985).
- Taylor, S.R. and McLennan, S.M., "The Continental Crust: its Composition and Evolution", Blackwell Scientific Publications, Oxford. 312pp (1985).
- Thamban, M., Rao, V.P. and Schneider R.R. and Grootes, P.M., "Glacial to Holocene fluctuations in hydrography and productivity along the southwestern continental margin of India", *Palaeogeography Palaeoclimatology Palaeoecology*, **165**, 113-127 (2001).
- Thamban, M., Rao, V.P. and Schneider R.R., "Reconstruction of late Quaternary monsoon oscillations based on clay mineral proxies using sediment cores from the western margin of India", *Marine Geology*, **186**, 527-539 (2002).

- Timothy, D. and S. Calvert, "Systematics of Variations in Excess Al and Al/Ti in Sediments from the Central Equatorial Pacific", *Paleoceanography*, **13**(2), 127-130 (1998).
- Tiwari, M., Ramesh, R., Bhushan, R., Somayajulu, B.L.K., Jull, A.J.T. and Burr, G.S., "Paleoproductivity variations from the Equatorial Arabian Sea, implications to east African and Indian summer rainfalls and the El Nino frequency", *Radiocarbon*, **48**(1), 17-29 (2006).
- Tiwari, M., Ramesh, R., Somayajulu, B.L.K., Jull, A.J.T., and Burr, G.S., "Early deglacial (~19-17 ka) strengthening of the northeast monsoon", *Geophysical Research Letters*, **32**, L19712, 1-4 (2005).
- Toggweiler, J.R., Dixon, K. and Bryan, K., "Simulations of radiocarbon in a coarse-resolution world ocean model. 1. Steady state pre-bomb distributions", *Journal of Geophysical Research*, 8217-8242 (1989a).
- Toggweiler, J.R., Dixon, K. and Bryan, K., "Simulations of radiocarbon in a coarse-resolution world ocean model. 2. Distributions of bomb-produced carbon 14", *Journal of Geophysical Research*, 8243-8264 (1989b).
- Tomczak, M. and J.S. Godfrey, "Regional Oceanography: An Introduction", *Pergamon*, 422pp (1994).
- Turekian, K.K. and Wedepohl, K.H., "Distribution of the Elements in some major units of the Earth's crust", *Geological Society of America Bulletin* **72**: 175-192 (1961).
- Unger, D., Ittekkot, V., Schafer, P., Tiemann, J. and Reschke, S., "Seasonality and interannual variability of particle fluxes to the deep Bay of Bengal: Influence of riverine input and oceanographic processes", *Deep-Sea Research II*, **50**, 897-923 (2003).
- Van der Weijden C. H., Reichert G.-J., and van Os B. J. H., "Sedimentary trace element records over the last 200 kyr from within and below the northern Arabian Sea oxygen minimum zone", *Marine Geology*, **231**(1-4), 69-88 (2006).
- Vance, D., Bickle, M., Ivy-Ochs, S. and Kubik, P.W., "Erosion and exhumation in the Himalaya from cosmogenic isotope inventories of river sediments", *Earth and Planetary Science Letters*, **206**, 273-288 (2003).
- Venkatachala, B.S.; Rajagopalan, G.; Kar, R.K.; Rajnikanth, A., "Palynological studies and ¹⁴C dating of a gravity core from the seabed west of Narcondam Island in the Andaman Sea", *Geological Survey India Special Publication*, **29**, 107-110 (1992).
- Walter, H.J., Hegner, E., Diekmann, B., Kuhn, G. and Rutgers van der Leoff, M.M., "Provenance and transport of terrigenous sediment in the South Atlantic Ocean and their relations to glacial and interglacial cycles: Nd and Sr isotopic evidence", *Geochimica et Cosmochimica Acta*, **64**(22), 3813-3827 (2000).

- Wanninkhof, R., "Relationship between wind speed and gas exchange over the ocean", *Journal of Geophysical Research*, 7373-7382 (1992).
- Wanninkhof, R., Ledwell, J.R. and Broecker, W.S., "Gas exchange - wind speed relation measured with sulfur hexafluoride on a lake", *Science*, 1224-1226 (1985).
- Weber, M.E., Wiedicke, M.H., Kudrass, H.R., Hubscher, C. and Erlenkeuser, H., "Active growth of the Bengal Fan during sea-level rise in highstand", *Geology*, 25(4), 315-318 (1997).
- Weber, M.E., Wiedicke-Hombach, M., Kudrass, H.R. and Erlenkeuser, H., "Bengal Fan sediment transport activity and response to climate forcing inferred from sediment physical properties", *Sedimentary Geology*, 155, 361-381 (2003).
- Wedepohl, 1960, "Minor element investigations of Atlantic bottom samples: geochemical comparison of pelitic sediments from different oceans.", *Geochimica et Cosmochimica Acta*, 18(3-4), 200-231 (1960).
- Weldeab, S., Emeis, K-C., Hemleben, C. and Siebel, W., "Provenience of lithogenic surface sediments and pathways of riverine suspended matter in the Eastern Mediterrameam Sea: Evidence from $^{143}\text{Nd}/^{144}\text{Nd}$ and $^{87}\text{Sr}/^{86}\text{Sr}$ ratios", *Chemical Geology*, 186, 139-149 (2002).
- Wijayananda N. P. and Cronan D. S., "The geochemistry and mineralogy of marine sediments from the eastern Indian Ocean", *Marine Geology* 117(1-4), 275-285 (1994).
- Winkler, G., Anderson, R. F. and Schlosser, P. "Equatorial Pacific productivity and dust flux during the mid-Pleistocene climate transition", *Paleoceanography* 20, PA4025, doi:10.1029/2005PA001177 (2005).
- Wyrtki, K., "Oceanographic Atlas of the International Indian Ocean Expedition", 531pp, (1971).
- Wyrtki, K., "Physical Oceanography of the Indian Ocean", *The Biology of the Indian Ocean*, B. Zeitzschel (ed.), Chapman and Hall Ltd., 19-36 (1973).
- Yadav, D.N., Sarin, M.M. and Somayajulu, B.L.K., "Western continental margins of India: Are they sink or source for trace elements in the Arabian Sea?", *Oceanography of the Indian Ocean*, Ed. B.N. Desai, Oxford & IBH Publishing Co. Pvt. Ltd., 359-367 (1992).
- Yadav D. N., "Manganese mobilization from the Western Continental margin of India", *Current Science*, 71, 900-905 (1996).
- Zonneveld, K.A.F., Ganssen, G., Troelstra, S., Versteegh, G.J.M. and Visscher, H., "Mechanisms forcing abrupt fluctuations of the indian ocean summer monsoon during the last deglaciation", *Quaternary Science Reviews*, 16(2), 187-201 (1997).